NOTICE

CERTAIN DATA CONTAINED IN THIS DOCUMENT MAY BE DIFFICULT TO READ IN MICROFICHE PRODUCTS.

FOSSIL

DOE/PC/79914-T12
(DE91004165)

MACROMOLECULAR COAL STRUCTURE AS REVEALED BY NOVEL DIFFUSION TESTS

Final Technical Report for the Period September 15, 1987—September 14, 1990

Work Performed Under Contract No. FG22-87PC79914

For
U.S. Department of Energy
Pittsburgh Energy Technology Center
Pittsburgh, Pennsylvania

By
Purdue University
West Lafayette, Indiana

DISCLAIMER

This report was prepared as an account of work sponsored by an agency of the United States Government. Neither the United States Government nor any agency thereof, nor any of their employees, makes any warranty, express or implied, or assumes any legal liability or responsibility for the accuracy, completeness, or usefulness of any information, apparatus, product, or process disclosed, or represents that its use would not infringe privately owned rights. Reference herein to any specific commercial product, process, or service by trade name, trademark, manufacturer, or otherwise does not necessarily constitute or imply its endorsement, recommendation, or favoring by the United States Government or any agency thereof. The views and opinions of authors expressed herein do not necessarily state or reflect those of the United States Government or any agency thereof.

This report has been reproduced directly from the best available copy.

Available to DOE and DOE contractors from the Office of Scientific and Technical Information, P.O. Box 62, Oak Ridge, TN 37831; prices available from (615)576-8401, FTS 626-8401.

Available to the public from the National Technical Information Service, U. S. Department of Commerce, 5285 Port Royal Rd., Springfield, VA 22161.

Printed in the United States of America. Office of Scientific and Technical Information, Oak Ridge, Tennessee

DOE/PC/79914-T12
(DE91004165)
Distribution Category UC-113

DOE/PC/79914--T12

DE91 004165

FINAL TECHNICAL REPORT

MACROMOLECULAR COAL STRUCTURE AS REVEALED BY NOVEL DIFFUSION TESTS

By

NIKOLAOS A. PEPPAS, PRINCIPAL INVESTIGATOR
JORGE OLIVARES
RICHARD DRUMMOND
STEVEN LUSTIG

School of Chemical Engineering
Purdue University
West Lafayette, Indiana 47907

Department of Energy
Pittsburgh Energy Technology Center
Contract No. DE-FG22-87PC79914

Progress Period: 9/15/87 - 9/14/90

ABSTRACT

The main goal of the present work was the elucidation of the mechanistic characteristics of dynamic transport of various penetrants (solvents) in thin sections of coals by examining their penetrant uptake, front swelling and stress development. The samples used were well characterized, and the experimentation temperature varied from 30 to 175°C. An important objective of this work was the study of coal network structure in different thermodynamically compatible penetrants and the analysis of dynamic swelling in terms of present anomalous transport theories. Interferometry/polariscopy, surface image analysis and related techniques were used to quantify the stresses and solvent concentration profiles in these sections. The swelling characteristics of selected coals were elucidated by penetration studies using a number of potentially swelling agents. Dynamic and equilibrium swelling behavior were correlated using the polar interaction contributions of the solvent solubility parameters. The penetrant front position was followed in thin coal sections as a function of time. The initial front velocity was calculated for various coals and penetrants. Our penetrant studies with thin coal sections from the same coal sample but with different thicknesses show that within the range of 150 μm to 1500 μm the transport mechanism of dimethyl formamide in the macromolecular coal network is non-Fickian. In fact, for the thickest samples the transport mechanism is predominately Case-II whereas in the thinner samples penetrant uptake may be diffusion-controlled. Studies in various penetrants such as acetone, cyclohexane, methanol, methyl ethyl ketone, toluene and methylene chloride indicated that penetrant transport is a non-Fickian phenomenon. However, the equilibrium swelling value at room temperature should be correlated with the polar contribution of the solvent solubility parameter. The penetrant front velocity was correlated to C% (dmmf) and $\overline{M}_c$ of the various coals studied, and to the solvent compatibility. Stresses and cracks were observed for transport of methylene chloride. In actual coal liquefaction and solvent treatment processes, the phenomena observed during the solvent transport in coal and the swelling of coal chunks and particles are characterized by large stresses created in the swelling system. These stresses are the consequence of purely relaxational transport mechanism, and are responsible for significant cracking of the coal samples. In actual applications, this continuous crazing may lead to significantly increased reaction rates and mass transfer of solvents in coal.

Page

LIST OF TABLES

LIST OF FIGURES

Figure Page

Figure Page

Figure Page

Figure | Page

Figure Page

Figure Page

Figure Page

1. INTRODUCTION

Coal may be utilized as an energy source in one of three ways. It can be burned directly to generate heat, or it can be converted to cleaner burning gaseous and liquid products. Coal can be converted to methane gas through a sequence of two reaction mechanisms, namely, the high temperature endothermic reaction with steam to produce carbon monoxide and hydrogen followed by the relatively low temperature exothermic reaction of the synthesis gas with additional hydrogen. The considerable thermal inefficiency of this reaction sequence limits its usefulness. The production of liquid fuels from coal is one of the options for alleviating projected shortages of energy sources.

Coal can be converted to liquid fuels by direct hydrogenation at extremely high temperatures and pressures. However the hydrogenation is a very cost inefficient process; therefore there has been efforts to reduce the hydrogen requirements for the process by maximizing the use of hydrogen in the coal itself or by the use of a coal-derived solvent that is capable of donating hydrogen (in situ) to the process. The chemistry of coal liquefaction is extremely complex. Indeed, the exact chemistry involved in the liquefaction process and the so called structure of coal itself is still only speculative.

The chemical objectives of coal liquefaction are (1) to reduce the effects of van der Waal's forces and hydrogen bonds, and, thus, separate fairly large units of coal structure into smaller units, (2) to bring about the decomposition of key aromatic; aliphatic; and a variety of carbon-heteroatom (i.e. nitrogen, oxygen, and sulfur) bonds within the coal to form smaller fragments, and, finally, (3) to increase the hydrogen/carbon atomic ratio from approximately 0.8 to produce a low-sulfur, ash-free liquid product that is comparable to crude oil, gasoline, or even the heavy oils and bitumens. This brings the importance of understanding the fundamentals of transport penetrants into the coal structure to aid and understand the liquefaction process of coal (Speight, 1983).

The widely accepted chemical structure of coal is one consisting of a system of aromatic/hydroaromatic/heterocyclic condensed ring clusters, crosslinked by methylenic, ethylenic, sulfidic, and/or etheric bridges (Given, 1960; Wiser, 1965; Davidson, 1980; Heredy and Wender, 1980; Wender et al., 1981; Hayatsu et al., 1978, 1980, 1981; Solomon, 1981; Evans and Hooper, 1981; Gerstein et al., 1981; Peppas and Lucht, 1984). Coals are extraordinarily complex heterogeneous substances, so complex that one must question the wisdom of applying to them models derived for homogeneous polymeric substances, especially quantitatively.

Considerable evidence exists from physicochemical experiments which suggests that bituminous coals consist of a highly crosslinked macromolecular network (Larsen and Kovac, 1978; Green et al., 1982; van Krevelen, 1981; Wert and Weller, 1982; Peppas and Lucht, 1984). The major source of experimental evidence favoring a crosslinked network is obtained from swelling experiments. It has been found that coal can swell in thermodynamically compatible solvents to twice its original volume without dissolution (Larsen and Kovac, 1978; Dryden, 1951a,b,c,d; Peppas and Lucht, 1984; Nelson, 1983; Lucht, 1983). Additional support for coal as a crosslinked, three dimensional network is obtained from thermomechanical analysis. When a crosslinked polymeric network is subjected to a stress, deformation occurs until it reaches the limit set by the extent of crosslinking. After the stress is removed, the polymeric network returns to its original conformation. A similar time-dependence of stress on strain has been observed in coal (Larsen and Kovac, 1978; Sanada and Honda, 1963; Howell and Peppas, 1984; Barr-Howell et al., 1985).

As mentioned before, the organic structure of coal consists of a system of aromatic/hydroaromatic/heterocyclic condensed ring clusters, crosslinked by methylenic, ethylenic, sulfidic, and/or etheric bridges. Figure 1.1 shows a model structure for the organic phase of coal proposed by Wiser (1965). Figure 1.2 shows a model structure for the organic phase of coal proposed by

Wender (1980). These proposed models represent structures for bituminous coals. To facilitate the analysis of coal as a macromolecular network, Lucht and Peppas (1981.a,.b), Lucht (1983), and Peppas and Lucht (1984) proposed a hypothetical and simplified representation of coals physicochemical organic structure. If one excludes mineral matter, ash and other impurities naturally found in coal, its structure can be described by two distinct by closely related phases. The first phase includes small and large molecules that are uncrosslinked and can be dissolved or extracted at low temperatures. The second phase, which constitutes the bulk of the coal structure, consists of a highly crosslinked macromolecular network. Figure 1.3 depicts this ideal swollen coal network showing various forms of macromolecular chains and defects. Included in this figure are covalent tetrafunctional and multifunctional crosslinks as well as effective crosslinks arising from physical entanglements and hydrogen-bonding. Also present are the molecules of the swelling agent and the extractable chains contained within the matrix.

Dynamic and equilibrium swelling studies have been utilized as molecular probes to elucidate the structure and morphology of polymeric networks. Both the thermodynamic equilibrium and the dynamic sorption behavior of penetrants can be interpreted in terms of molecular models that are related to material characteristics such as crystal structure, degree of crosslinking, and distribution of free-volume. In an analogous fashion, studies of equilibrium and dynamic sorption penetrants into coal networks can be used as a means of elucidating aspects of the molecular structure and physical state of coal will enhance its efficient utilization.

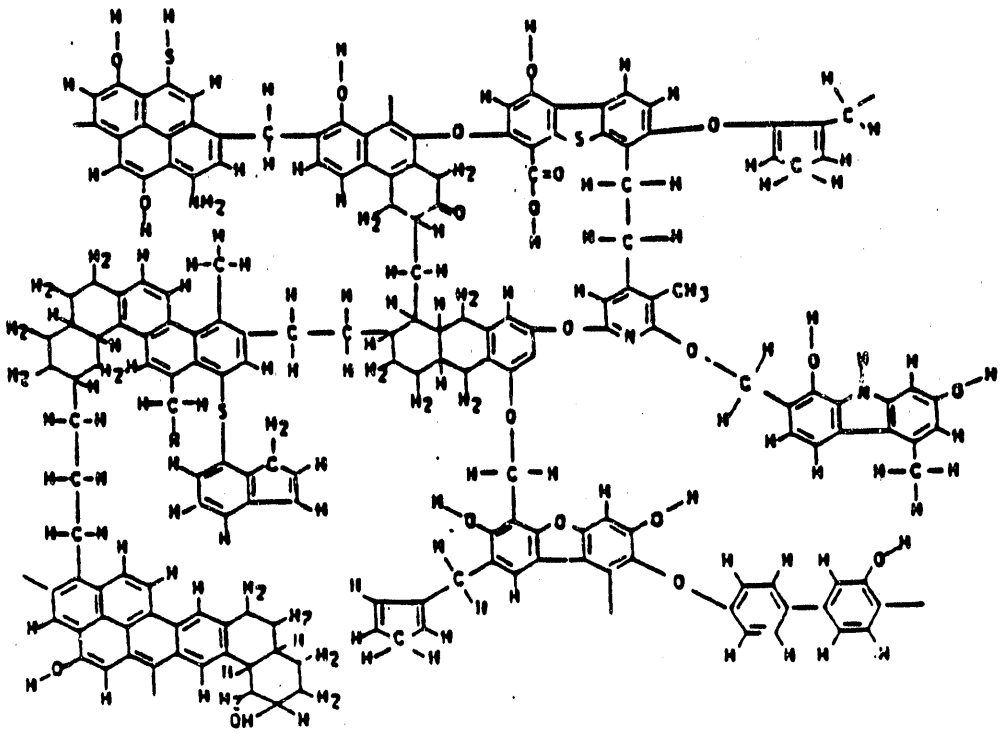

Figure 1.1 Model Structure of the Organic Phase of Coals According to Wiser (1965).

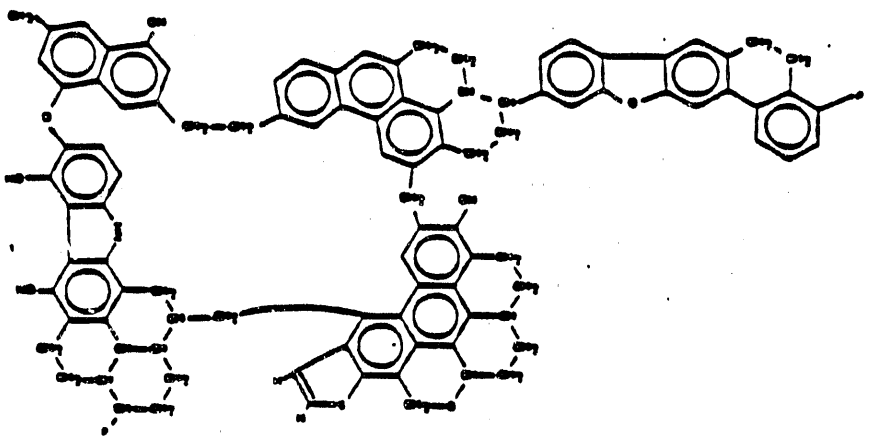

Figure 1.2 Model Structure of the Organic Phase of Coals According to Heredy and Wender (1980).

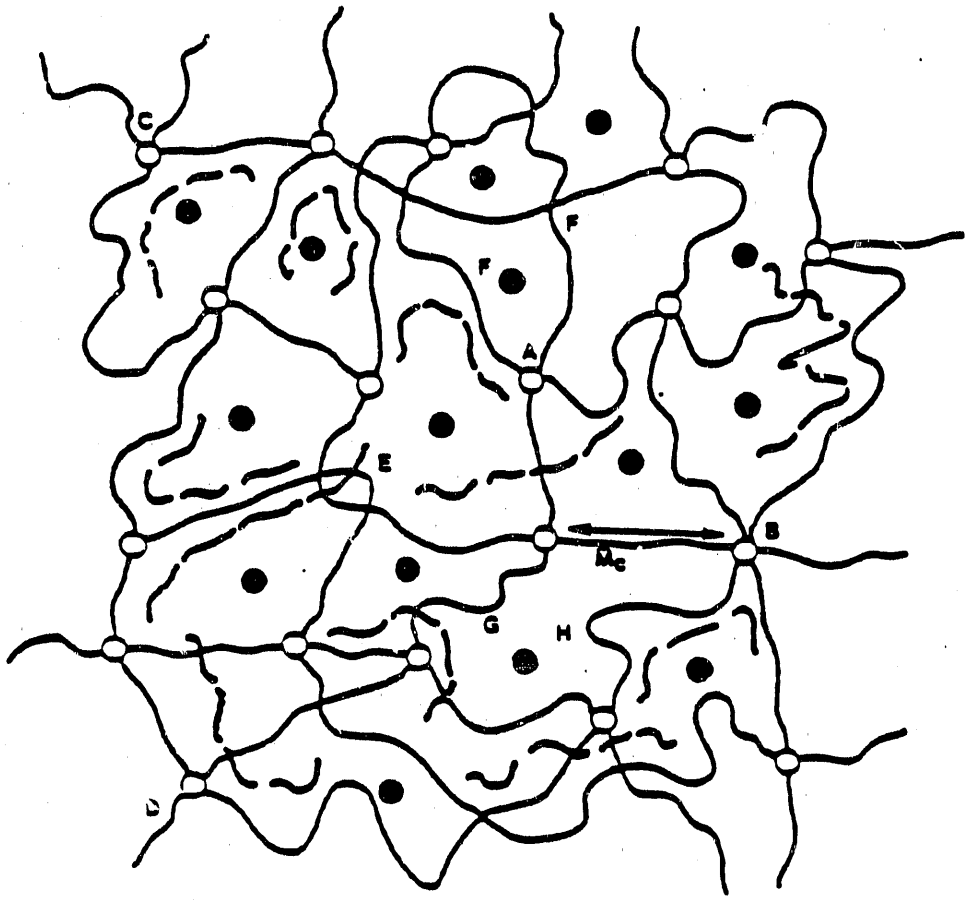

Figure 1.3 Simplified model of the crosslinked structure of coal including possible defects. - chains participating in network structure; – extractable (unreacted or degraded) chains; (O) crosslinks (junctions); (O) molecules of penetrant; M_c molecular weight between crosslinks; A tetrafunctional crosslink; B multifunctional crosslink; C unreacted functionalities; D chain end; E entanglement; F chain loop; G effective network chain; H mesh size.

2. BACKGROUND

2.1 Introduction

Diffusion into coals is of considerable technological importance since many coal modification processes, such as direct liquefaction, desulfurization, demineralization, and chemical modification, involve diffusion of liquids or gasses into the coal. Additionally, much of the fundamental chemical research on coals requires diffusion of liquids or dissolved reagents into the coal so that reactions can occur. Precise interpretation of these experiments often requires an understanding of the diffusional behavior. The rate of reactants diffusing into the particles is often the rate-limiting step.

Besides the variations in particle shapes and sizes, there are a number of other factors that complicate diffusion in coal. These factors include cracks and holes through the coal, the variety of macerals having different chemical and physical properties which make up the coal, the heterogeneity of the structure even within individual macerals, and the effects of intermaceral interfaces and mineral matter (Brenner and Hagan, 1985). Even though these variations within the coal network make the characterization of coal difficult, one may give approximate results to describe the structure of coal. Having described coal as a macromolecular structure in chapter one, a polymeric model with mathematical and physical similarities to coal would be a good approximation to describe the structure of coal.

2.2 Transport of Penetrants in the Macromolecular Structure of Coal

Analysis of dynamic swelling results from macromolecular networks swollen by thermodynamically good solvents yields information about the structure of the network and its solvent-network interactions. Diffusion studies can be used to identify the thermodynamic state of the network,

i.e., whether the network exists in the glassy or rubbery state. For a macromolecular network, it is possible to determine whether sorption is due to Fickian diffusion, macromolecular chain relaxations, or due to a coupling of the two phenomena. In order to understand the mechanisms that govern the sorption of penetrants into the coal network, it is necessary to study and understand the concentration, temperature, and penetrant activity effects on diffusion, as well as particle geometry, network crosslinking density, and penetrant-network compatibility.

2.2.1 Concentration Effects

Introduction of a penetrant into a glassy macromolecular network can have the same effect on the system as increasing the temperature (Ritger and Peppas, 1987b). As the penetrant enters the network, the network density decreases, resulting in an increase in large molecular chain motions. This change in density is due to the breakage and formation of chemical bonds. Increasing the penetrant concentration in the network can be viewed as an effective decrease of the glass transition temperature. Peppas and Lucht (1985) determined that the glass transition temperatures for a variety of coals ranged from 350 to 400° C. The concentration dependence on the temperature at which the transition from the glassy state to the rubbery state occurs is reflected in the fact that the glass transition temperature is defined by a curve and not a single point. This relationship between concentration and temperature, the effective glass transition curve, is depicted in Figure 2.1 for a coal/penetrant system.

Penetrant transport in polymers may induce structural changes such as swelling, microcavity formation, primary phase transition and secondary phase transition. Obviously these changes require rearrangement of molecular chains. Therefore penetrant uptake may be controlled by transport phenomenon, by structural relaxations, or by coupling of the two phenomena.

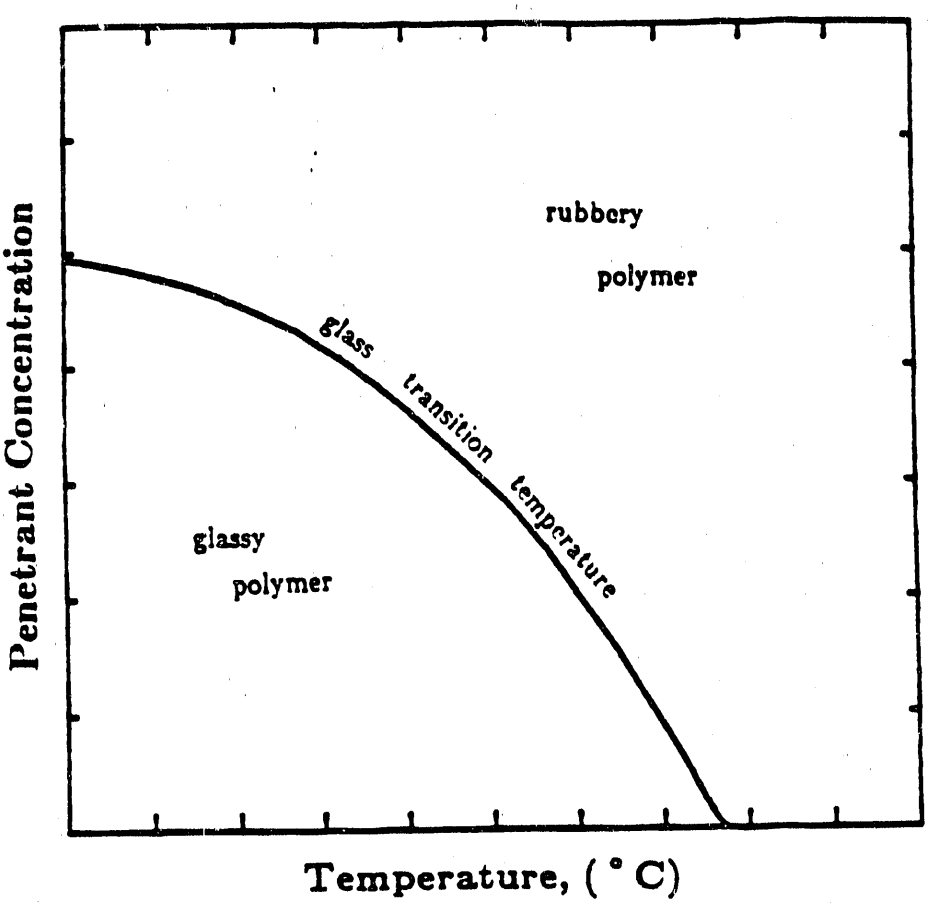

Figure 2.1 Thermodynamic state of a macromolecular network as a function of penetrant concentration and temperature.

Astarita and Nicolais (1983) classified the relaxation phenomena observed during solvent transport in glassy macromolecular systems into two broad categories. The first category, termed bulk structural changes (BSC), includes those processes where the structural changes occur gradually over the entire volume of the macromolecular network. Those processes exhibiting an abrupt transition in the structure are included in the second category, moving boundary phenomena (MBP). In this second category, a sharp front often divides the two structurally different regimes of the polymeric material. This front moves in time until the whole sample achieves the same new structure.

The limiting case that characterizes moving boundary phenomena is termed Fickian diffusion. It is strictly concentration-dependent, and usually occurs in glassy systems where the penetrant activity is low. Fickian diffusion may also occur in the rubbery state. The other limiting case, termed Case-II transport, is characterized by a moving front at nearly constant velocity and a region behind it in which relaxation of the macromolecules takes place. The boundary between rubbery and the glassy state is generally very sharp (Ritger and Peppas, 1987a). Most transport processes in glassy polymers fall between these two limiting cases and are termed anomalous transport. This occurs when the diffusional and relaxational kinetic rates are comparable, and can be thought of as the coupling of the Fickian and Case-II transport processes.

2.2.2 Temperature and Penetrant Activity Effects

The transport of penetrants into a polymer network depends on temperature and activity of the penetrant (Hopfenberg and Frisch, 1969). Concentration-independent and concentration-dependent Fickian diffusion, time-dependent diffusion anomalies, Case-II transport, and solvent crazing-stress cracking may occur in the same polymer structure if parameters such as temperature, penetrant activity, and penetrant type are varied. Figure 2.2 shows the transport features in the various regions of the temperature-penetrant activity plane. In this case penetrant activity is defined as P^{par}/P_o, where P^{par} is the penetrant partial pressure and P_o is the penetrant vapor pressure (Hopfenberg and Frisch, 1969).

When a macromolecular structure is below its glass transition temperature, i.e., in the glassy state, all large molecular motions are restricted although segmental motion may still be exhibited. As the temperature is increased, the extent of vibrations also increases, the chains move further apart, and the density of the whole material decreases (Hopfenberg and Stannett, 1973). Thus, an increase in the diluent concentration in a macromolecular system as well as an increase of the system temperature decreases the network density.

The polymer network can also be altered by varying penetrant activity. The activation energy characterizing solvent crazing decreases with decreasing penetrant activity (Hopfenberg and Frisch, 1969). The effects of temperature and penetrant activity on the transport of normal hydrocarbons in glassy polymers may be summarized as follows (Michaels et al., 1968).

(1) At high penetrant activities (ca. 0.85-1.0) over a range of temperatures well below T_g, solvent crazing accompanies the transport of penetrant into the polymer.

(2) The crazing kinetics of Case-II transport, i.e., the boundary between crazed polymer and the uncrazed, glassy core moves at a constant rate to the film midplane.

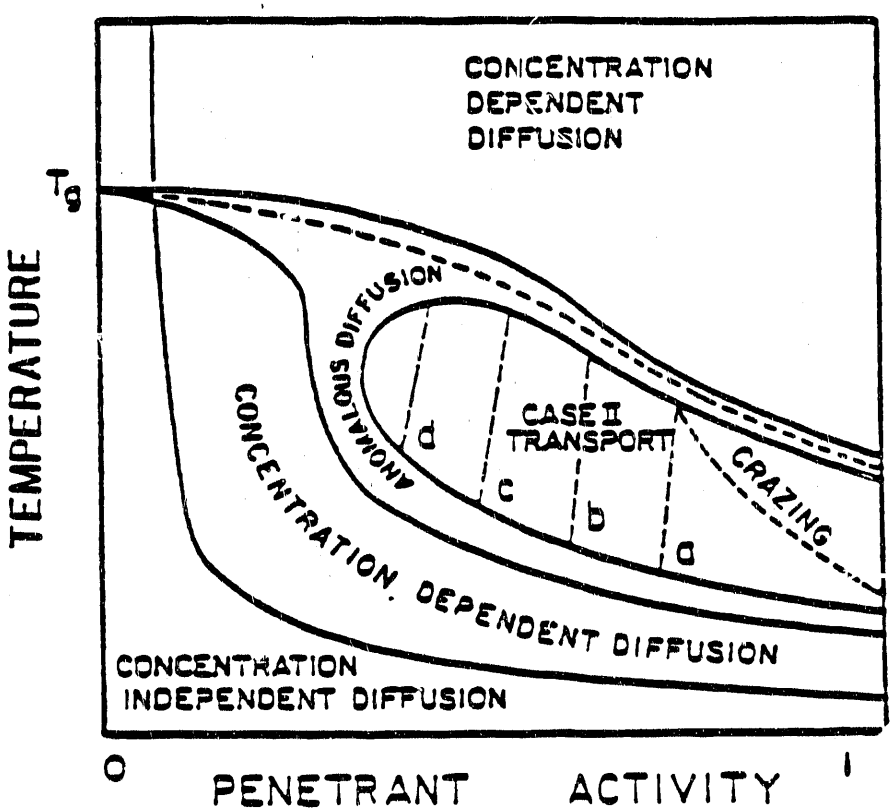

Figure 2.2 Regions of penetrant diffusion mechanisms in macromolecular structures as a function of temperature and penetrant activity (from Hopfenberg and Frisch, 1969).

(3) The activation energy characterizing solvent crazing is quite large (ca. 50-60 Kcal/mol) suggesting that the primary bond breakage probably contributes to the rate-determining relaxations at the boundary between swollen and unswollen polymer.

(4) Case-II transport occurs over a similar temperature range at activities between 0.5 and 1.0. Crazing is only observed at the very high activities corresponding to penetrant concentrations sufficient to produce osmotic stresses which are sufficiently large to cause local fracture of the material.

(5) Case-II sorption is also a highly activated process (ca. 20-50 Kcal/mol). The activation energy decreases with decreasing penetrant activity.

(6) As activity is reduced to values lower than 0.5, time-dependent or anomalous diffusion is observed.

(7) At very low activities and/or very low temperatures, thermally activated diffusion controls the transport of penetrant in polymers. The activation energy for diffusion is less than 10 Kcal/mol, and if activity is reduced to very small values the diffusion coefficients are independent of concentration as well as time.

The work of Lucht (1983) and Hsieh (1984) have shown that the coal structure may exhibit the same dynamic swelling behavior as glassy polymers. Therefore the just mentioned temperature and penetrant activity effects on glassy polymers, may also apply to the coal structure. Later, Ritger and Peppas (1987b) also conducted studies of penetrant transport into coal at high penetrant activities. They concluded that Case-II governed the overall transport process. These coal studies support the theory established by Hopfenberg and Frisch (1969), even though studies at low activities need to be done on coal to conclude that coals and glassy polymers behave similarly.

Barr-Howell et al. (1986a), studied the transport of penetrants in the macromolecular structure of coal as a function of temperature. The results showed a decrease in penetrant uptake as temperature was increased. It was mentioned in this section that an increase in temperature lowers the density of the network; therefore one would expect higher diffusion rates and higher penetrant uptakes with a temperature increase. Obviously there is some contradiction in the experimental results and the theoretical prediction for high temperature studies. This case needs to be looked more in detail.

2.2.3 Crosslinking Effects

Analysis of the physical behavior of macromolecular networks in coals and determination of the number average molecular weight between crosslinks and the crosslinking density of the network are important factors in the development of structure/properties relationships of coal samples, and in the elucidation of technical problems during coal extraction, liquefaction and modification through chemical reactions (Lucht and Peppas, 1981.a). An attractive method of investigating the structure of coal is to observe the response of coal to a swelling agent (penetrant). The degree to which coal swells in the presence of a specific swelling agent is a measure of the solvent-coal compatibility and of the flexibility of the coal structure itself.

Peppas and Lucht (1985), Barr-Howell et al. (1986b), and Ritger and Peppas (1987b) conducted swelling studies on coal to elucidate the transport of penetrants into the macromolecular structure of coal. The studies were done over a range of coals consisting of different carbon contents. To analyze the data and to characterize the transport processes, they used a semi-empirical expression:

$$\frac{M_t}{M_\infty} = kt^n \qquad (2.1)$$

here M_t is the mass uptake of penetrant at time t, M_∞ is the mass uptake of penetrant at infinite time, k

is a constant incorporating characteristics of the macromolecular network system and the penetrant, and n is the diffusional exponent which is indicative of the transport mechanism.

For transport in thin films, if n=0.5 the mechanism is Fickian diffusion. For values of $0.5<n<1.0$ the mechanism is anomalous transport. Values of n=1.0 indicate Case-II transport, and values $n>1.0$ indicate Super Case-II transport. In all cases, the first 60% of the data of the penetrant uptake curve is used for the determination of the values of n.

The results from Peppas and Lucht (1985), Barr-Howell et al. (1986b), and Ritger and Peppas (1987b) based on equation (2.1) show that the transport mechanism varies with carbon content. As the carbon content increases, the diffusional exponent n also increases. Since coal crosslinking increases with carbon content, the transport mechanism of penetrants is affected by the crosslinking density.

In conventional polymeric systems, the characteristic relaxation time, λ, and the penetrant diffusion coefficient, D, are strongly dependent upon the degree of crosslinking (which can be related to the molecular weight between crosslinks) of the sample. The molecular weight between crosslinks in coal as a function of carbon content was previously investigated by Lucht (1983) and Barr-Howell et al.(1986b). They used a modified Gaussian network equation to analyze their swelling studies and to determine values for the average molecular weight between crosslinks, M_c, the number of repeating units between crosslinks, and the average molecular weight of the repeating unit. The results of their analysis are presented graphically in Figure 2.3. It is evident from Figure 2.3 that the molecular weight between crosslinks reaches a maximum at a carbon content between 75 to 80% and decreases for carbon contents greater than or less than this range. Therefore one would expect the highest swelling ratios for coals that contain a 75 to 80% carbon content, due to the fact that the chains within the network are longer making the spacing available for swelling larger. Since the swelling ratio increases for the coals within this range, indicates that the penetrant concentration increases and the diffusion process becomes

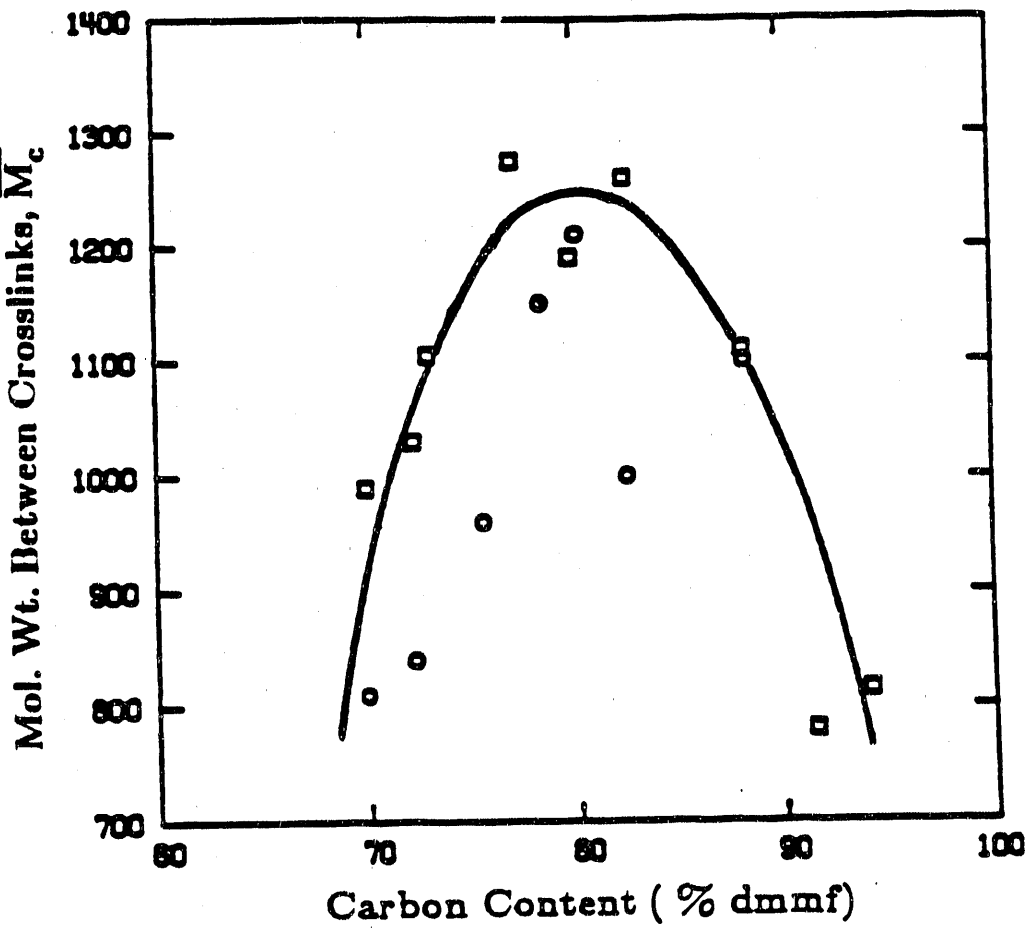

Figure 2.3 Molecular weight between crosslinks as a function of carbon content for 600-850 μm coal particles. Values of M_c obtained from equilibrium pyridine swelling studies at 35°C by Barr-Howell (1984) (○), and Lucht (1983) (□).

faster.

2.2.4 Film Thickness Effect

The Deborah number, De, was first presented by Vrentas et al. (1975) and Vrentas and Duda (1977) as a mean of predicting the mechanism of penetrant transport. The diffusional Deborah number is defined as the ratio of the relaxation time of the system to the time corresponding to the diffusion process of the same system. The characteristic diffusion time for one-dimensional diffusion in a thin film is defined as:

$$\Theta = \frac{\delta^2}{D} \tag{2.2}$$

where the characteristic diffusion length, δ, is the film half thickness $l/2$, and D is the penetrant diffusion coefficient. Therefore the Deborah number can be written as:

$$De = \frac{\lambda D}{l^2} \tag{2.3}$$

where λ is the characteristic relaxation time. Equation (2.3) predicts that the Deborah number can be altered if the sample thickness is changed at constant relaxational and diffusional times. However Ritger and Peppas (1987b) concluded that the mechanism governing the transport of pyridine in thin coal films ranging between 150 and 1000 μm thick is Case-II transport and Supercase Case-II transport with a diffusional exponent n in the range $0.95<n<1.05$. These results show that by varying the sample thickness between 150 and 1000 μm, the transport mechanism remains almost constant.

2.2.5 Solvent Chemistry

In the classification of coal solvents presented by Dryden (1951a), a good solvent for coal contains a nitrogen or oxygen atom possessing an unshared pair of electrons. All factors being equal,

nitrogen-containing compounds are better solvents than oxygen-containing compounds. Dryden inferred that the possibility of hydrogen bonding must play a part in these interactions. The swelling ratios in hydrogen bonding solvents are much higher than those in the non-hydrogen bonding solvents particularly with solvents containing nitrogen (Quinga and Larsen, 1987).

Basic organic solvents tend to be good swelling solvents for coal. The high swelling caused by such solvents (hydrogen bond-accepting solvents in general) is attributed to the replacement of coal-coal hydrogen bonds with coal-solvent hydrogen bonds. This phenomenon causes the coal to swell more, because replacement of a coal-coal hydrogen bond by a coal-solvent hydrogen bond reduces the crosslink density of the coal (Larsen et al., 1985). However swelling studies with non-polar solvents have been reported before. In order to make use of a non-polar solvent as a penetrant, the coal network would have to be pre-extracted with a polar solvent with good hydrogen bonding properties to lower the density of the network (Larsen et al., 1983; Hall et al., 1988; Barr-Howell et al., 1986b).

A solvent can also be described in terms of its electron-donor and electron-acceptor properties. Szeliga and Marzec (1983) characterized swelling agents for coal in terms of its electron-donor numbers. They found that solvents with electron-donor numbers between 0-16 either do not swell the coal or swell it only slightly. Solvents with electron-donor within the range 16-30 show an increase in the swelling ratio. The conclusions to their work are that coal macromolecules are bound together by means of electron-donor-acceptor interactions and that electron-donor sites in coal macromolecules have donor numbers of 16-30 approximately.

Solubility parameters is another method to characterize solvent-coal compatibility. Solubility parameter δ is defined as as $(C.E.D.)^{1/2}$ where C.E.D. is the cohesive energy density. This C.E.D. is defined as the sum of interaction energies of all molecules present in a unit volume of a solid or liquid. Numerous types of cohesive forces act between molecules, the most important ones are due to

dispersion (d), polar (p), and hydrogen-bond (h) interactions. Hansen (1967) suggested a relationship for the solubility parameter which accounts for the most important cohesive energy forces:

$$C.E.D.= \delta^2 = \delta_d^2 + \delta_p^2 + \delta_h^2 \tag{2.4}$$

The solubility parameter for a solvent but not for coal can be determined from the molar heat of vaporization H_v. The solubility parameter can also be written as:

$$\delta^2 = C.E.D.= \frac{(H_v - RT)\rho}{M} \tag{2.5}$$

where R is the universal gas constant, T is the absolute temperature, M is the molecular weight and ρ is the density. The heat of vaporization can be determined calorimetrically or can be calculated either from the vaporization of vapor pressure with temperature or from the boiling point (Hildebrand and Scott, 1962).

The solubility parameter of nonvolatile polymers including coal can not be determined directly, because some of the endothermic heat of mixing and the endothermic heat of crystal melting are much larger than the entropy of mixing. Some investigators have determined solubility parameters for some nonvolatiles and crystalline solids empirically. For this method the δ of the polymer is said to be equal to the δ of the solvent in which the polymer dissolves without showing heat of mixing. In practice, the solubility parameter for coals can be estimated using a series of solvents of various δ values. The δ at the maximum swelling is assigned to the coal (Hansen, 1967).

Two materials are miscible when the free energy of mixing, ΔG_m, is zero or negative. This quantity can be calculated from the heat of mixing, ΔH_m, the entropy of mixing, ΔS_m, and the absolute temperature, T, using the equation:

$$\Delta G_m = \Delta H_m - T\Delta S_m \tag{2.6}$$

The heat of mixing of a solvent and polymer, coded with subscripts 2 and 1, respectively, can be

calculated from the difference of δ_1 and δ_2 values by the Hildebrand-Scatchard formula (Hildebrand and Scott, 1962):

$$\Delta H_m = V_1(\delta_1 - \delta_2)^2 V_2^2 \tag{2.7}$$

here V_1 is the molar volume of the solvent and V_2 is the volume fraction of the polymer. ΔH_m is either positive or zero; therefore the dissolution process is either endothermic or athermal. Since the entropy change is always positive, the $-T\Delta S_m$ term in equation (2.6) always promotes mixing. Its absolute value must exceed the value of ΔH_m for dissolution to take place; only under this conditions is ΔG_m negative. If all this assumptions hold, a solvent is "best" if it gives zero heat of mixing, i.e., if its δ value matches that of the solute (Hildebrand and Scott, 1962).

2.3 Mathematical Description of the Method

Two limiting mechanisms of penetrant transport may be observed in glassy macromolecular systems: Fickian diffusion and Case-II transport as defined by Alfrey et al. (1966). Fickian diffusion is described by a diffusion coefficient while Case-II transport is described by a characteristic relaxation constant. Non-Fickian behavior or anomalous transport falls between these two limiting cases and requires two or more parameters to describe the coupling of diffusional and relaxational phenomena.

2.3.1 Fickian Diffusion in a Thin Section of Coal

Consider one-dimensional, isothermal penetrant diffusion into a thin coal slab of thickness, l, where the structure is initially maintained at a constant uniform penetrant concentration, C_1, and the surfaces are kept at a constant penetrant concentration, C_o. This situation is referred to as the perfect sink conditions and applies to sorption as well as desorption. Assuming constant penetrant diffusion coefficient, D, with one-dimensional diffusion in the x-direction, Fick's Second Law, the transport

process may be described by:

$$\frac{\partial C}{\partial t} = D \frac{\partial^2 C}{\partial x^2} \tag{2.8}$$

where:

$$t=0, \qquad -\frac{l}{2} < x < \frac{l}{2}, \quad C = C_1$$

$$t>0, \qquad x = \pm \frac{l}{2}, \quad C = C_o$$

The solution to Fick's law (Crank, 1968) in the form of a trigonometric function with the proper boundary and initial conditions is as follows:

$$\frac{M_t}{M_\infty} = 1 - \sum_{n=0}^{n=\infty} \frac{8}{(2n+1)\pi^2} \exp\left[\frac{-D(2n+1)^2\pi^2}{l^2} t\right] \tag{2.9}$$

where M_t is the mass of penetrant uptake at time t, and M_∞ is the mass of penetrant uptake as time approaches infinity. An alternative solution to equation (2.9) which is useful for interpretation of short time behavior is given in the form of an error function series:

$$\frac{M_t}{M_\infty} = 4\left[\frac{Dt}{l^2}\right]^{1/2} \left[\frac{1}{\pi^{1/2}} + 2\sum_{n=1}^{n=\infty} (-1)^n \text{ ierfc } \frac{nl}{2(Dt)^{1/2}}\right] \tag{2.10}$$

where ierfc x is the integrated complementary error function of x. For "small" times, i.e. small values of the dimensionless time, defined as $4Dt/l^2$, equation (2.10) can be approximated to:

$$\frac{M_t}{M_\infty} = 4\left[\frac{Dt}{\pi} l^2\right]^{1/2} \tag{2.11}$$

As indicated by equation (2.11), Fickian diffusion is characterized by an initial $t^{1/2}$ - time dependence of the penetrant uptake. Equation (2.11) is valid for the first 60% of the total penetrant uptake ($M_t/M_\infty \leq 0.60$) (See Figure 2.4). A deviation from the straight line in Figure 2.4 occurs when there is an appreciable overlap of fluid diffusing in from one side of the slab with fluid which diffused in through

the other side.

2.3.2 Case-II Transport in a Thin Section of Coal

The analysis here is presented by analogy to the first order relaxation model presented by Enscore et al., (1977) for polymers. Consider a thin coal section of cross-sectional area, A, and thickness, l, undergoing Case-II penetration (see Figure 2.5). In the swollen region defined by $X \leq x \leq l/2$, where X is the position of the advancing front, there is a uniform concentration of penetrant equal to the equilibrium penetrant concentration, C_o. In the glassy region defined by $0 \leq x \leq X$, there is essentially no solvent. The sorption kinetics are assumed to be controlled by a rate-limiting relaxation phenomenon positioned at the advancing front. Defining a Case-II relaxation constant, k_o, and describing the sorption process by a first order kinetic expression, the sorption into a thin section may be given by:

$$\frac{dM_t}{dt} = k_o A \tag{2.12}$$

In the swollen region of volume $V = A(\frac{l}{2} - X)$, the mass balance at any time, t, is given by

$$M_t = C_o A \left[\frac{l}{2} - X \right] \tag{2.13}$$

Substituting M_t into the first order kinetic expression and simplifying one gets:

$$\frac{dX}{dt} = - \frac{k_o}{C_o} \tag{2.14}$$

Solving for X and substituting into the mass balance:

$$M_t = \left[\frac{4k_o A}{l} \right] \tag{2.15}$$

which may also be written in the form:

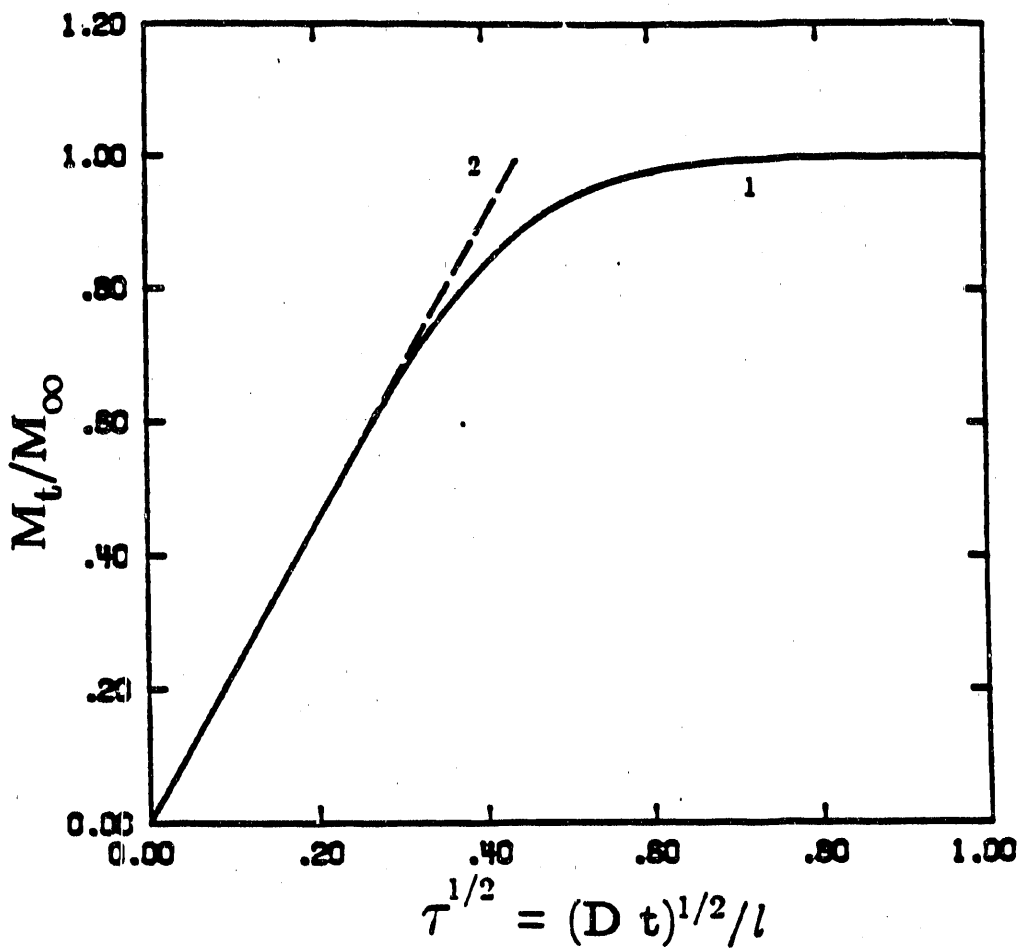

Figure 2.4 Normalized penetrant uptake, M_t/M_∞, versus square root of dimensionless time, $\tau^{1/2}$, for Fickian diffusion in a plane sheet. Comparison of the solutions to equation (2.8) given by: (1) equation (2.9); and (2) equation (2.11).

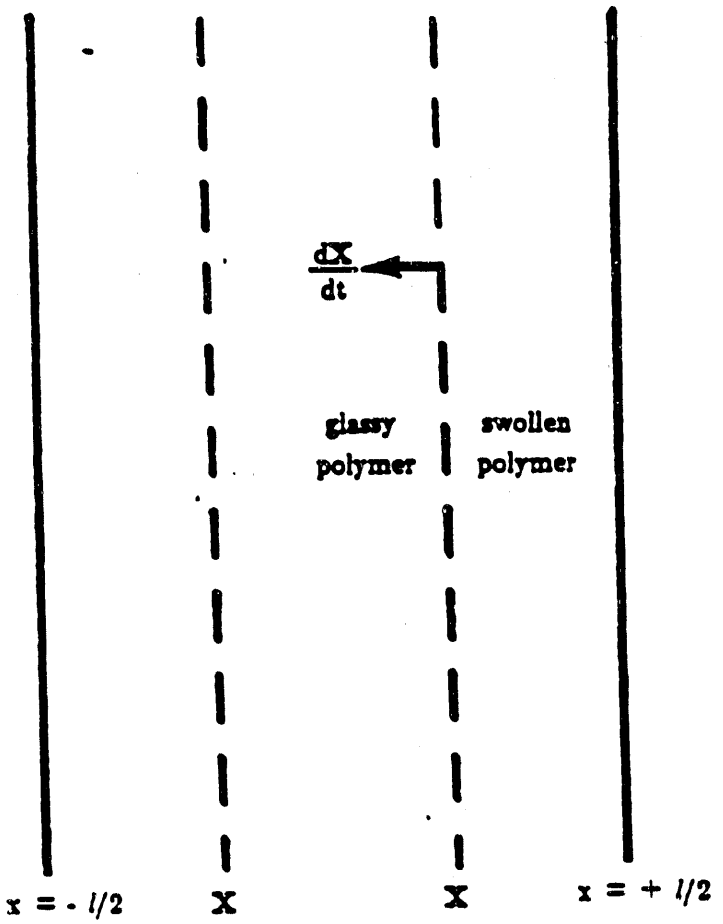

Figure 2.5 Thin coal section of cross-sectional area A and Thickness *l* under-going Case-II penetration.

$$M_t = \left[2C_o\frac{A}{l}\right]\left[2\frac{k_o}{C_o l}t\right] \tag{2.16}$$

The term $2C_oA/l$ is the uptake at long times M_∞, therefore for short times equation (2.16) becomes:

$$\frac{M_t}{M_\infty} = \frac{2k_o t}{C_o l} \tag{2.17}$$

Obviously equation (2.17) shows that Case-II transport is characterized by a t-time dependence of the penetrant uptake.

2.3.3 Semi-Empirical Equations for the Analysis of Penetrant Transport into Thin Sections of Coal

Most transport processes in glassy polymers can be represented by a coupling of the Fickian diffusion and Case-II transport. Therefore one may combine equations (2.11) and (2.17) in an additive form and write an expression for M_t/M_∞:

$$\frac{M_t}{M_\infty} = k_1 t^{1/2} + k_2 t \tag{2.18}$$

where

$$k_1 = \left[\frac{4D}{\pi l^2}\right]^{1/2} \tag{2.19}$$

and

$$k_2 = \left[\frac{2k_o}{C_o l}\right] \tag{2.20}$$

A generalized expression of the previous equation can be written as:

$$\frac{M_t}{M_\infty} = kt^n \tag{2.21}$$

here k incorporates characteristics of the macromolecular network system and the penetrant, and n is the diffusional exponent, which is indicative of the transport mechanism. For Fickian diffusion in a plane

sheet n=0.5, for Case-II transport in a plane sheet n=1.00, and for anomalous transport 0.5<n<1.0. This short time approximation applies only to the first 60% of the normalized penetrant uptake. This model has been proposed before by Peppas and Lucht (1985), Barr-Howell et al. (1986b), Alfrey et al. (1966), Enscore et al. (1977), Jacques et al. (1974) and Sinclair and Peppas (1984).

2.3.4 Determination of Diffusion and Relaxation Coefficients

The analysis here is taken as an analogy to the mathematical model for diffusion and relaxation in glassy polymer powders by Berens and Hopfenberg (1978). The sorption process in glassy polymer is considered as the linear superposition of phenomenologically independent contribution, from Fickian Diffusion and chain relaxations. Therefore the total amount of sorption per unit weight of coal at time t may be expressed as:

$$M_t = M_{t,F} + M_{t,R} \tag{2.22}$$

here $M_{t,F}$ and $M_{t,R}$ are the contributions of the Fickian and relaxational processes, respectively. $M_{t,F}$ is the solution to Fick's Second Law, and given as:

$$\frac{M_{t,F}}{M_{\infty,F}} = 1 - \sum_{n=0}^{n=\infty} \frac{8}{(2n+1)\pi^2} \exp\left[\frac{-D(2n+1)^2\pi^2}{l^2} t\right] \tag{2.23}$$

where $M_{\infty,F}$ is the equilibrium amount of sorption in the unrelaxed polymer (coal). For a short time approximation one may obtain

$$\frac{M_{t,F}}{M_{\infty,F}} = 4\left[\frac{Dt}{\pi l^2}\right]^{1/2} \tag{2.24}$$

The relaxation process is assumed to be first order in the concentration difference which drives the relaxation. The differential equation for the relaxation process is therefore:

$$\frac{dM_{t,R}}{dt} = k(M_{\infty,R} - M_{t,R}) \tag{2.25}$$

where k is the relaxation-rate constant and $M_{\infty,R}$ is the ultimate amount of sorption due to relaxation.

Integration of equation (2.25) with the initial condition that t=0, $M_{t,R}$=0, leads to:

$$M_{t,R} = M_{\infty,R}\left[1 - \exp(kt)\right] \tag{2.26}$$

Substitution of equations (2.23) and (2.26) into equation (2.22) results in:

$$M_t = M_{\infty,F}\left[1 - \sum_{n=0}^{n=\infty} \frac{8}{(2n+1)\pi^2} \exp\left[\frac{-D(2n+1)^2\pi^2}{l^2} t\right]\right] + M_{\infty,R}\left[1 - \exp(kt)\right] \tag{2.27}$$

which has the constraints:

$$M_{\infty,F} = M_\infty \phi_F \tag{2.28}$$

$$M_{\infty,R} = M_\infty \phi_R \tag{2.29}$$

$$\phi_F + \phi_R = 1 \tag{2.30}$$

where ϕ_F and ϕ_R are the fractional contributions due to Fickian diffusion and relaxation process respectively. Therefore equation (2.28) may be written as:

$$\frac{M_t}{M_\infty} = \phi_F\left[1 - \sum_{n=0}^{n=\infty} \frac{8}{(2n+1)\pi^2} \exp\left[\frac{-D(2n+1)^2\pi^2}{l^2} t\right]\right] + \phi_R\left[1 - \exp(kt)\right] \tag{2.31}$$

and for a short time approximation one may use equation (2.11) to replace the Fickian diffusion term in equation (2.31) to obtain:

$$\frac{M_t}{M_\infty} = \phi_F\, 4\left[\frac{Dt}{\pi l^2}\right]^{1/2} + \phi_R\left[1 - \exp(kt)\right] \tag{2.32}$$

The model embodied in equation (2.32) assumes that the Fickian contribution is driven by a gradient which is related to the invariant equilibrium concentration $M_{\infty,F}$. The relaxation term in equation (2.24) is independent of particle size and is related to the dissipation of swelling stresses induced by entry of the penetrant. This dissipation, or stress relaxation, is initiated by the plasticizing penetration, but is considered here to be otherwise independent of the superimposed diffusive transport.

Equations (2.31) and (2.32) are nonlinear with three unknowns (D, k, and ϕ_F, or ϕ_R) which may be solved using a nonlinear-regression analysis method.

2.4 In Situ Microscopic Studies of Coal

The swelling of coal in solvents is an important means for obtaining information on the physicochemical structure of coal. In situ observations can provide information about the coal-penetrant interaction and furthermore extend the observations into valuable kinetic information.

Brenner (1981) performed in-situ studies on coal and found that when the swelling is allowed to proceed beyond a certain stage, the process becomes substantially irreversible. This irreversibility is attributed to fractures or dislocations within the coal which occur when sufficiently high stresses are generated by uneven swelling of the coal structure. Brenner (1985) observed in-situ at the macroscopic level for the first time the diffusion of pyridine into coal. The studies were conducted on thin films of coal with dimensions of 15 μm thickness and 0.50 mm across. Qualitative work was reported on the elucidation of pyridine diffusion into the thin coal sample. Also included in Brenner's in-situ studies is a graphical interpretation of the position front as a function of time; however the data lack of information. No units of magnitude are reported in his work. Brenner claims that equilibrium is attained after 800 seconds without any further explanation.

2.5 Dynamic Swelling of Stiff Polymer Networks that Simulate the Coal Structure

Since the work of Van Krevelen (1961), polymers have been recognized as appropriate models for aiding in the investigation of the coal network structure. In 1983, Squires et al. synthesized a new class of polymers to aid the investigation of coal. These polymers are poly (1,4-dimethylnaphthalene), poly (1,4-dimethylnaphthaleno-1,2-dioxybenzene), and poly (1,4-dimethylnaphthaleno-2,5-

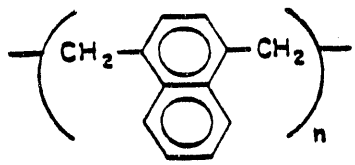

POLYMER I

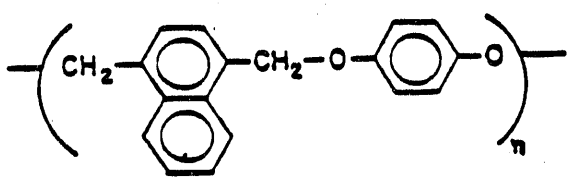

POLYMER II

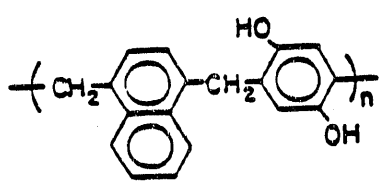

POLYMER III

Figure 2.6 Model polymer structures simulating the coal structures (from Squires et al., 1983).

dihydroxybenzene) (Figure 2.6). The naphthalene nucleus was selected because it represents a reasonable average ring size for a bituminous coal; the ethylene and oxymethylene linkages were selected because they are thought to be the most reactive sites in the coal macromolecular network (Vernon, 1980; Schlosberg et al., 1981). Tne pyridine uptake of poly (1,4-dimethylnaphthaleno-2,5-dihydroxybenzene) appeared most to resemble the pyridine uptake in coal networks (Howell et al., 1986a). The swelling studies on the three polymer models were conducted at low penetrant activities, and compared with swelling studies on coals at high penetrant activities. Obviously low penetrant activity studies on coal need to be done to use these polymer models as a comparison to coal.

2.6. Prediction of Penetrant Transport

Figures 2.7 through 2.10 indicate the predictions of the model presented by equation (2.31) for the case of various coal samples exhibiting different degrees of crosslinking. Thus, these samples have different values of penetrant diffusion coefficients or different values of the relaxation constant k.

For example, Figure 2.7 indicates the uptake of a penetrant in a thin coal section when the relaxation constant is $k = 6 \times 10^{-6}\ s^{-1}$ and for varying diffusion coefficients. The case of 50% Fickian diffusion and 50% non-Fickian diffusion is examined. By reducing the relaxation constant to 50% of the previous, it is seen that the penetrant uptake becomes slower (Figure 2.8). Figure 2.9 shows the same data in real times.

Figure 2.10 indicates the influence of the Fickian diffusion on the overall rate of transport of the penetrant. It can be seen that as the Fickian portion decreases the penetrant uptake becomes slower.

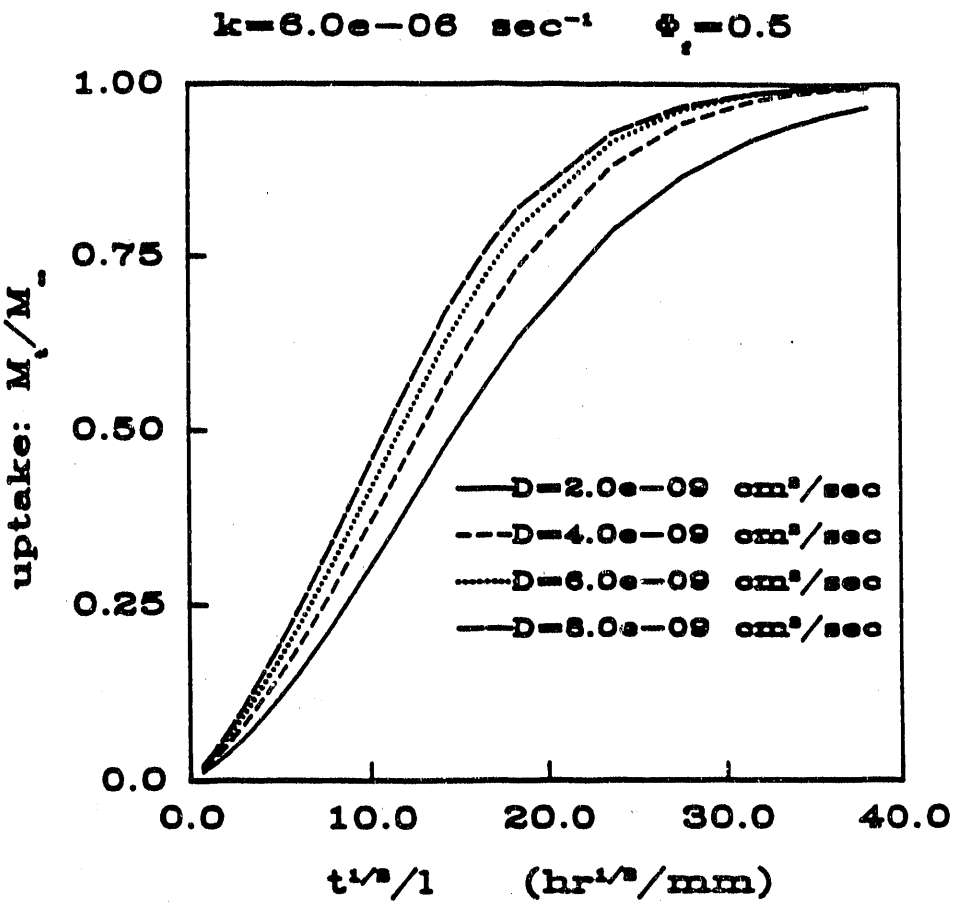

Figure 2.7 Penetrant uptake in coal samples of thickness 1 (mm) as a function of time and diffusion coefficient, for $k = 6 \times 10^{-6}$ sec^{-1} and 50% Fickian diffusion.

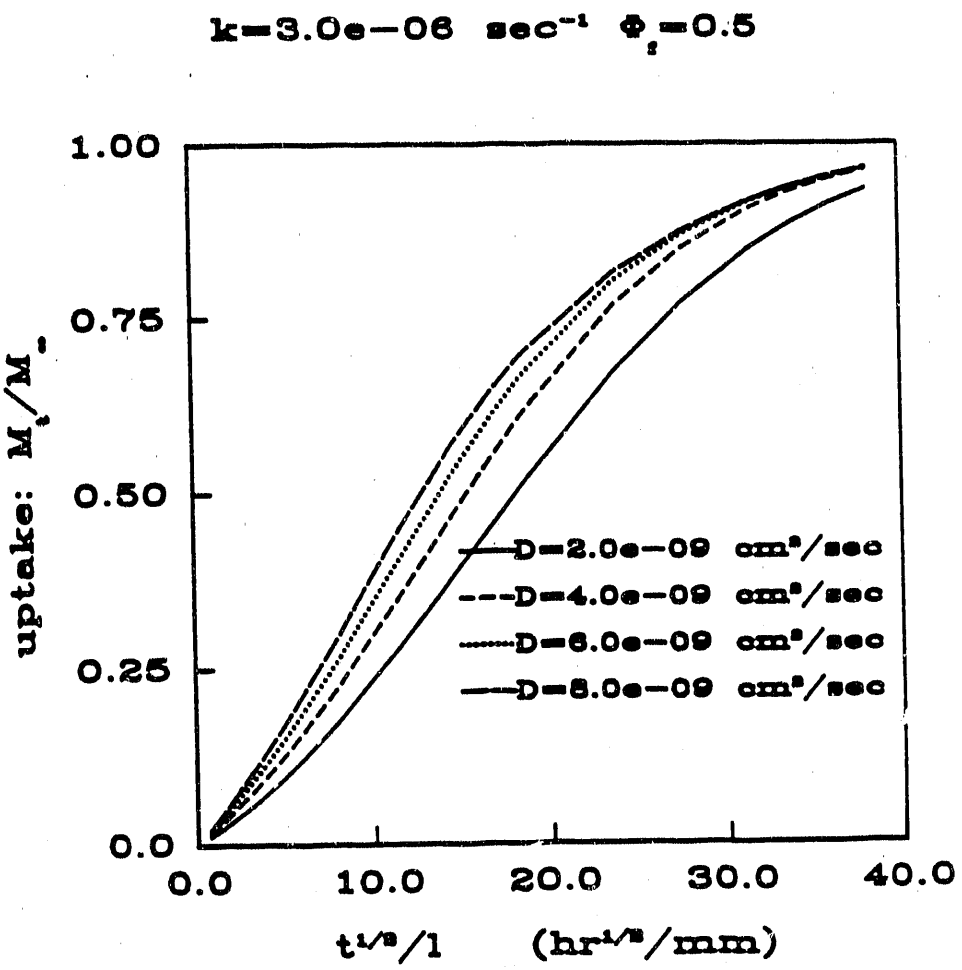

Figure 2.8 Penetrant uptake in coal samples of thickness 1 (mm) as a function of time and diffusion coefficient, for k = 3 x 10^{-6} sec^{-1} and 50% Fickian diffusion.

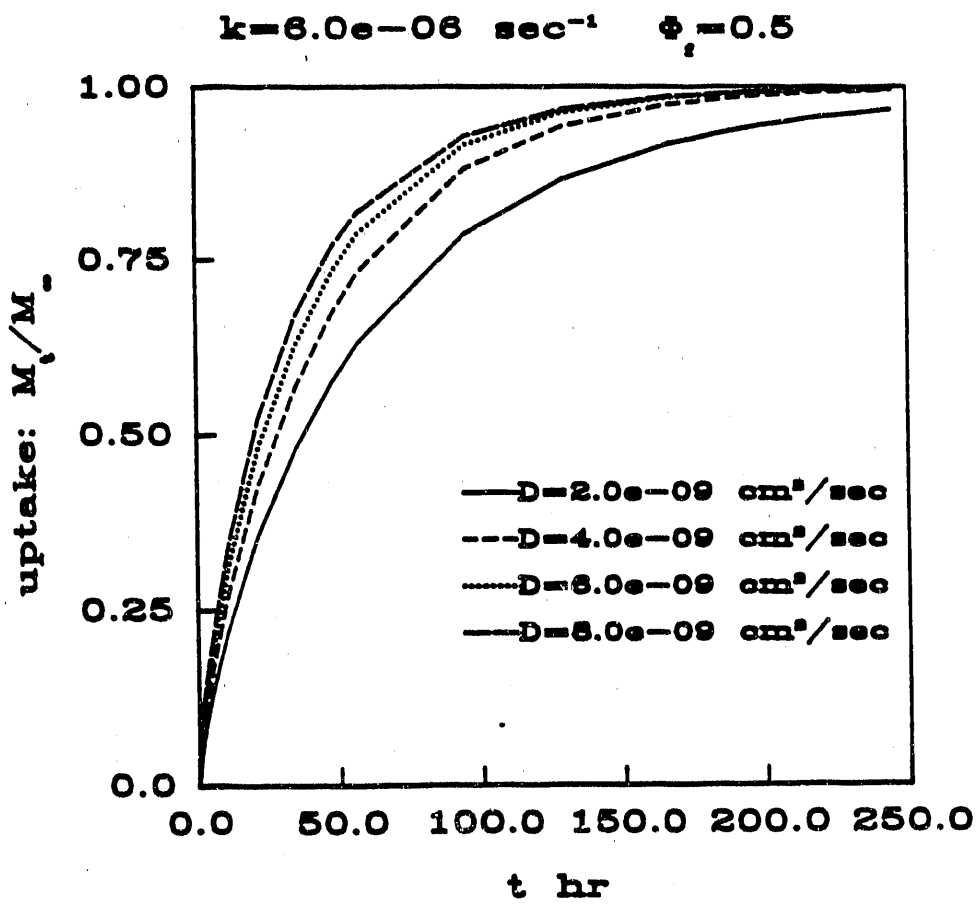

Figure 2.9 Penetrant uptake in coal samples of thickness 1 (mm) as a function of time and diffusion coefficient, for $k = 6 \times 10^{-6}$ sec^{-1} and 50% Fickian diffusion.

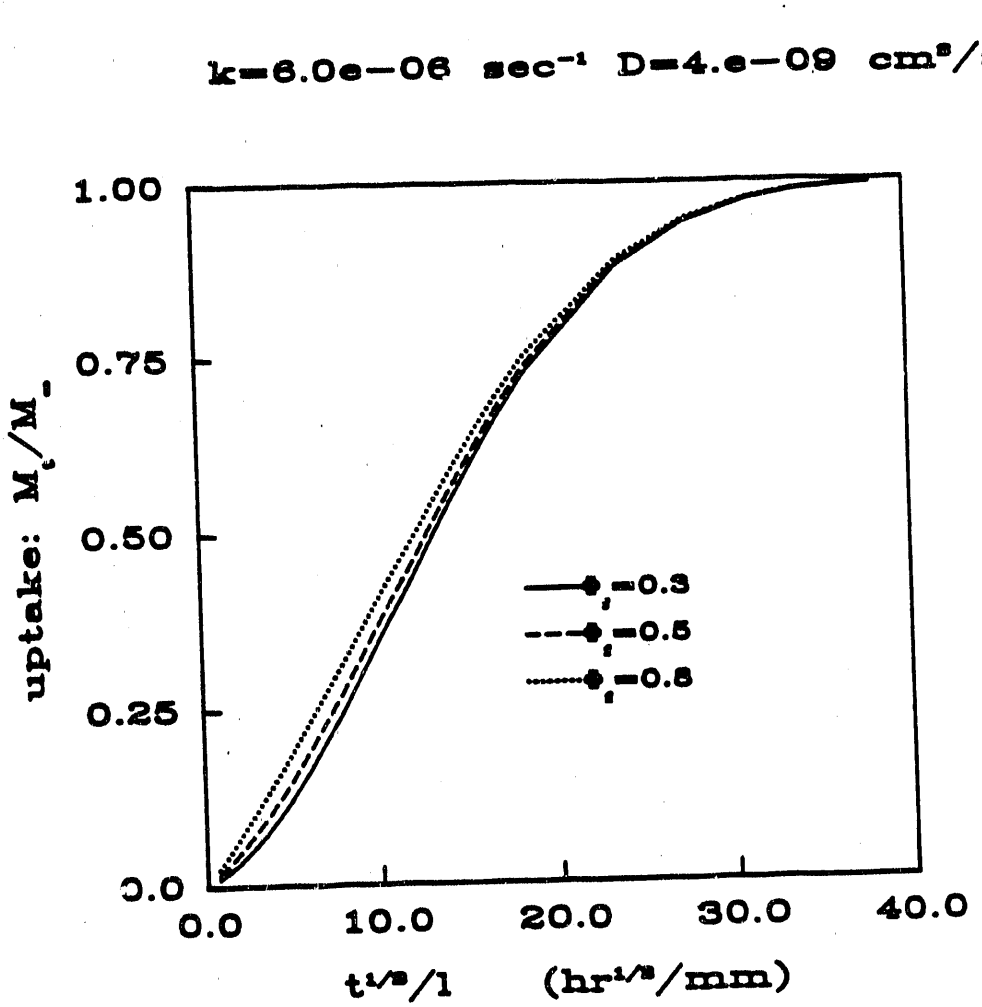

Figure 2.10 Penetrant uptake in coal samples of thickness 1 (mm) as a function of the Fickian diffusion portion (0.3, 0.5 or 0.8) for $k = 6 \times 10^{-6}$ sec^{-1} and $D = 4 \times 10^{-9}$ cm^2/s.

3. EXPERIMENTAL DESIGN OF POLARISCOPE

3.1. Interferometry and Polariscopy

The penetrant concentration and normal stress profile histories can be measured simultaneously with changes in the sample dimensions by the novel, interferometric-photoelastic technique proposed here. Since both techniques involve imaging the sample, the coal and swelling interface positions can also be recorded as a function of time. Although the measurements are made simultaneously, each is independent of the others. The penetrant concentration profile is measured via interferometry as the normal stress profile is measured via photoelasticity.

A plan of the experimental apparatus is shown in Figure 3.1. The swelling sample is constrained on all but two opposing faces by rigid optical flats and one birefringent flat. Thus solvent exposure to the coal and swelling strain is permitted only along one axis. Viewing is normal to the penetration axis, perpendicular to the side faces shown. Brief descriptions of both measurements ensue.

A modification of the classical Mach-Zender interferometer is utilized to measure the penetrant concentration profile. The interference pattern seen at the camera is the result of spatial variations of penetrant concentration. When the interferometer is aligned initially for the infinite fringe, the increment in penetrant concentration between fringes is given below.

$$\Delta\rho_2 = \frac{\lambda_o \, \Delta m}{L \, dn_s/d\rho_2} \tag{3.1}$$

when Δm is the local fringe displacement and $dn_s/d\rho_2$ expresses the change in mixture refractive index with composition. Thus, the concentration profile is determined by counting fringe displacements in an interferogram with a knowledge how n_s changes with composition. Although stresses in the swelling coal induce birefringence, this change in coal optical density on linearly polarized light is very small

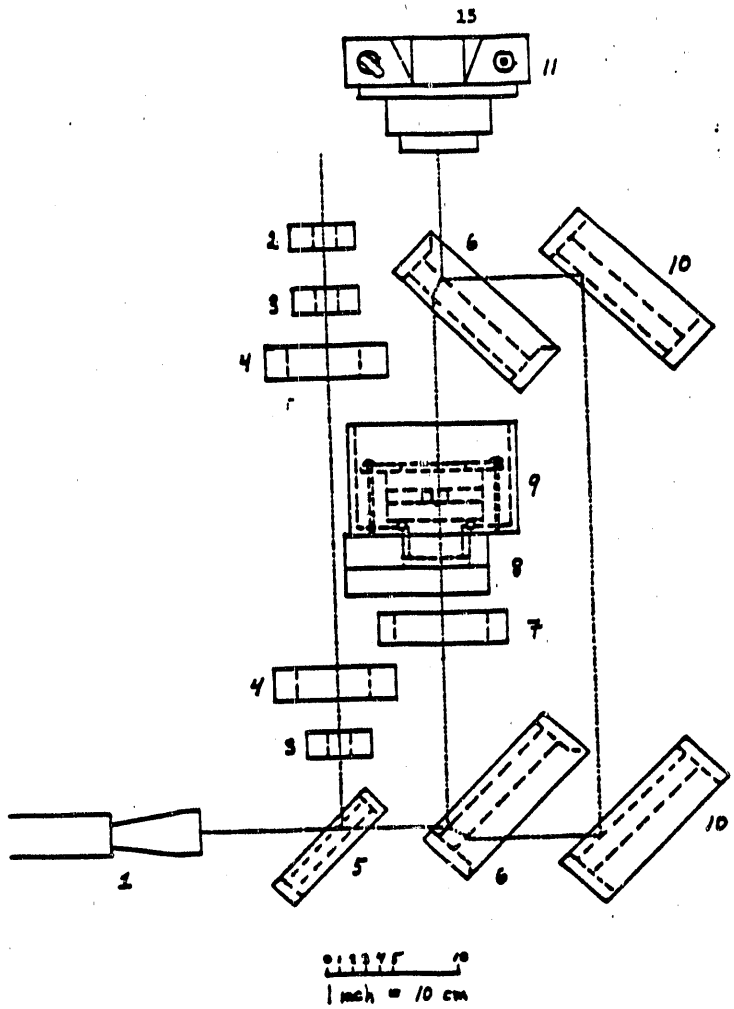

Figure 3.1 Interferometer constructed for the transport studies (for explanation of symbols, see next page).

Figure 3.1 Explanation of Symbols

1. Laser & Beam Expander Unit
2. Polarizer
3. $\lambda/4$ Retarder
4. Partial Mirror
5. Removable Mirror
6. Beamsplitter
7. Optical Flat
8. Object mount
9. Temperature-regulated object stage
10. Mirror
11. Camera

with respect to the effect of change in composition, especially since polarizers will not be used in the interferometer beams.

The local normal stress at the coal surface is a quantity which can be computed from the aforementioned predictive model. This profile must be equal to the vertical component of stress profile in the birefringent flat at the interface. Since the birefringent flat does not swell, its optical response can be easily measured and the stress profile at the interface computed. Thus, the birefringent flat acts as a pressure transducer.

The measurement of normal stresses requires two fringe patterns recorded using the micropolariscope. The first polarigram is taken with the apparatus configured as shown in Figure 3.1. The second polarigram is recorded after the sample is rotated about an oblique angle, θ, in the plane of the figure. The principal stresses can then be computed using equations (3.2) and (3.3).

$$\sigma = \frac{\lambda_o \cos\theta}{LC \sin^2\theta} [N_\theta - N_o \cos\theta] \tag{3.2}$$

$$\sigma_2 = \frac{\lambda_o}{LC} \csc^2\theta [N_\theta \cos\theta - N_o] \tag{3.3}$$

Here N_o and N_θ are the local fringe orders associated with the normal and oblique incidence fringe patterns, respectively. Aside from an accurate optical arrangement, this technique requires only a calibrated value of the relative stress-optical coefficient, C, for the birefringent flat. This value can be easily calibrated by measuring the birefringence of the flat as a function of known loading.

3.2. Stress Analysis

Using the polariscope-interferometer we analyzed some of the coal samples tested. Figures 3.2 and 3.3 show the stress pattern of two thin sections of PSOC 418 and 384, respectively, upon exposure

to pyridine for 24 hours. It can be seen that the pyridine transport led to significant molecular relaxations and stresses in the coal samples. These stresses are shown as anisotropic birefringence pattern.

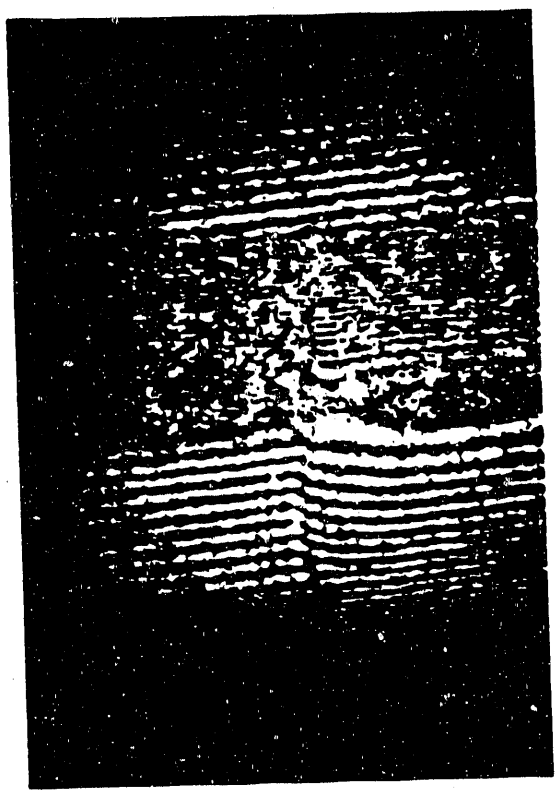

Figure 3.2 Interferometric patterns of stress in a thin coal section of PSOC-418 after exposure to pyridine for 24 hours at 35°C.

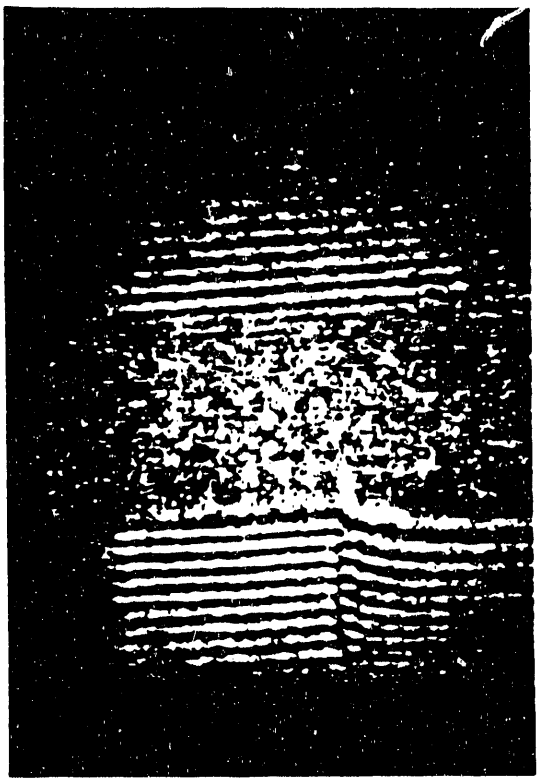

Figure 3.3 Interferometric patterns of stress in a thin coal section of PSOC-384 after exposure to pyridine for 24 hours at 35°C.

4. EXPERIMENTAL PART

4.1 Preparation of Thin Coal Sections

Coal samples, average size of 10 mm and packed under nitrogen, were supplied by the Pennsylvania State University Coal Bank (PSU). The identification numbers used throughout are those assigned by PSU. Table 4.1 includes pertinent information provided by PSU for the coals used in this investigation.

The techniques presented here for preparing uncontaminated thin section specimens of coal are based on the method of preparation employed by Brenner (1982). Epoxy resins which are normally used as embedding compounds in the preparation of geographic thin sections are not easily or even completely removed from the sample after preparation. Such contamination would drastically alter the penetrant transport behavior in the coal network. Uncontamined coal samples were prepared using a parraffin-based adhesive which could be completely removed from the sample.

A chunk of PSOC coal was ground flat in a direction parallel to the geographic bedding plane on a horizontal diamond grinding wheel using progressively finer diamond grits. The flat surface of the coal was then heat-cemented to a preconditioned microscope slide. Preparation of the microscope slide consisted of rough grinding to a uniform thickness to provide a textured surface for enhanced adhesion. The adhesive used was a hexane-soluble, paraffin-based, thermoplastic compound (Paraplast, American Scientific Products, St. Louis, MO). When the adhesive had hardened, the coal chunk was cut with a diamond saw leaving approximately a 2 mm thick slab of coal mounted on the glass slide. The slab was then ground using a vertical diamond grinding wheel to the desired final thickness.

The thin section specimens of coal were removed from the glass slide by soaking in n-hexane for several hours. Hexane does not swell the coal sample. The original solvent was decanted off and a large

Table 4.1 Analysis of PSU Coal Samples*.

PSOC Code No.	County, State	Rank**	%C (dmmf)	%H (dmmf)	%MM (dry)
418	Titus,TX	LigA	69.94	6.18	27.50
791	Titus,TX	LigA	72.25	5.39	20.77
247	Burke,ND	LigA	75.53	4.84	12.77
312	Navajo,AR	HVC	78.38	5.72	7.51
853	Delta,CO	HVC	80.12	5.08	3.74
402	Craig,OK	HVA	82.40	5.64	18.46
341	Jefferson,PA	HVA	86.01	5.79	14.53
384	Sullivan,PA	SAn	94.17	3.58	24.11

* Elemental analysis performed by Pennsylvania State University

** LigA = Lignite A; HVC = high volatile C bituminous;
HVA = high volatile A bituminous; SAn = semi-anthracite.

excess of additional solvent was added to insure removal of any residual adhesive from the coal sections. After a few days of immersion, the solvent was removed and the samples were oven-dried at 60°C. The samples were stored in a dry nitrogen atmosphere at room temperature until use. The uncontamined samples obtained ranged in thickness from 200 μm to 500 μm and were used for swelling studies using a thermogravimetric analyzer. Also samples ranging in thickness from 7 μm to 15 μm were obtained in a similar way and used for in-situ studies using a polarized microcope.

4.2 Dynamic Penetrant Transport Studies

Two different dynamic swelling studies were performed to elucidate the phenomenological and mechanistic analyses of swelling. The first method is the dynamic swelling desiccator studies which consist of high penetrant activity vapor swelling studies. The second method is the thermogravimetric analyzer studies which consists of low penetrant activity vapor swelling studies.

4.2.1 Dynamic Swelling Desiccator Studies

Thin coal sections, 200 μm to 500 μm thick, of 2 mg to 100 mg were dried and weighed to ± 0.05 mg on a Sartorius electronic analytical balance. The samples were then suspended in a 15 x 45 mm vials which were placed in a dessicator over a pool of solvent. The solvents used in the studies were methylene chloride, pyridine, methyl ethyl ketone, toluene, benzene, methanol, acetone, cyclohexane, and tetrahydrofuran. The desiccator was sealed and placed in a water bath to maintain a constant temperature of 35 ± 0.5°C. At set time intervals, the coal samples were removed, weighed and then returned to the dessicator.

4.2.2 Thermogravimetric Analyzer Studies

Swelling studies were carried out using a thermogravimetric analyzer (model TGA2, Perkin Elmer, Norwalk, Conn.). The instrument consists of a microbalance which operates on an optics system and a temperature controlled microfurnace. The TGA measures the weight loss or weight gain of a sample as it is subjected to a precisely controlled temperature environment.

Approximately 5 mg of a thin film of coal was placed in a platinum pan which was suspended from the lever arm balance. For thermally treated samples, coal films were heated at the desired temperature. A weight loss was observed due to water and low volatiles contained within the coal network. The samples were heated until a weight loss equilibrium was obtained, then cooled at a rate of 5°C/min to room temperature. The swelling process followed immediately by introducing an equilibrated mixture flow of nitrogen and solvent. Nitrogen (99.99% pure) at a constant flow rate of 95 ± 2 cc/min was purged through the solvent contained in the three gas washing bottles (Figure 4.1), and carried over the microfurnace which contained the coal sample. The penetrant weight uptake as a function of time was obtained from a chart recorder which was connected to the TGA. The solvents used for these studies are pyridine, N,N-dimethylformamide, chloroform.

4.2.3 Determination of Penetrant Activity

Penetrant activity is defined as P^{par}/P_o (Hopfenberg et al., 1969), where P^{par} is the penetrant partial pressure and P_o is the penetrant vapor pressure. The penetrant partial pressure is defined as the penetrant mole fraction, x_p, in the nitrogen/solvent mixture times the total pressure, P. To determine the penetrant mole fraction, the output flow from the thermogravimetric analyzer was analyzed using a gas-chromatograph (Varian Aerograph Series 1400, Walnut Creek, CA) equipped with a thermal conductivity detector and an 1/8 in. packed column (SE-30 nonpolar). The penetrant activity for

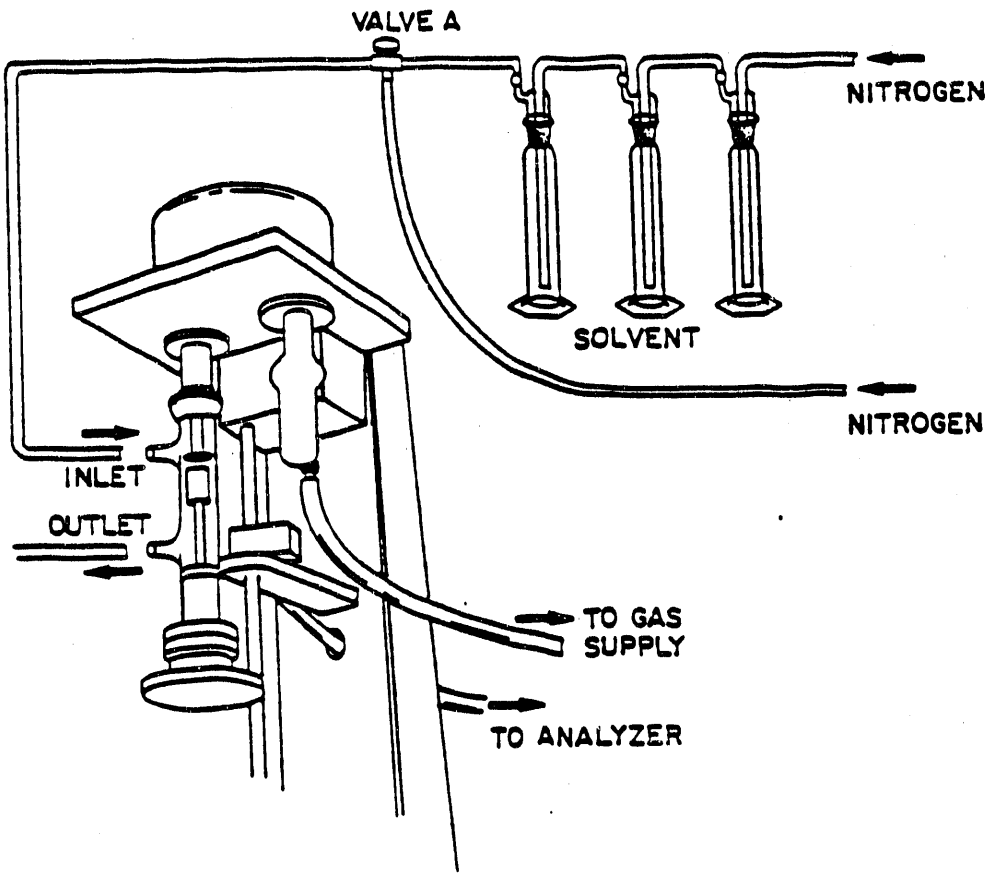

Figure 4.1 Thermogravimetric Analyzer.

chloroform at room temperature was calculated to be 0.04 and that of pyridine and N,N-dimethylformamide to be less than 0.04.

4.3 In-Situ Microscopy Studies

Thin coal samples of thickness ranging from 7 μm to 15 μm were obtained based on the method of preparation employed by Brenner (1982). Quantitative and qualitative work on coal was obtained using a polarized microscope (Microstar Series 110, Scientific Instruments, Buffalo, NY). The polarized microscope was connected to a video camera which sent the signal to a videocassette recorder and a monitor. Proper use of formulae given by the manufacturers were used to determine the magnification magnitude of the observed picture on the monitor screen. A hot plate source which fits in the polarized microscope was used to conduct diffusion studies at 40°C, 70°C, and 100°C.

Direct exposure of the coal film to a solvent, results on immediate cracking of the coal due to strong stresses from the concentration gradient of the solvent. Therefore it is desirable to prevent the solvent from penetrating through the top or bottom of the thin section and to allow it to penetrate only from one edge.

A grease-immersion technique was used to elucidate the diffusion of a penetrant into a semi-infinite coal medium (Figure 4.2). A thin film of coal was immersed in silicone grease (high vacuum grease, Dow Corning, Midland, MI), and both coal and grease were sandwiched between a 1 mm thick glass slide on the bottom and a glass coverslip on top. Careful practice was used to place the exposed edge of coal at the same level as the coverslip to prevent any fast diffusion of penetrant. For the high temperature in-situ studies the 1 mm thick glass slide containing the coal sample was placed on top of the heating plate source. The sample was allowed to equilibrate at the desired temperature. The diffusion process followed immediately by introducing the solvent into the glass slide container.

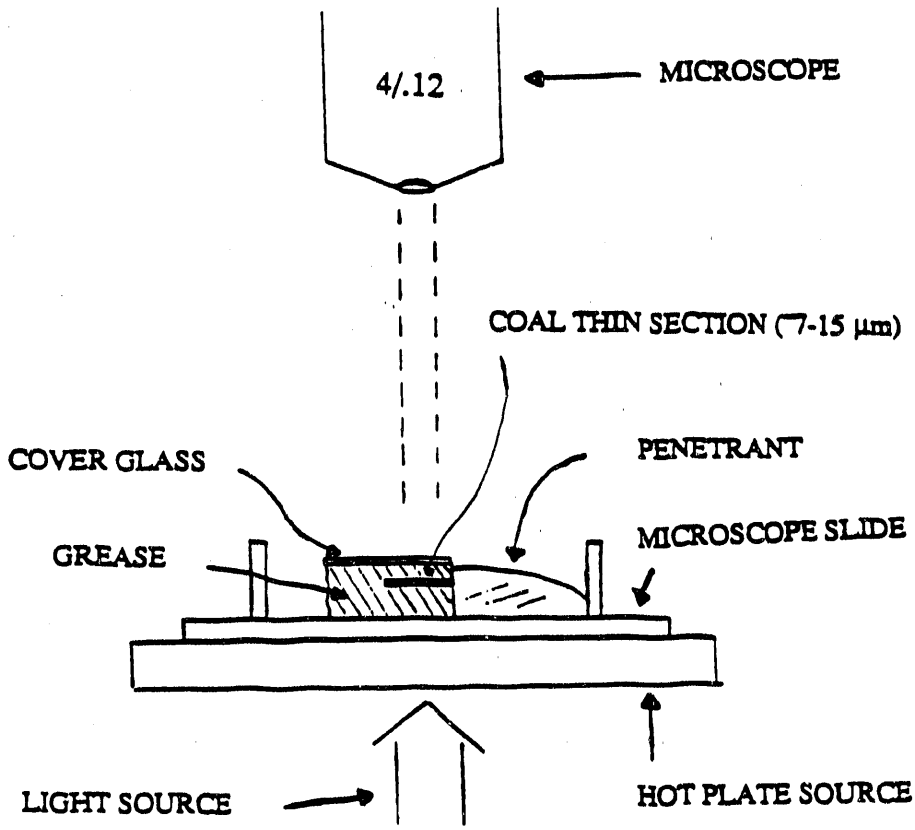

Figure 4.2 Grease-immersion technique.

Many observations were recorded, and some showed characteristics of a sharp advancing front which divided the glassy region from the swollen region. The distance separating the advancing penetrant front from a fixed point in space was recorded as a function of time. The diffusion process was conducted until an equilibrium was reached.

5. RESULTS AND DISCUSSION

In this chapter the results of equilibrium and dynamic swelling studies of coal as well as in-situ diffusion studies are described. Both phenomenological and mechanistic analyses of the dynamic swelling behavior and the in-situ process are considered. The chapter is divided into three sections, the first of which contains the equilibrium swelling studies of coal with high penetrant activity solvents. Equilibrium is analyzed as a function of penetrant type, carbon content of coal, and solubility parameter, δ. Also, the swelling behavior of coal with different carbon contents is compared to the swelling behavior of poly(methyl methacrylate) (PMMA) crosslinked with different amounts of ethylene glycol dimethacrylate (EGDMA). Section 5.2 contains dynamic swelling studies for different penetrants as a function of temperature treatment and carbon content, and Section 5.3 summarizes the in-situ diffusion studies for different temperatures, carbon contents and different penetrant type.

5.1 Equilibrium Swelling Studies of Coal

Equilibrium swelling studies with high activity penetrants were performed in thin sections of coal (200 μm to 500 μm) to study the effect of penetrant type, carbon content, and polar, dispersive and hydrogen-bond contributions. These results are presented in Figures 5.1 through 5.16. The experiments were conducted in desiccators at 35°C.

5.1.1 Penetrant Uptake in Coal Samples as a Function of Penetrant Type and Carbon Content

The swelling behavior of coals PSOC 418, 853 and 384 in acetone, cyclohexane, methanol, methyl ethyl ketone (MEK), toluene, and methylene chloride at 35°C are presented in Figures 5.1, 5.2 and 5.3, respectively. In all cases, the amount of penetrant per initial dry weight of coal, M_t/M_c, is reported as a function of time. In fact, to account for minor changes in coal samples thickness, l, the data

are plotted versus t/l^2, a normalized time expressed in h/cm^2. It can be seen in Figure 5.1 that methylene chloride is the penetrant that exhibits the largest coal swelling followed by acetone, and toluene. When exposed to a high penetrant activity solvent, the thin coal sections swell immediately (within 1.0 hr). However, a good deal of information can be obtained from these studies such as classification of penetrants in terms of their solubility parameters. An explanation for the high swelling of coal PSOC-418 with methylene chloride may be that the methylene chloride solubility parameter matches that of the coal sample PSOC-418. As discussed before, the free energy of mixing is minimum when the solubility parameters of coal and penetrant are equal.

The swelling of coals PSOC 853 and 384 with acetone, cyclohexane, methanol, MEK, toluene and methylene chloride are depicted in Figures 5.2 and 5.3, respectively. In these cases, methylene chloride exhibits the largest swelling followed by MEK and toluene. Therefore, methylene chloride shows the highest swelling regardless of the coal used.

Increasing the carbon content of coals does not necessarily increase the crosslinking amount. It was mentioned that the average molecular weight between crosslinks does not increase linearly with carbon content, but exhibits a maximum for coals with carbon contents between 75-80% C. This effect is depicted in Figure 5.4 for coal swelling with methylene chloride. In this case, methylene chloride was selected as the penetrant due to its good compatibility with PSOC coals. The highest swelling is exhibited by PSOC-247 followed by PSOC 418, 853, 341, 384 and 312. With the exception of PSOC-312 the equilibriurn uptake for the five coals follows the same pattern as the average molecular weight between crosslinks follows when plotted as a function of carbon content (Figure 5.42). This indicates that the equilibrium penetrant uptake increases as the average molecular weight between crosslinks increases.

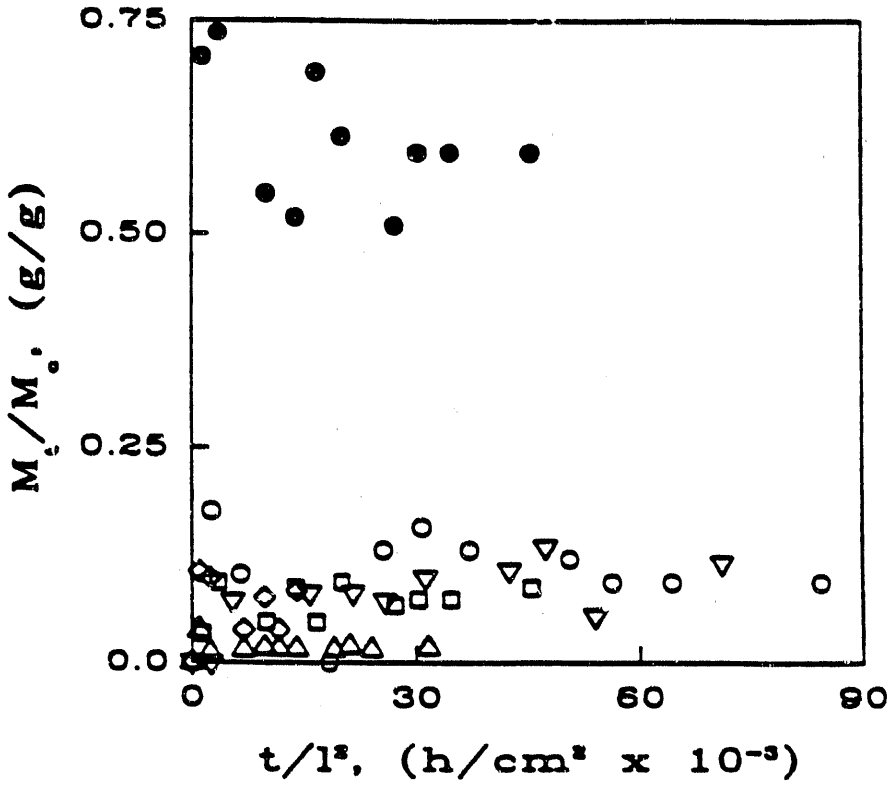

Figure 5.1 Penetrant uptake (in g penetrant/g dry coal) in thin coal sections of PSOC-418 at 35°C as a function of normalized timet/l^2 (h/cm^2). Acetone (○), cyclohexane (□),methanol (◇), MEK (△), toluene (▽), methylene chloride (◐).

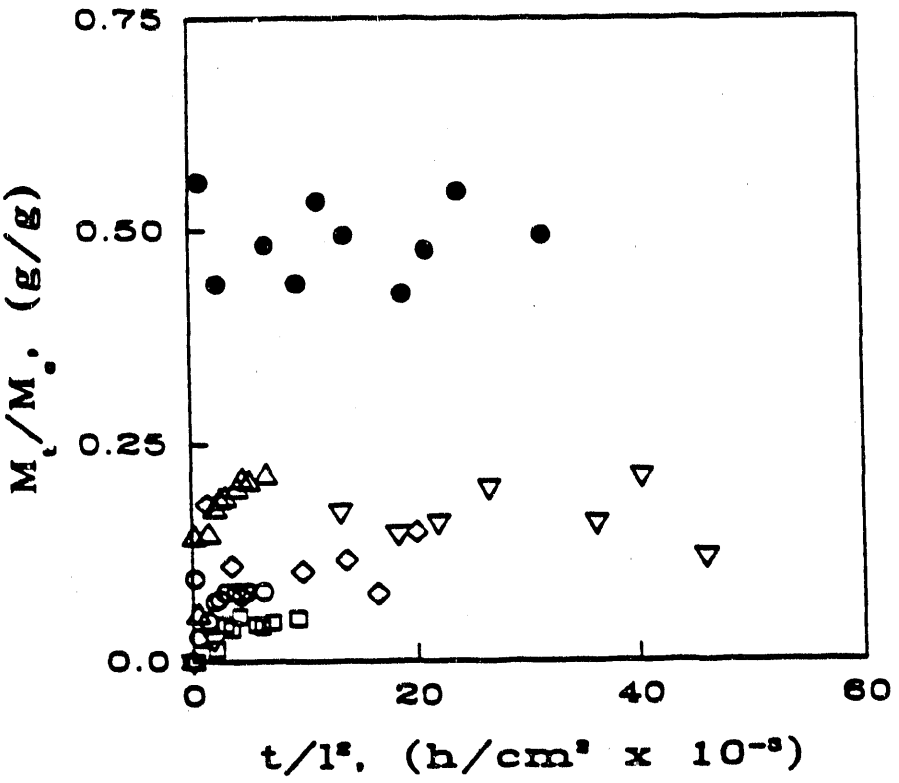

Figure 5.2 Penetrant uptake (in g penetrant/g dry coal) in thin coal sections of PSOC-853 at 35°C as a function of normalized timet/l^2 (h/cm^2). Acetone (○), cyclohexane (□),methanol (◇), MEK (△), toluene (▽), methylene chloride (●).

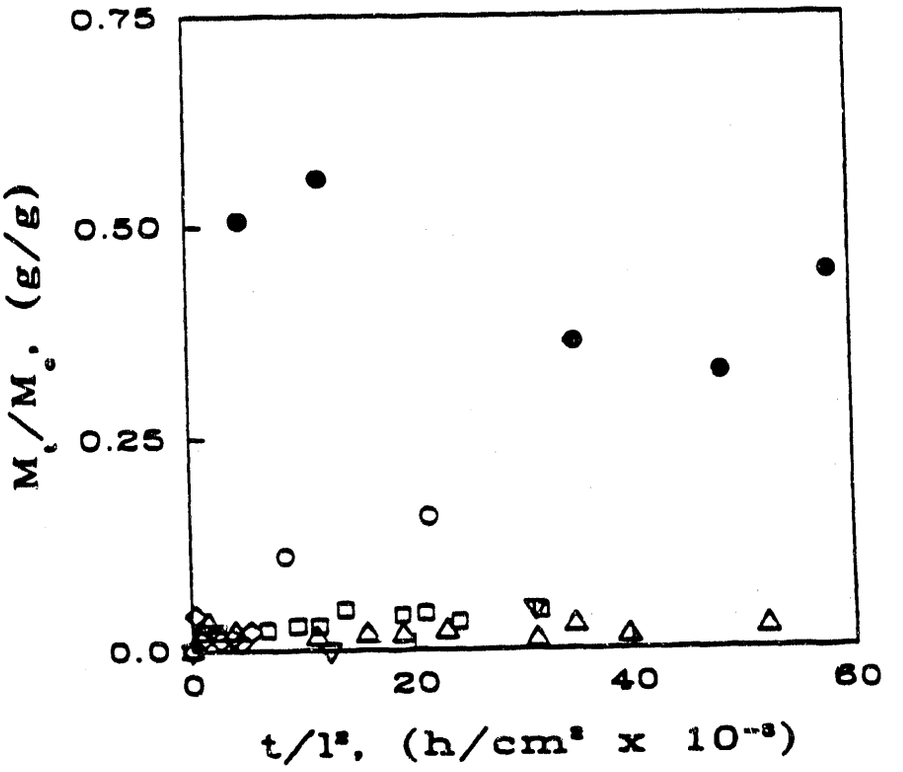

Figure 5.3 Penetrant uptake (in g penetrant/g drycoal) in thin coal sections of PSOC-384 at 35°C as a function of normalized time t/l^2 (h/cm^2). Acetone (○), cyclohexane (□),methanol (◇), MEK (△), toluene (▽), methylene chloride (●).

5.1.2 Penetrant Uptake in Coal Samples as a Function of Solubility Parameters

The solubility parameter of coal can be estimated from swelling studies using penetrants of different solubility parameters. The free energy of mixing is minimized when the solubility parameters of the solvent and the solute are comparable. Therefore, the solubility parameter for coal is equivalent to the solubility parameter of the penetrant exhibiting the highest swelling to coal. Equilibrium swelling studies of coal with various penetrants (see Table 5.1 for description) were conducted to elucidate the compatibility of coal and the penetrant. Figure 5.5 depicts the equilibrium penetrant uptake in thin coal sections of PSOC-418 as a function of the penetrant solubility parameter, δ_1. It can be seen that the maximum equilibrium penetrant uptake occurs at a solubility parameter of about 9.5 $cal^{1/2}/cm^{3/2}$.

Figure 5.6 depicts the equilibrium penetrant uptake in thin coal sections of PSOC-853 as a function of the penetrant solubility parameter. It can be seen again that the maximum penetrant uptake occurs at a δ_1 equal to 9.5 $cal^{1/2}/cm^{3/2}$. The same observation is made in Figure 5.7 for the swelling of coal PSOC-384. Based on these results an estimated solubility parameter, δ_2, for coal is equal to 9.5 $cal^{1/2}/cm^{3/2}$.

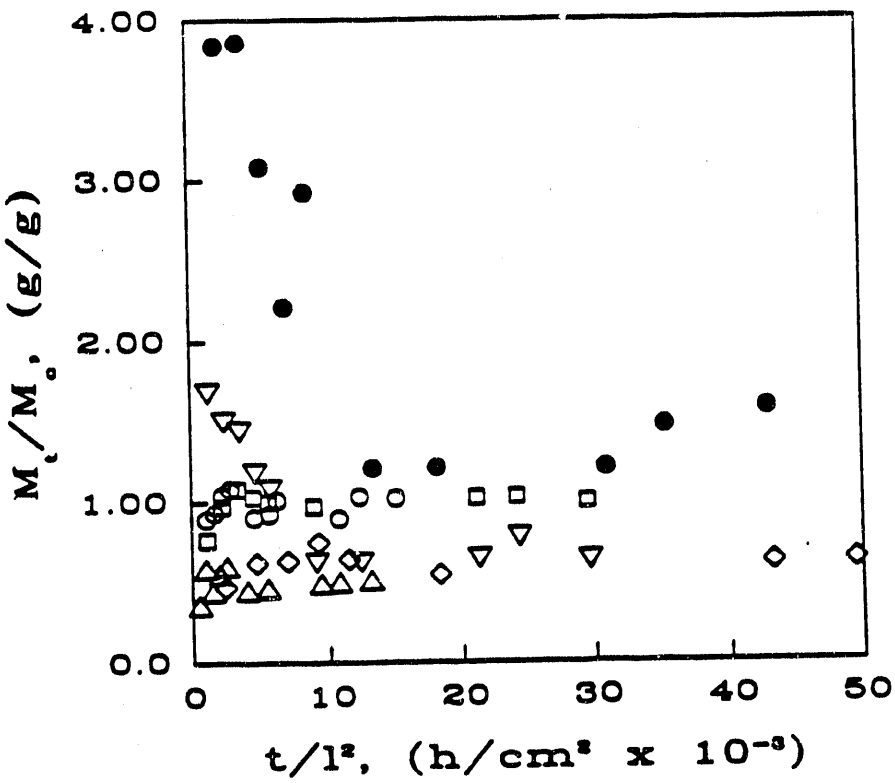

Figure 5.4 Methylene chloride uptake (in g penetrant/g drycoal) in thin coal sections at 35°C as a function of normalized time t/l^2 (h/cm^2). PSOC-418 (○), PSOC-853 (□), PSOC-384 (◇), PSOC-312 (△), PSOC-341 (▽), PSOC-247 (●).

Table 5.1 Solubility Parameters (in $cal^{1/2}/cm^{3/2}$) *

Solvent	δ_t	δ_d	δ_p	δ_h
Methylene Chloride	9.93	8.91	3.1	3.0
Chloroform	9.21	8.65	1.5	2.8
Pyridine	10.61	9.25	4.3	2.9
Methyl ethyl ketone	9.27	7.77	4.4	2.5
Toluene	8.91	8.82	0.7	1.0
Benzene	9.15	8.95	0.5	1.0
Methanol	14.28	7.42	6.0	10.9
Acetone	9.77	7.58	5.1	3.4
Cyclohexane	8.18	8.18	0.0	0.0
Tetrahydrofuran	9.1	-	-	-
N,N-Dimethylformamide	12.1	-	-	-

* Adopted from Gardon and Teas (1976).

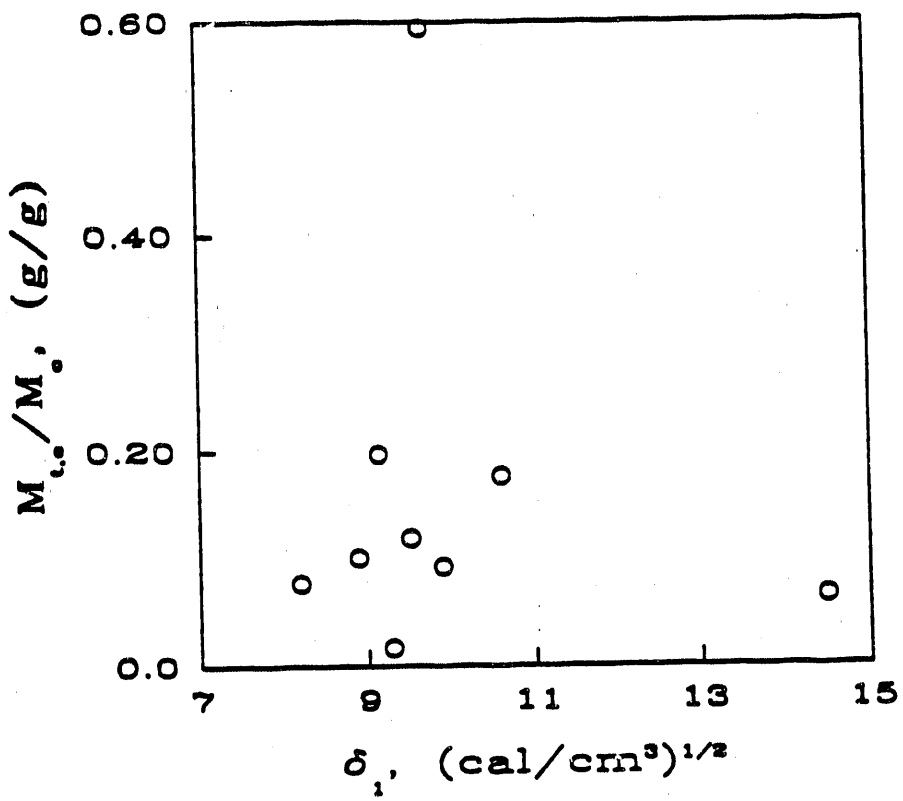

Figure 5.5 The equilibrium penetrant uptake in (g penetrant/g dry coal) in thin coal sections of PSOC-418 at 35°C as a function of the penetrant solubility parameter, δ_1, (in $cal^{1/2}/cm^{3/2}$).

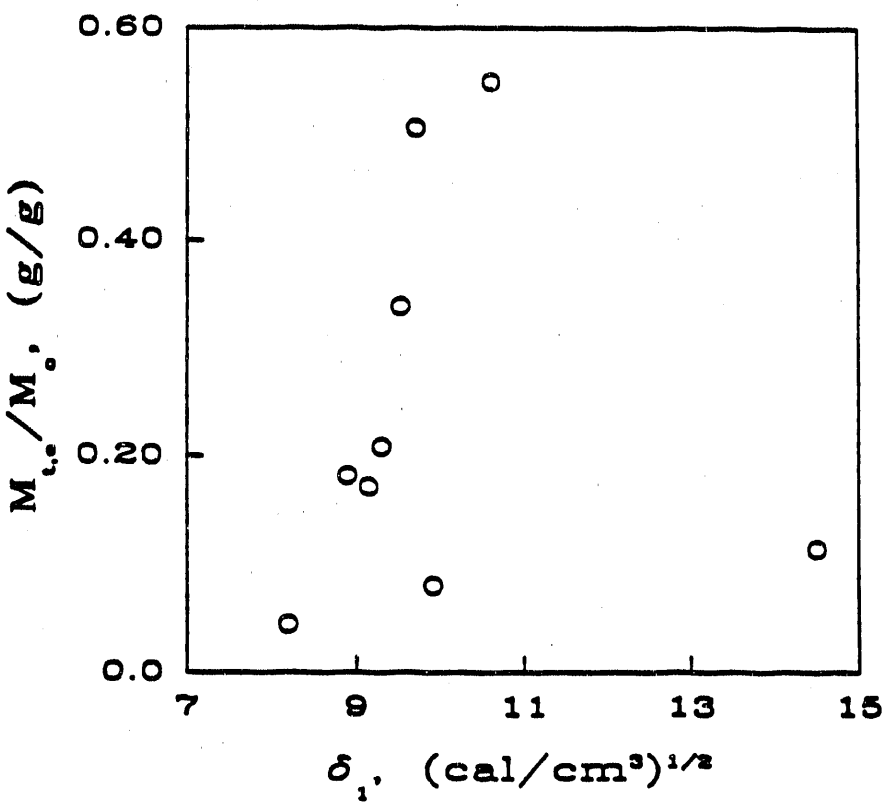

Figure 5.6 The equilibrium penetrant uptake in (g penetrant/g dry coal) in thin coal sections of PSOC-853 at 35°C as a function of the penetrant solubility parameter, δ_1, (in $cal^{1/2}/cm^{3/2}$).

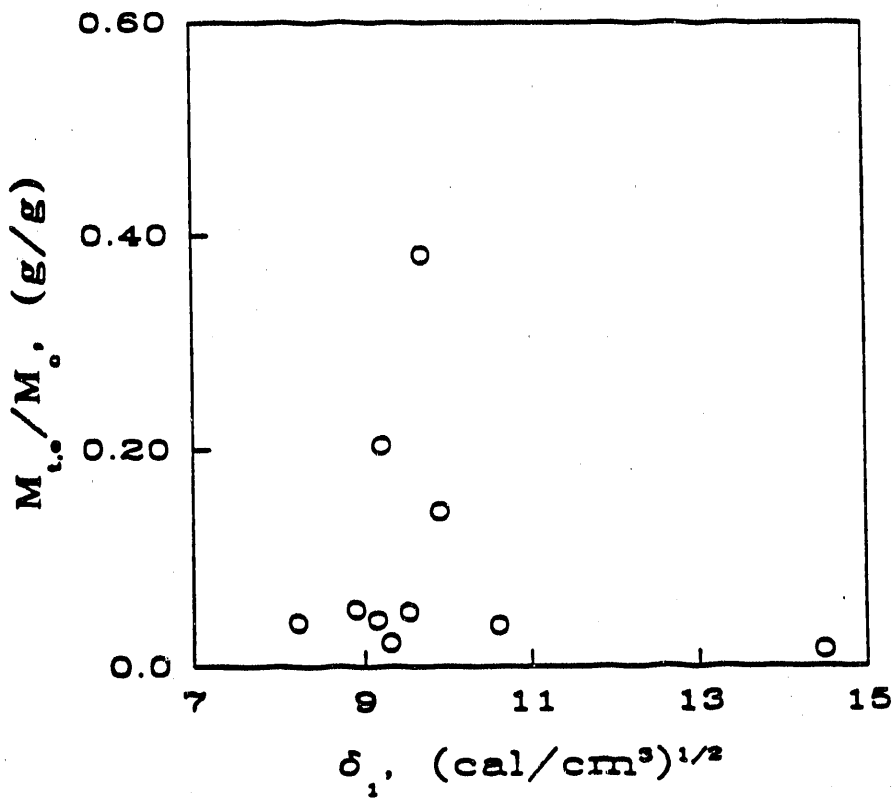

Figure 5.7 The equilibrium penetrant uptake in (g penetrant/g dry coal) in thin coal sections of PSOC-384 at 35°C as a function of the penetrant solubility parameter, δ_1, (in $cal^{1/2}/cm^{3/2}$).

In this case, δ_l is the solubility parameter of the solvent, δ_d is the dispersive interaction contribution to the solubility parameter, δ_p is the polar interaction contribution and δ_h is the hydrogen-bond interaction contribution.

The initial penetrant uptake rate, dM_p/dt, can also be analyzed in terms of the penetrant solubility parameter. Figures 5.8 through 5.10 depict the initial penetrant uptake rate in thin coal sections of PSOC 418, 853 and 384, respectively, as a function of the penetrant solubility parameter. For coals PSOC 418 and 853, a maximum initial penetrant uptake rate is exhibited around a solubility parameter of 9.5 $cal^{1/2}/cm^{3/2}$. However, coal PSOC-384 shows a maximum initial penetrant uptake rate at a solubility parameter of 14.5 $cal^{1/2}/cm^{3/2}$, which then decreases almost linearly as the solubility parameter decreases. These results apply to the initial rates only; as the swelling process reaches equilibrium the solubility parameter of the maximum rate approaches 9.5 $cal^{1/2}/cm^{3/2}$.

It is also possible to study the swelling behavior of penetrants in terms of their cohesive energy properties. Table 5.1 lists values for the dispersive interaction contribution, δ_d, polar interaction contribution, δ_p, and hydrogen-bond interaction contribution, δ_h, to the solubility parameter for a variety of solvents. Swelling studies can be conducted with penetrants of different cohesive energies to elucidate the effect of δ_d, δ_p and δ_h upon coal swelling. These interaction effects are exhibited in Figures 5.11 through 5.13 for the swelling of coals PSOC 418, 853 and 348, respectively. Figure 5.11 depicts the equilibrium penetrant uptake in thin coal sections of PSOC-418 as a function of the penetrant solubility parameter, δ_l, and its dispersive, polar and hydrogen-bonding contributions. It can be seen that the swelling due to dispersive forces exhibits a maximum at a δ_d of 9.0 $cal^{1/2}/cm^{3/2}$; for the swelling due to polar and hydrogen-bond contributions, the maximum occurs at a δ_h of 3.0 $cal^{1/2}/cm^{3/2}$. In other words, the dispersive forces are more significant to the swelling of PSOC-418 than any other force contribution. For the swelling of coal PSOC-853 depicted in Figure 5.12, the maximum swelling

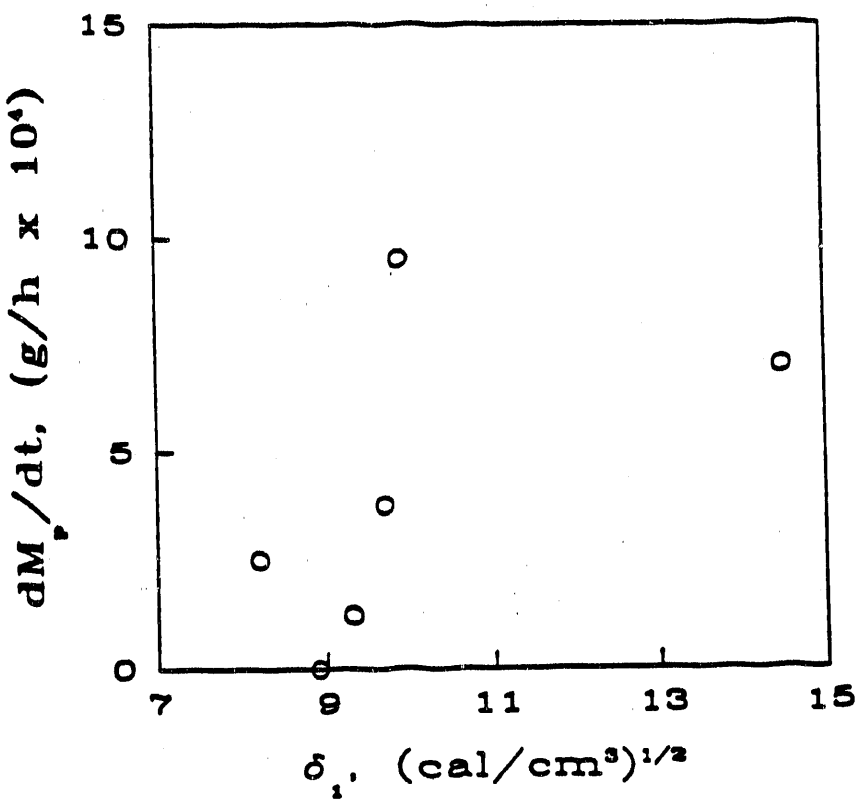

Figure 5.8 Initial penetrant uptake rate (in g/h) inthin coal sections of PSOC-418 at 35°C as a function of the penetrant solubility parameter, δ_1.

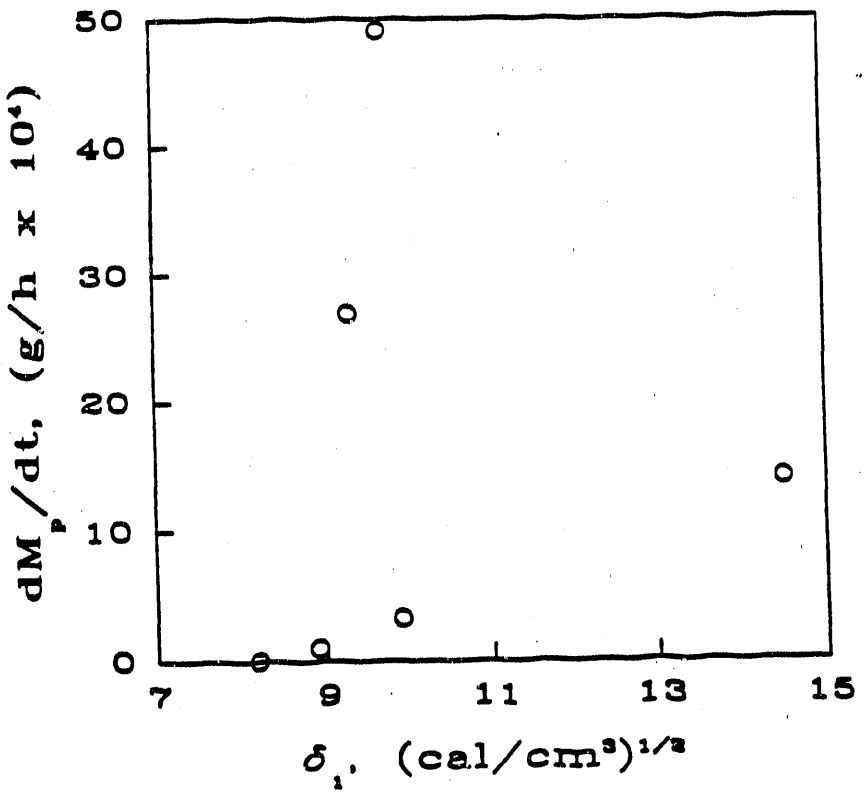

Figure 5.9 Initial penetrant uptake rate (in g/h) in thin coal sections of PSOC-853 at 35°C as a function of the penetrant solubility parameter, δ_1.

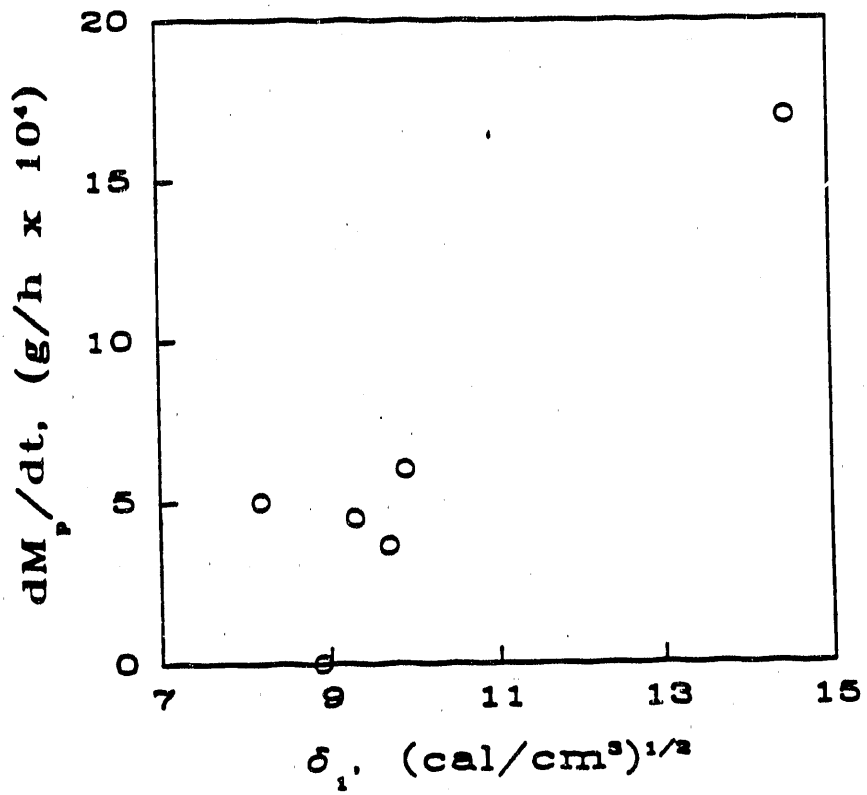

Figure 5.10 Initial penetrant uptake rate (in g/h) in thin coal sections of PSOC-384 at 35°C as a function of the penetrant solubility parameter, δ_1.

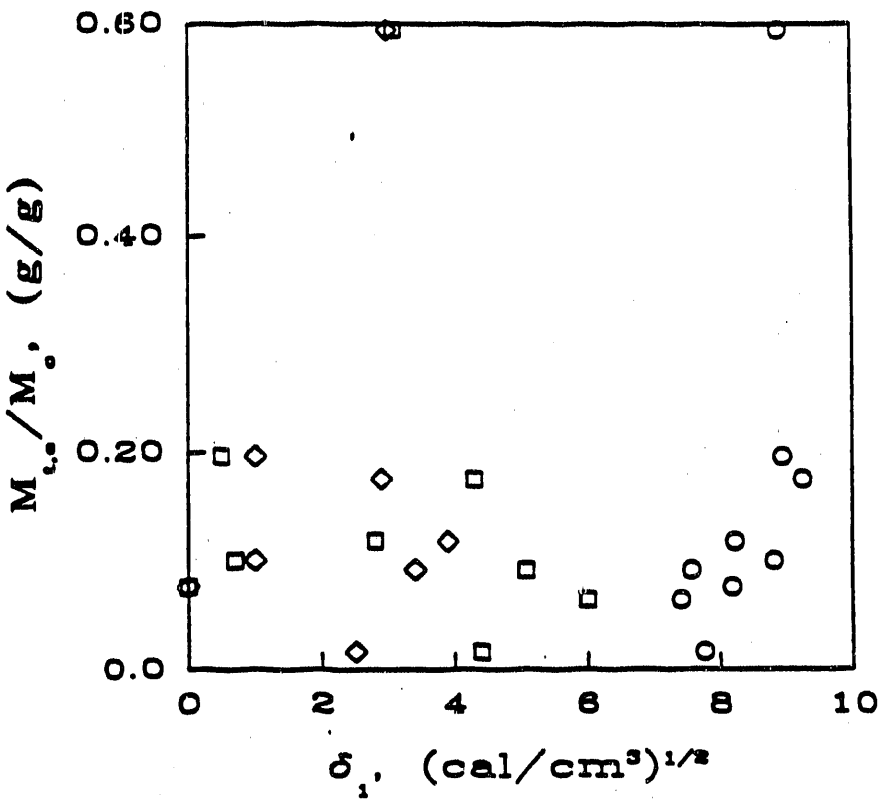

Figure 5.11 Equilibrium penetrant uptake (g penetrant/g dry coal) in thin coal sections of PSOC-418 at 35°C as a function of the penetrant solubility parameter, δ_1, (in $cal^{1/2}/cm^{3/2}$) and its dispersive (O), polar (□), and hydrogen bonding (◊) contributions.

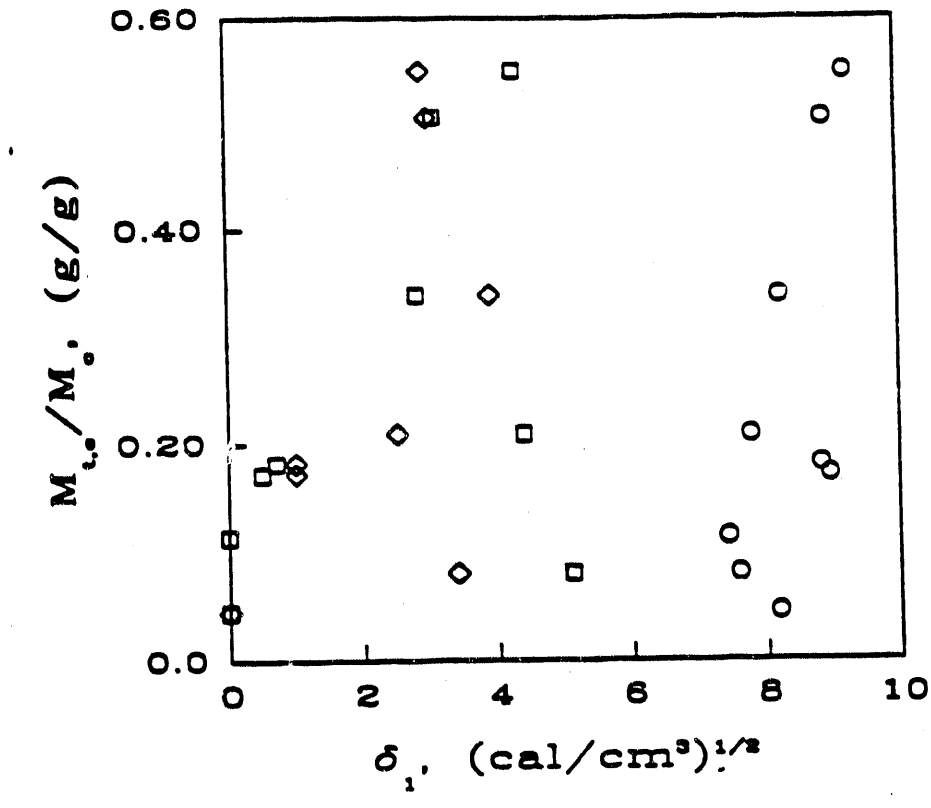

Figure 5.12 Equilibrium penetrant uptake (g penetrant/g dry coal) in thin coal sections of PSOC-853 at 35°C as a function of the penetrant solubility parameter, δ_1, (in $cal^{1/2}/cm^{3/2}$) and its dispersive (○), polar (□), and hydrogen bonding (◇) contributions.

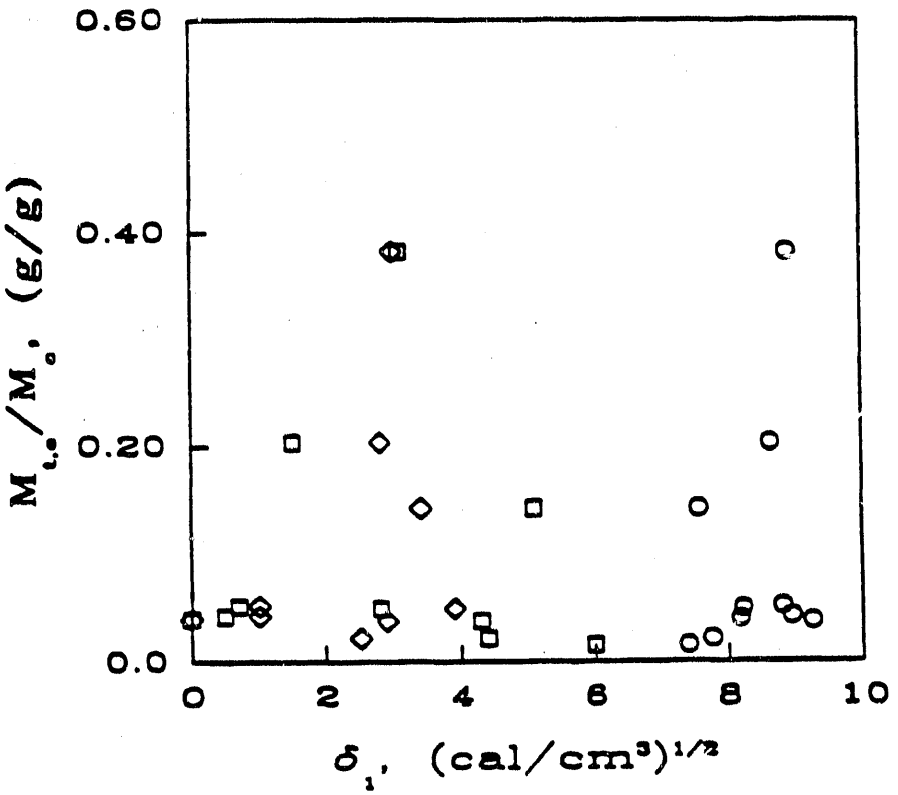

Figure 5.13 Equilibrium penetrant uptake (g penetrant/g dry coal) in thin coal sections of PSOC-384 at 35°C as a function of the penetrant solubility parameter, δ_1, (in $cal^{1/2}/cm^{3/2}$, and its dispersive (○), polar (□), and hydrogen bonding (◇) contributions.

due to the dispersive forces occurs at a δ_d of 9.5 $cal^{1/2}/cm^{3/2}$, the maximum swelling due to polar contributions occurs at a δ_p of 4.5 $cal^{1/2}/cm^{3/2}$, while the maximum swelling due to hydrogen-bonding occurs at a δ_h of 3.0 $cal^{1/2}/cm$. In the case of PSOC-384, the maximum swelling due to dispersive forces occurs at a δ_d of 9.0 $cal^{1/2}/cm^{3/2}$, and the maximum swelling due to polar and hydrogen-bond contributions occurs at a δ_p or δ_h of 3.0 $cal^{1/2}/cm^{3/2}$. Therefore, the cohesive energy contributions to the swelling of coals PSOC 418, 853 and 384 is approximately the same for all three coals.

Another practical way to elucidate the swelling of coals due to the penetrant polar interactions is to use a fractional parameter, f_p, defined as δ_p/δ_t. Plotting solvent behavior by the solvents' fractional solubility parameters permits more lucid analysis of solubility and other interactions. Figures 5.14, 5.15 and 5.16 exhibit the equilibrium penetrant uptake in coals PSOC 853, 418 and 384, respectively, as a function of the polar contribution to the solubility parameter. In all three cases, the maximum swelling is observed with penetrants having a polar contribution which is approximately 30% of the total solubility parameter.

Thus, liquids with solubility parameters around δ_t=9.5 $cal^{1/2}/cm^{3/2}$ exhibit the greatest swelling regardless of the coal used. The maximum coal swelling is attained with methylene chloride. Also, liquids with dispersive contributions around δ_d=9.0 $cal^{1/2}/cm^{3/2}$, and polar and hydrogen-bond contributions around δ_p and δ_h equal to 3.0 $cal^{1/2}/cm^{3/2}$ exhibit the greatest compatibility regardless of the coal used.

5.1.3 Swelling of PMMA

Comparison of the coal behavior in various penetrants was achieved by conducting swelling studies in well characterized, crosslinked poly(methyl methacrylate) (PMMA). Figure 5.17 shows the dynamic uptake of methylene chloride by PMMA crosslinked with 1, 2 and 5 wt% EGDMA. In general,

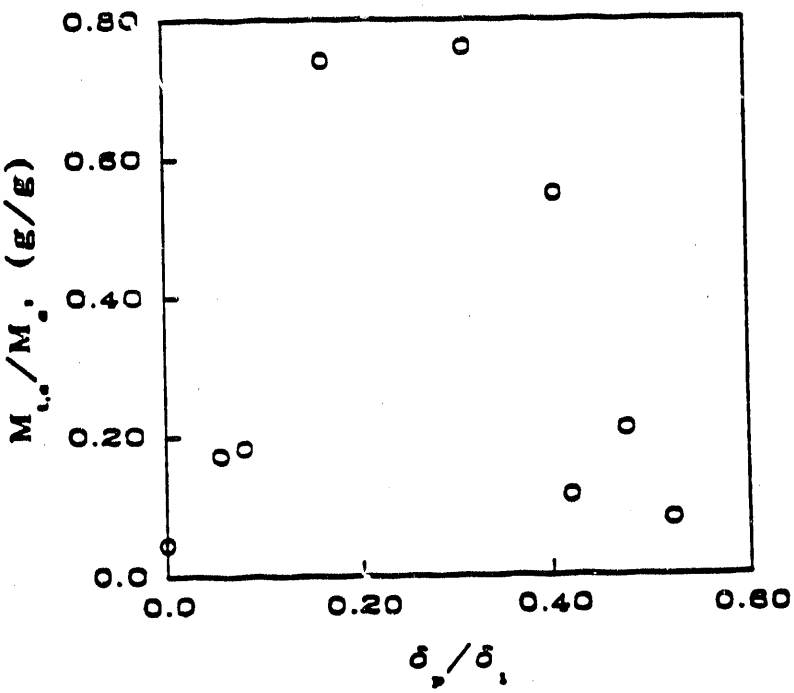

Figure 5.14 Equilibrium penetrant uptake (g penetrant/g dry coal) in thin coal sections of PSOC-853 at 35°C as a function of the polar contribution to the solubility parameter, δ_p/δ_1.

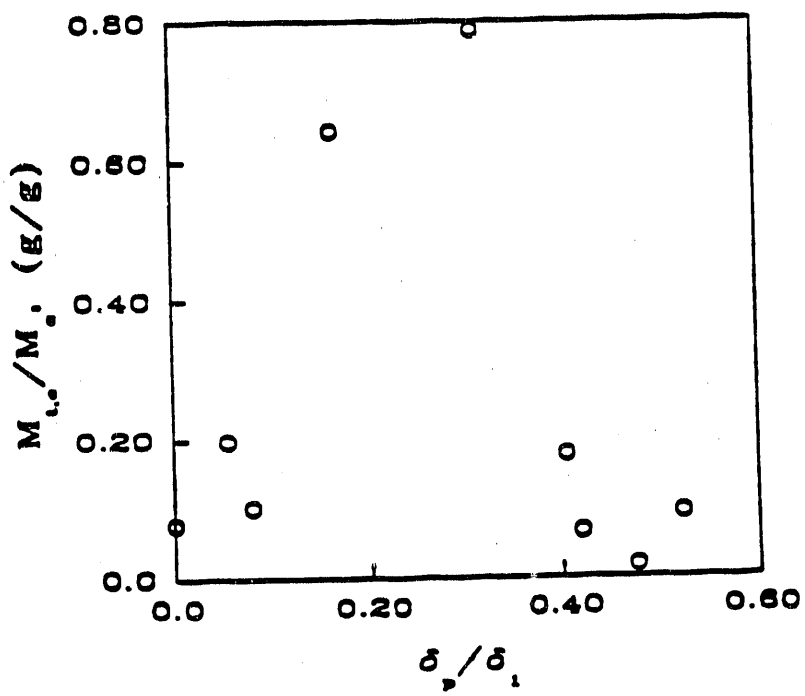

Figure 5.15 Equilibrium penetrant uptake (g penetrant/g dry coal) in thin coal sections of PSOC-418 35°C as a function of the polar contribution to the solubility parameter, δ_p/δ_1.

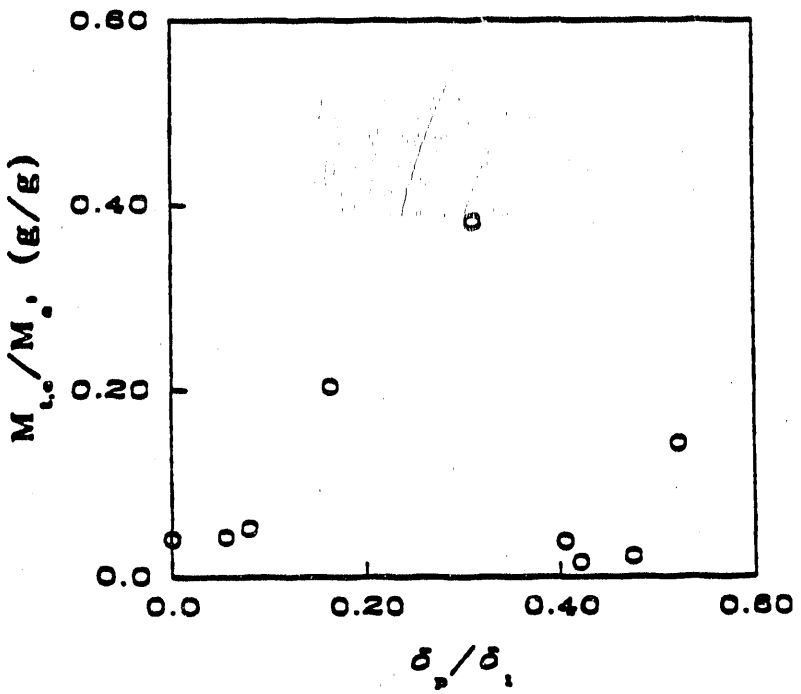

Figure 5.16 Equilibrium penetrant uptake (g penetrant/g dry coal) in thin coal sections of PSOC-384 at 35°C as a function of the polar contribution to the solubility parameter, δ_p/δ_1.

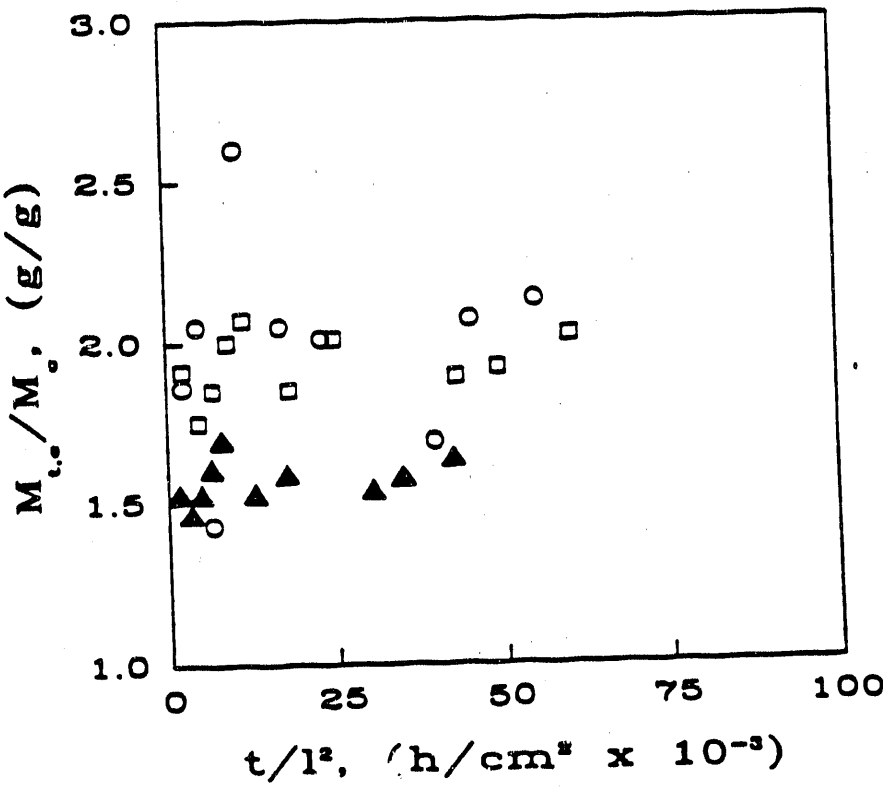

Figure 5.17 Methylene chloride uptake at 35°C in crosslinked PMMA with 1, 2, or 5% EGDMA crosslinking agent. 1.0% (O), 2.0% (□) and 5.0% (▲).

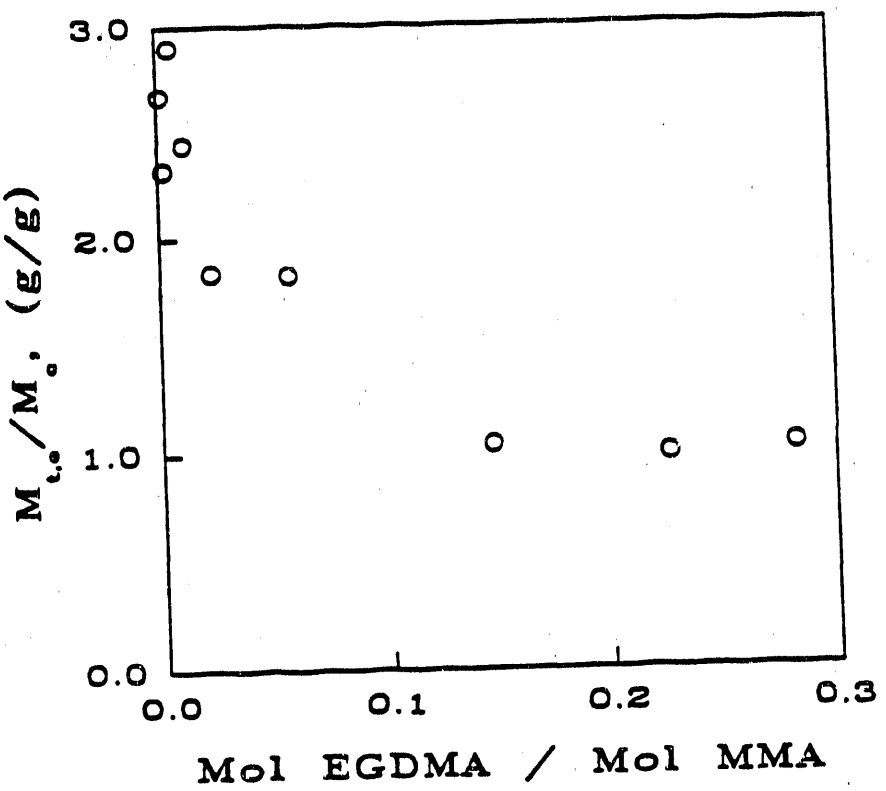

Figure 5.18 Methylene chloride uptake at 35°C in crosslinked PMMA as a function of the moles EGDMA per mole MMA.

the uptake is higher for the lower degree of crosslinking polymer samples. This is shown even better in Figure 5.18, where the equilibrium methylene chloride uptake is shown as a function of the degree of crosslinking expressed as moles EGDMA per mole MMA. These results are in good agreement to those for coal, which also show that the equilibrium penetrant uptake decreases as the crosslinking increases. In the case of coals, the crosslinking is best expressed by the average molecular weight between crosslinks, and not necessarily by the carbon content.

5.2 Dynamic Penetrant Uptake in Coal Samples

Dynamic penetrant uptake studies in thermally treated coal samples were performed with various penetrants to elucidate the phenomenological and mechanistic effects of the diffusion process. Coal swelling by thermodynamically good solvents is due to two main processes. The first is a pure Fickian diffusion and the second is the relaxation of the macromolecular chains which are positioned at the advancing penetrant front. The reader should recall that Fickian diffusion is described by a diffusion coefficient, D, (in cm^2/s), and characterized by an initial square root of time dependence. Case-II transport or relaxation controlled transport is described by a relaxation constant, k, (in s^{-1}), and characterized by an initial linear time dependence. In this section both phenomenological and mechanistic analyses will be discussed for the diffusion of penetrants into thin sections of coals treated at different temperatures.

The thermogravimetric analyzer (TGA) was used to obtain the dynamic penetrant uptake in thin sections of coal (200 μm to 500 μm thick) after various temperature treatments. The coal samples were exposed to a low penetrant activity atmosphere (0.04 for chloroform and less than 0.04 for pyridine and DMF), so that the diffusion of penetrants occurred in all directions. Thin square sections of coal were used with aspect ratio (width or length to thickness) of 10:1, so that an one dimensional diffusion

process could be assumed.

Studies with temperature treated coal samples elucidated the effects of temperature on the diffusion of penetrants into coal. The temperatures at which the coal was treated were 35°C, 100°C and 150°C. Thermal treatment consisted of heating the coal samples at constant temperature for 20 hours; however, equilibrium weight loss was obtained after approximately 3 hours. Then, the diffusion studies were conducted at room temperature with varying carbon content and penetrant types. The coals used in these studies were PSOC- 791 (72.2% C on a dry mineral matter free basis (dmmf)), PSOC-247 (75.5% C dmmf), PSOC-312 (78.3% C dmmf) and PSOC-853 (80.1% C dmmf). The penetrants used were pyridine, N,N-dimethylformamide (DMF) and chloroform.

5.2.1 Penetrant Uptake in Coal Samples as a Function of Carbon Content

Diffusion studies were conducted in thermally treated coal samples containing different carbon content to elucidate the effects of crosslinking and coal heterogeneity. Coals are so inhomogeneous that their chemical structure varies from microregion to microregion and an exact mechanistic analysis is impossible. However, one may use an analysis for homogeneous studies to obtain an approximate result. In this section the coal crosslinking effects will be studied. It must be noted that some deviations from the phenomenological studies may be due to the inhomogeneity of coals and not experimental error.

Figures 5.19 through 5.26 present the phenomenological (without coal porosity correction) amount of penetrant adsorbed per initial dry weight of coal, M_t/M_c, as a function of time. Again, to account for minor changes in the coal samples thickness, l, the data are plotted versus t/l^2, a normalized time expressed in h/cm^2. Figure 5.19 shows the pyridine uptake as a function of normalized time for four different coals treated at 35°C. It can be seen that the equilibrium penetrant adsorbed is higher for coals PSOC 853 and 247, and lower for coals PSOC 791 and 312. This phenomenon was expected since

the average molecular weight between crosslinks is higher for coals PSOC 247 and 853. Therefore, the mesh size available for swelling is larger. It can also be seen that the initial penetrant uptake rate increases from PSOC 312, to 853, to 791, and to 247 (see Table 5.2). Figure 5.20 shows the pyridine uptake as a function of normalized time for four different coals treated at 100°C. The equilibrium penetrant uptake is higher for coal PSOC 791, followed by PSOC 247, 312 and 853. In this case, the penetrant uptake increases as the carbon content decreases. An observed Fickian diffusion in coal PSOC-853 deviates to anomalous then Case-II transport as the carbon content decreases. These results differ from the results for the diffusion of pyridine in coals treated at 35°C. This may be due to the higher temperature treatment,(100°C). As the temperature increases, the chains rearrange and the network density is decreased. Also, an increase of temperature reduces some of the stresses within the coal network. The results show that a temperature increase decreases the network density of the lower carbon content coals more than it decreases the network density of the higher carbon content coals.

Figure 5.21 shows the pyridine uptake as a function of normalized time for four different coals treated at 100°C. In this case, the equilibrium penetrant uptake as well as the initial diffusion rate is higher for the lower carbon content coals. The equilibrium pyridine uptake as well as the initial diffusion rate are highest in PSOC 247 and 791 followed by PSOC 853 and 312. The same sequence was observed for the diffusion of high penetrant activity vapors, where PSOC-312 gave the lowest swelling ratio. There is another phenomenon occurring in this case. At about 12.4 hours (7.5×10^3 h/cm^2 in Figure 5.21) the diffusion rate increases again until it reaches an equilibrium. This may be the time when the penetrant and coal network equilibrate, and the macromolecular chains relax allowing the coal network to reach a new equilibrium. Numerical results for the initial diffusion rates and the pyridine, DMF and chloroform equilibrium uptakes are listed in Tables 5.2, 5.3 and 5.4, respectively. Initial diffusion rate is defined as the change of coal mass with respect to normalized time, $dM_c/dt/l^2$.

Thus, for pyridine diffusion studies into coals PSOC 791, 247, 312 and 853 treated at 35°C, the initial diffusion rates as well as the equilibrium penetrant uptake increase with an increase between crosslinks. At high temperature treatments, the diffusion process decreases as the carbon content of coals increases.

Figures 5.22, 5.23 and 5.24 exhibit the DMF uptake as a function of normalized time for four different coals treated at 35°C, 100°C and 150°C, respectively. It can be seen from Figure 5.22 that the initial diffusion rates as well as the equilibrium DMF uptake are higher for the lower carbon content coals. The initial diffusion rate is higher for PSOC-247 followed by PSOC 791, 312 and 853, respectively. This phenomenon indicates that PSOC-247 would have the highest average molecular weight between crosslinks.

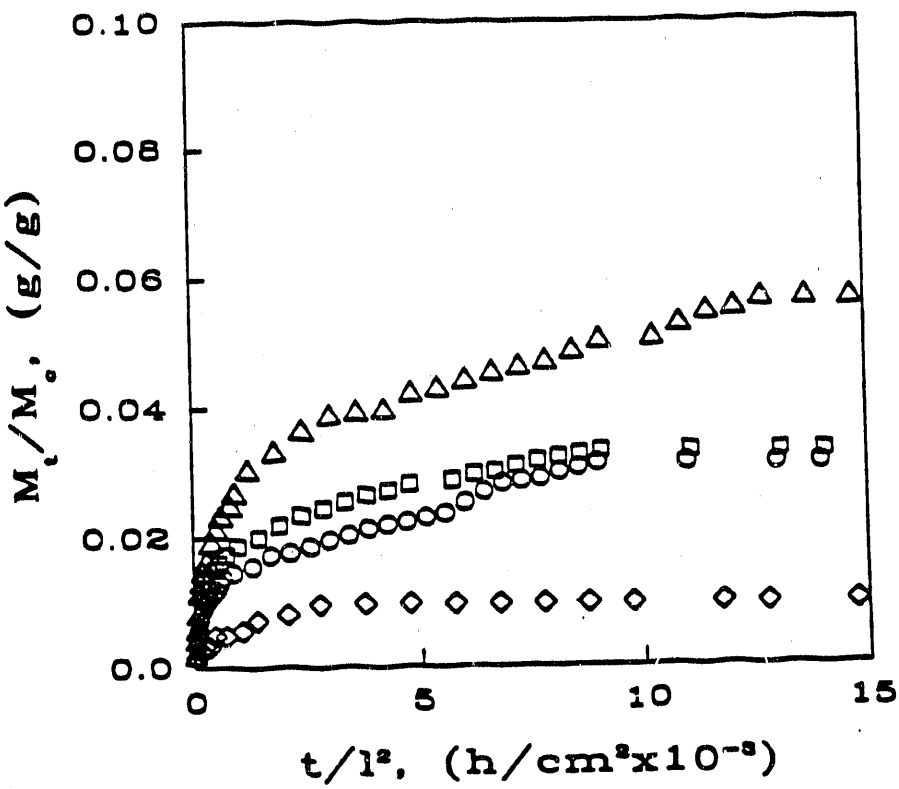

Figure 5.19 Phenomenological pyridine (penetrant activity < 0.04) uptake, M_t/M_c, as a function of normalized time, t/l^2, in coals treated at 35°C. PSOC-791 (○), PSOC-247 (□), PSOC-312 (◇), PSOC-853 (△).

Table 5.2

Initial Rates and Equilibrium Uptakes for the

Diffusion of Pyridine into PSOC Coals

Coal PSOC	%C	Treatment Temp.(°C)	M_c *	Initial Rate (g-cm^2/h)	Equilibrium Uptake (g/g)
791	72.2	35	1027	8.6×10^{-4}	0.031
247	75.5	35	1250	9.2×10^{-4}	0.033
312	78.3	35	1210	1.4×10^{-4}	0.010
853	80.1	35	1200	8.2×10^{-4}	0.056
-	-	-	-	-	-
791	72.2	100	1027	1.5×10^{-3}	0.050
247	75.5	100	1250	1.6×10^{-3}	0.039
312	78.3	100	1210	1.9×10^{-4}	0.040
853	80.1	100	1200	9.7×10^{-4}	0.021
-	-	-	-	-	-
791	72.2	150	1027	2.2×10^{-3}	0.047
247	75.5	150	1250	1.8×10^{-3}	0.064
312	78.3	150	1210	4.2×10^{-4}	0.025
853	80.1	150	1200	4.6×10^{-4}	0.035

* Average weight between crosslinks, M_c, values are obtained from Lucht (1983).

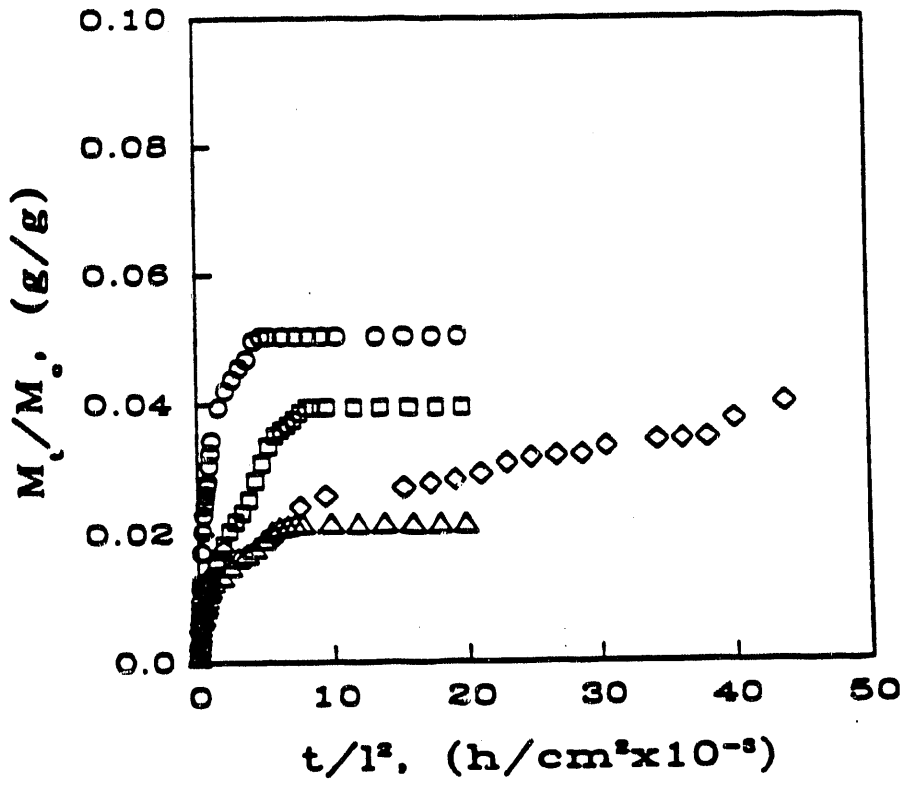

Figure 5.20 Phenomenological pyridine (penetrant activity < 0.04) uptake, M_t/M_c, as a function of normalized time, t/l^2, in coals treated at 100°C. PSOC-791 (○), PSOC-247 (□), PSOC-312 (◇), PSOC-853 (△).

Table 5.2

Initial Rates and Equilibrium Uptakes for the

Diffusion of Pyridine into PSOC Coals

Coal PSOC	%C	Treatment Temp.(°C)	M_c *	Initial Rate (g-cm^2/h)	Equilibrium Uptake (g/g)
791	72.2	35	1027	8.6×10^{-4}	0.031
247	75.5	35	1250	9.2×10^{-4}	0.033
312	78.3	35	1210	1.4×10^{-4}	0.010
853	80.1	35	1200	8.2×10^{-4}	0.056
-	-	-	-	-	-
791	72.2	100	1027	1.5×10^{-3}	0.050
247	75.5	100	1250	1.6×10^{-3}	0.039
312	78.3	100	1210	1.9×10^{-4}	0.040
853	80.1	100	1200	9.7×10^{-4}	0.021
-	-	-	-	-	-
791	72.2	150	1027	2.2×10^{-3}	0.047
247	75.5	150	1250	1.8×10^{-3}	0.064
312	78.3	150	1210	4.2×10^{-4}	0.025
853	80.1	150	1200	4.6×10^{-4}	0.035

* Average weight between crosslinks, M_c, values are obtained from Lucht (1983).

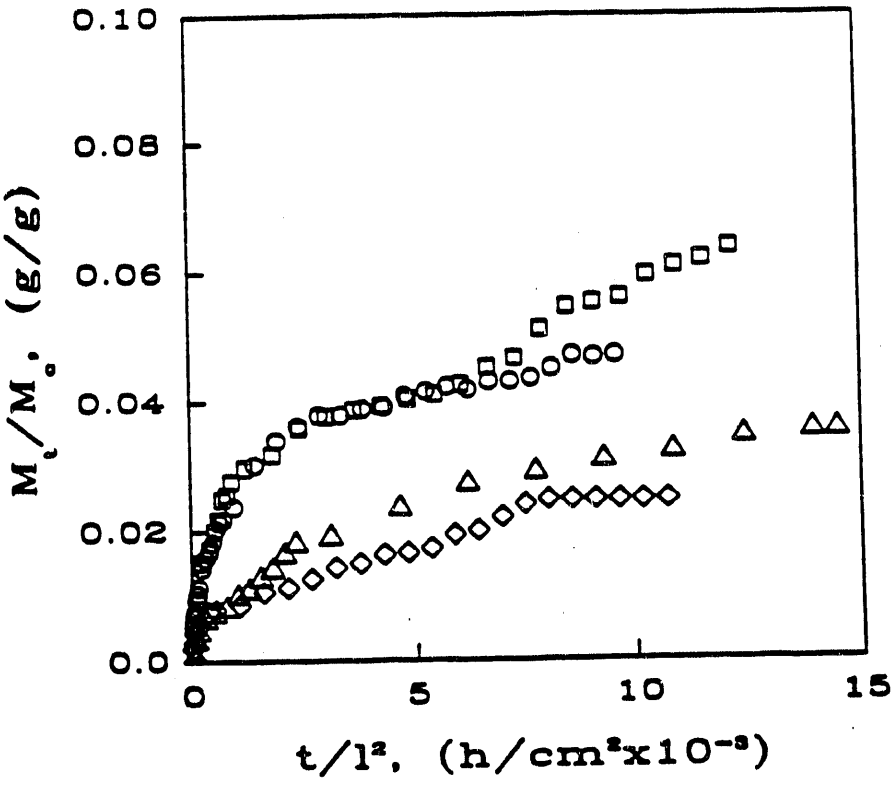

Figure 5.21 Phenomenological pyridine (penetrant activity < 0.04) uptake, M_t/M_c, as a function of normalized time, t/l^2, in coals treated at 150°C. PSOC-791 (○), PSOC-247 (□), PSOC-312 (◇), PSOC-853 (△).

Table 5.3 Initial Rates and Equilibrium Uptakes for

the Diffusion of DMF into PSOC Coals.

Coal PSOC	%C	Treatment Temp.(°C)	M_c *	Initial Rate (g-cm^2/h)	Equilibrium Uptake (g/g)
791	72.2	35	1027	2.4×10^{-3}	0.081
247	75.5	35	1250	2.6×10^{-3}	0.067
312	78.3	35	1210	3.4×10^{-4}	0.020
853	80.1	35	1200	2.4×10^{-4}	0.012
-	-	-	-	-	-
791	72.2	100	1027	1.6×10^{-3}	0.061
247	75.5	100	1250	1.4×10^{-4}	0.043
312	78.3	100	1210	9.5×10^{-5}	0.021
853	80.1	100	1200	9.7×10^{-5}	0.018
-	-	-	-	-	-
791	72.2	150	1027	1.0×10^{-4}	0.033
247	75.5	150	1250	2.0×10^{-4}	0.045
312	78.3	150	1210	6.7×10^{-5}	0.018
853	80.1	150	1200	6.6×10^{-5}	0.009

* Average weight between crosslinks, M_c, values are obtained from Lucht (1983).

Table 5.4 Initial Rates and Equilibrium Uptakes for

the Diffusion of Chloroform into PSOC Coals.

Coal PSOC	%C	Treatment Temp.(°C)	M_c *	Initial Rate (g-cm^2/h)	Equilibrium Uptake (g/g)
791	72.2	35	1027	7.4×10^{-5}	0.043
247	75.5	35	1250	1.2×10^{-4}	0.045
312	78.3	35	1210	6.3×10^{-5}	0.015
853	80.1	35	1200	2.0×10^{-5}	0.012
-	-	-	-	-	-
791	72.2	100	1027	6.2×10^{-5}	0.043
247	75.5	100	1250	5.2×10^{-5}	0.028
312	78.3	100	1210	2.2×10^{-5}	0.008
853	80.1	100	1200	4.8×10^{-5}	0.035
-	-	-	-	-	-
791	72.2	150	1027	2.4×10^{-4}	0.042
247	75.5	150	1250	4.1×10^{-5}	0.029
853	80.1	150	1200	3.1×10^{-5}	0.013

* Average weight between crosslinks, M_c, values are obtained from Lucht (1983).

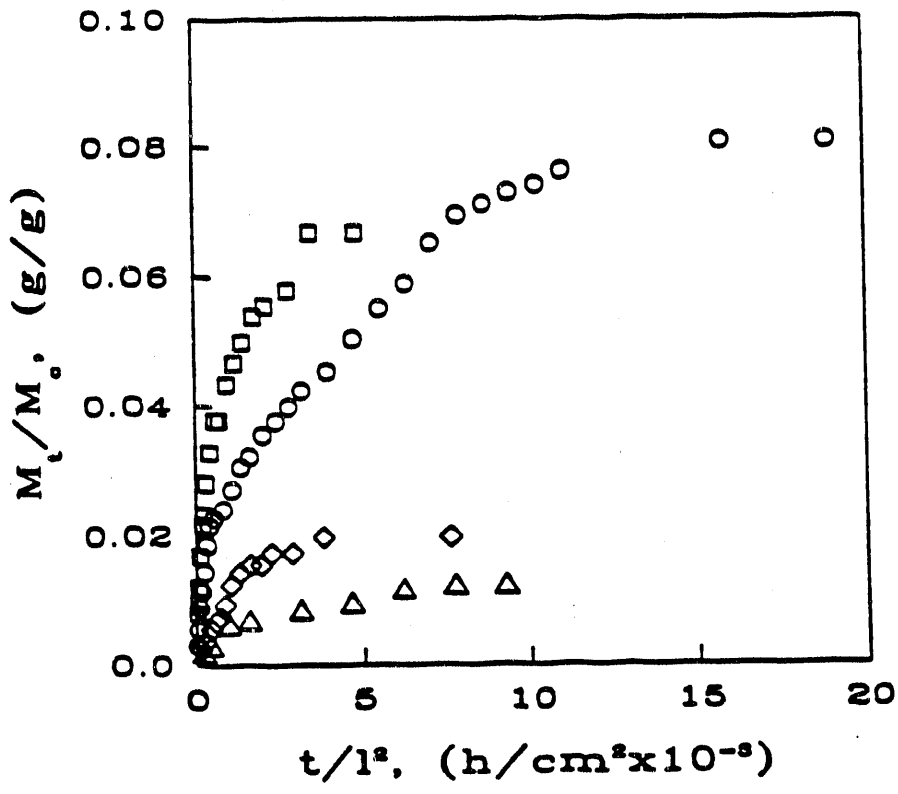

Figure 5.22 Phenomenological DMF (penetrant activity < 0.04) uptake, M_t/M_c, as a function of normalized time, t/l^2, in coals treated at 35°C. PSOC-791 (O), PSOC-247 (□), PSOC-312 (◇), PSOC-853 (Δ).

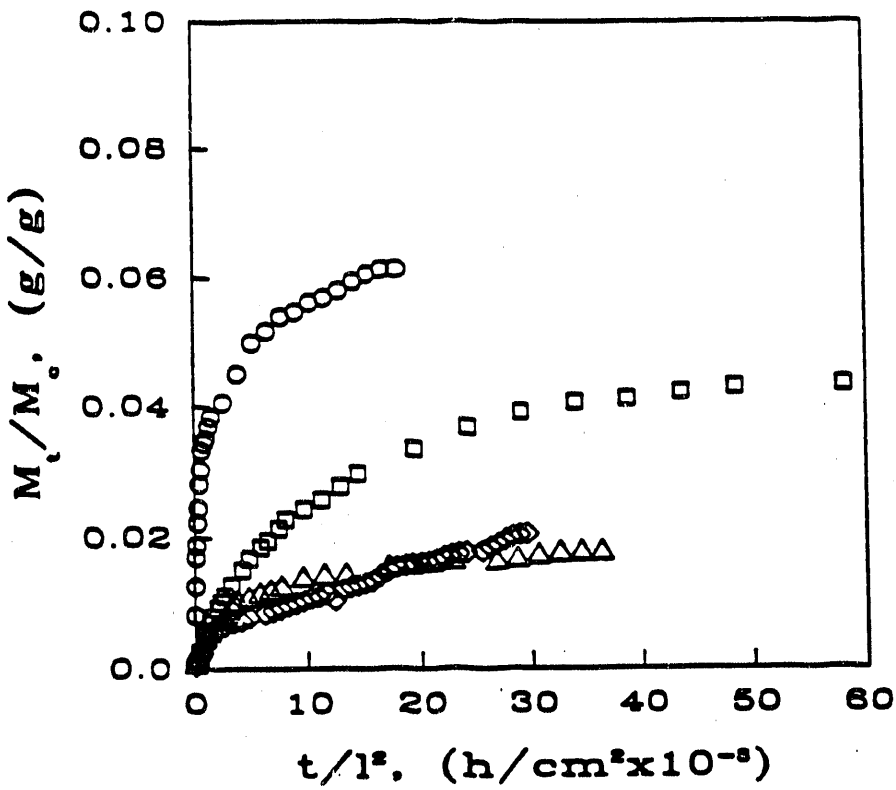

Figure 5.23 Phenomenological DMF (penetrant activity < 0.04) uptake, M_t/M_c, as a function of normalized time, t/l^2, in coals treated at 100°C. PSOC-791 (○), PSOC-247 (□), PSOC-312 (◇), PSOC-853 (△).

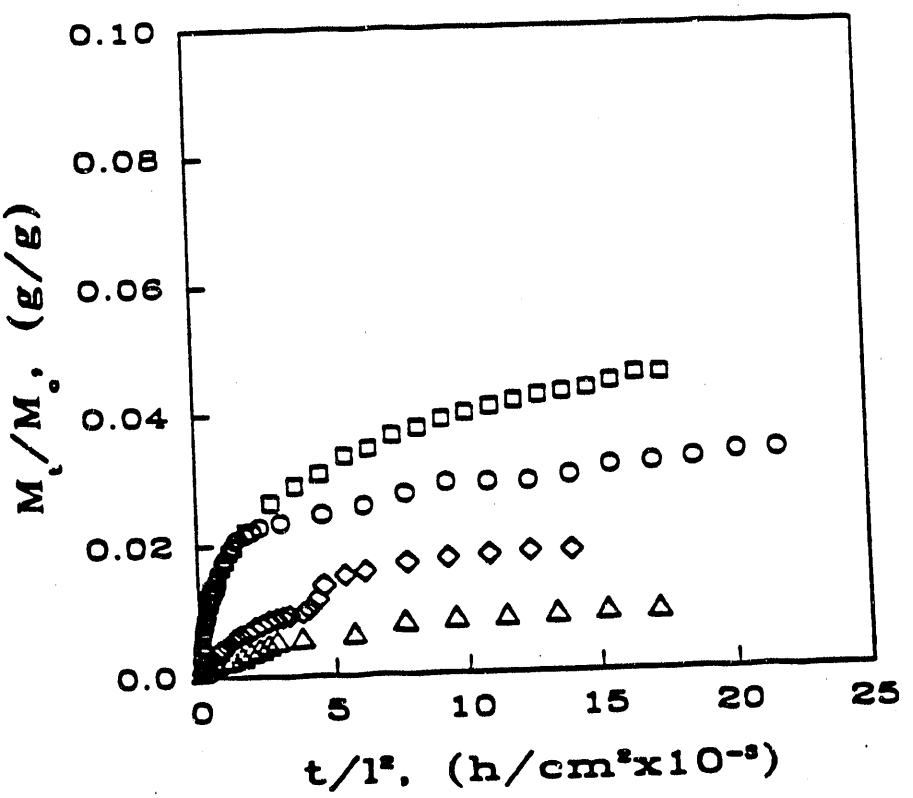

Figure 5.24 Phenomenological DMF (penetrant activity < 0.04) uptake, M_t/M_c, as a function of normalized time, t/l^2, in coals treated at 150°C. PSOC-791 (O), PSOC-247 (□), PSOC-312 (◇), PSOC-853 (Δ).

In the case of the DMF diffusion into coal treated at 100°C depicted in Figure 5.23, the equilibrium uptake was highest for PSOC-791 followed by PSOC 247, 312 and 853, respectively. This observations are in good agreement with the pyridine diffusion into coals treated at higher temperatures. The observed initial diffusion rates also increase as the carbon content decreases (Table 5.3). Figures 5.23 and 5.24 exhibit the DMF uptake in coals treated at 150°C as a function of normalized time. In this case the equilibrium penetrant uptake as well as the initial diffusion rate was higher for PSOC-247 followed by PSOC 791, 312 and 853, respectively. These results suggest that PSOC-247 has the highest average molecular weight between crosslinks, and the results are in good agreement with the pyridine diffusion into coal results.

Thus, coal PSOC-247 exhibits the highest DMF equilibrium uptake as well as the highest initial diffusion rates among all samples tested. A temperature increase favors the DMF diffusion in the lower carbon content coals. The diffusion of DMF and pyridine in coals treated at 35°C increase as the average molecular weight between crosslinks increases. Therefore, the swelling studies with pyridine and DMF show many similarities.

Three types of penetrants were used to elucidate the effects of penetrant type on the diffusion process. Pyridine and DMF have already been discused. The third penetrant is chloroform, which elucidates the effects of chlorinated solvents on the diffusion process. Figure 5.25 exhibits the chloroform uptake in coals treated at 35°C as a function of normalized time. In this case, the equilibrium uptake is higher for PSOC-247 followed by PSOC 791, 312 and 853, respectively. This is the same as the pattern exhibited in the diffusion of DMF into coals treated at 35°C, but with different equilibrium uptake values. It can also be seen that the initial diffusion rates are higher for the lower carbon content coals. At about 12.4 hours (7.5×10^3 h/cm^2), coals PSOC 791 and 247 exhibit an accelerated diffusion rate until equilibrium is attained. This same phenomenon has been previously

observed for the diffusion of pyridine into coals and it occured at the same normalized time.

Figure 5.26 exhibits the chloroform uptake in coals treated at 100°C as a function of normalized time. It can be seen that the equilibrium uptake as well as the initial diffusion rate are higher for PSOC 791 followed by PSOC 247, 853 and 312, respectively. In this case, a temperature treatment increase favored the diffusion in the lower carbon content coals. Probably, the stresses are removed within the coal network as the temperature increases. Therefore, the transport process becomes relaxation controlled. The transport process deviates from Fickian diffusion to anomalous transport then to Case-II transport with a temperature treatment and carbon content increase. Finally, Figure 5.27 exhibits the chloroform uptake in coals treated at 150°C as a function of normalized time. Similarly to the diffusion of chloroform in coals treated at 100°C, the diffusion rates are higher for the lower carbon content coals. The chemical bonds break at high temperatures, and the coal network density decreases.

The results from the aforementioned studies can be combined to provide conclusions of the penetrant uptake in coals as a function of carbon content at different temperatures.

i) For coals treated 35°C, the initial diffusion rates as well as the equilibrium uptake of pyridine, DMF and chloroform into coals PSOC 791, 247, 312 and 853 increase with the average molecular weight between crosslinks.

ii) For the high temperature treated coals, the diffusion of pyridine, DMF and chloroform decreases as the carbon content in coals increases. Coal PSOC-247 exhibits the highest initial diffusion rates and equilibrium uptakes. This suggest that coal PSOC-247 has the highest average molecular weight between crosslinks of the coals studied.

iii) All three penetrants show similar swelling observations, and a mechanistic analysis is necessary to elucidate penetrant diffusion into coals.

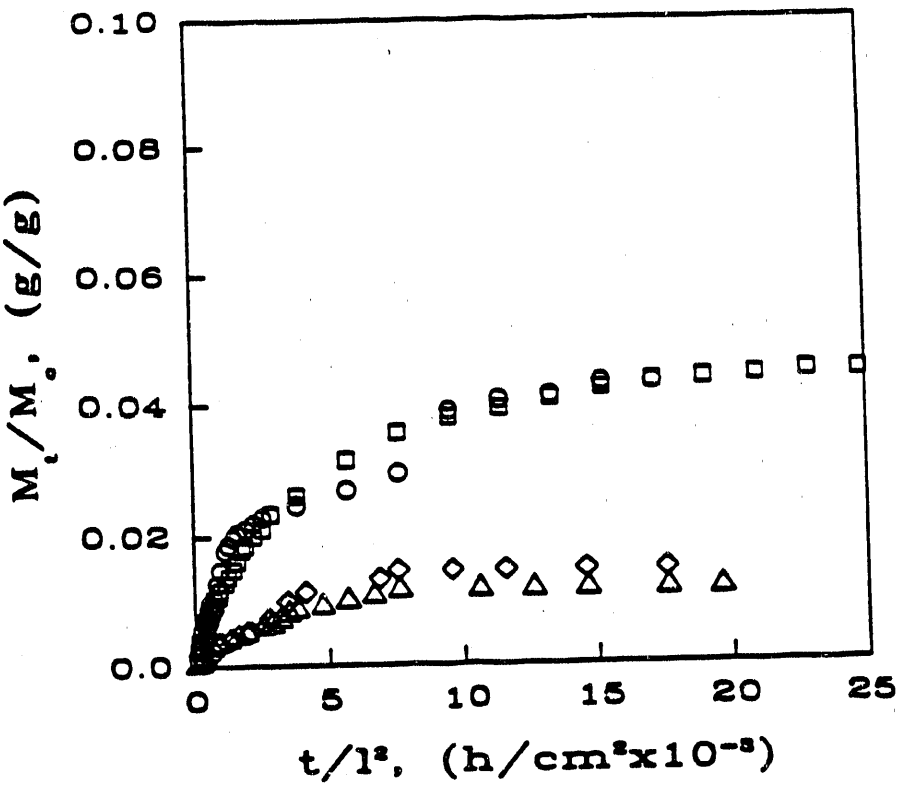

Figure 5.25 Phenomenological chloroform (penetrant activity = 0.04) uptake, M_t/M_c, as a function of normalized time, t/l^2, in coals treated at 35°C. PSOC-791 (O), PSOC-247 (□), PSOC-312 (◇), PSOC-853 (Δ).

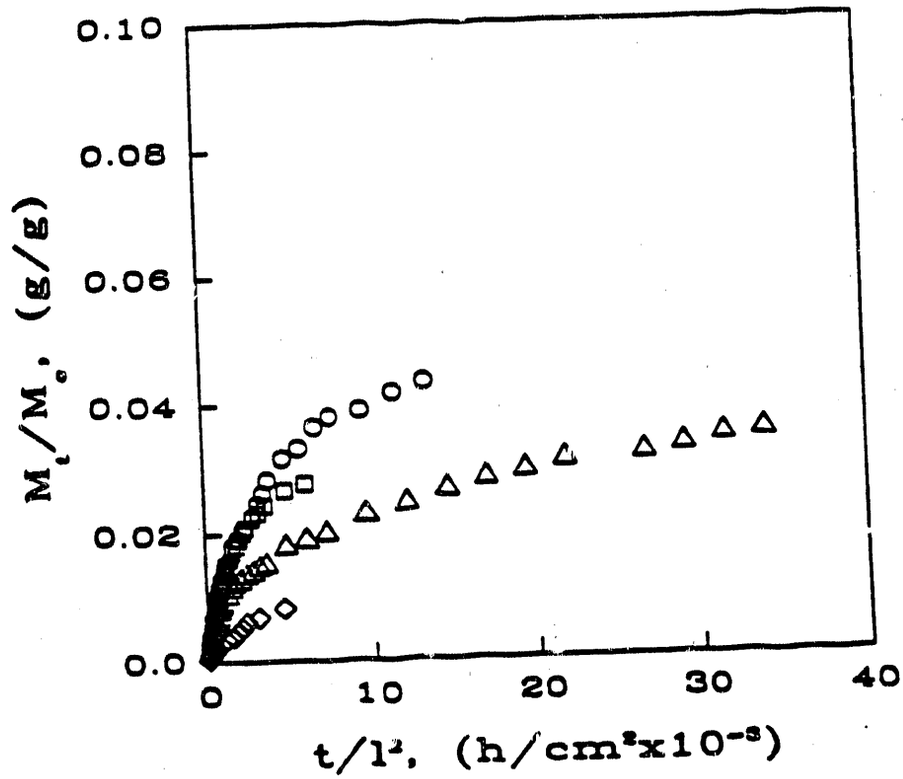

Figure 5.26 Phenomenological chloroform (penetrant activity = 0.04) uptake, M_t/M_c, as a function of normalized time, t/l^2, in coals treated at 100°C. PSOC-791 (O), PSOC-247 (□), PSOC-312 (◊), PSOC-853 (Δ).

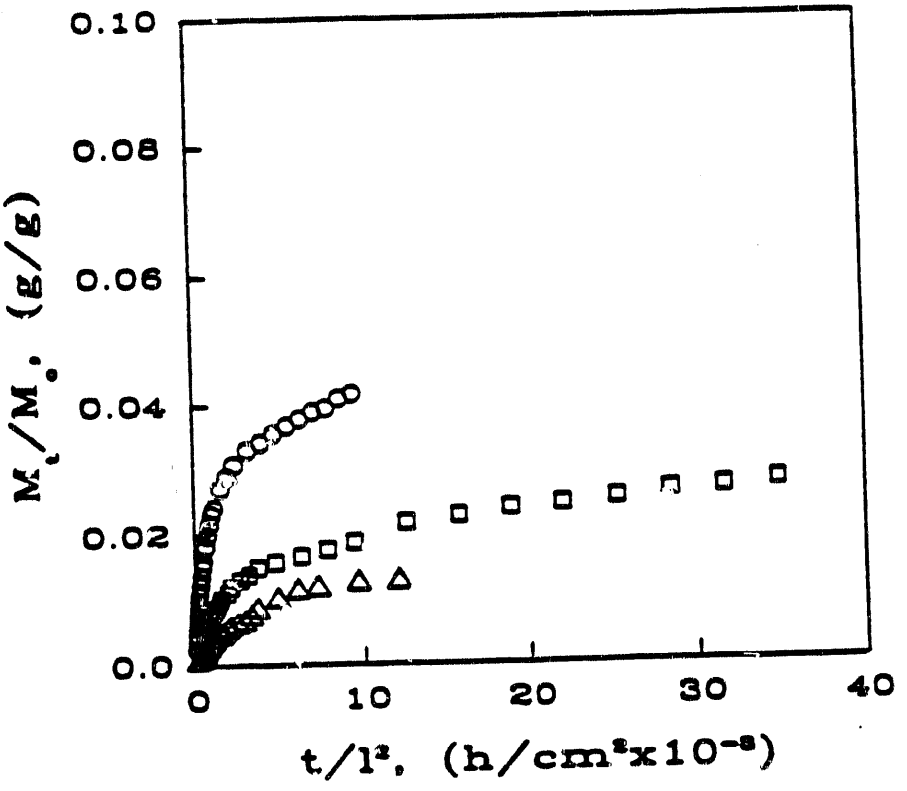

Figure 5.27 Phenomenological chloroform (penetrant activity = 0.04) uptake, M_t/M_c, as a function of normalized time, t/l^2, in coals treated at 150°C. PSOC-791 (O), PSOC-247 (□), PSOC-853 (Δ).

iv) The diffusion rates depend on the average molecular weight between crosslinks of the coals studied.

5.2.2 Penetrant Uptake in Coal Samples as a Function of Temperature

The effects of temperature treatment in penetrant diffusion in coal are discussed in this section. The swelling studies discussed before are presented as a function of temperature treatment to elucidate the temperature effects in the diffusion process. Three temperature treatments, 35°C, 100°C and 150°C for each coal will be discussed. Figures 5.26 through 5.39 exhibit the penetrant uptake as a function of normalized time for coals PSOC 791, 247, 312 and 853 at different temperature treatments.

The pyridine uptake in coals is shown in Figures 5.28 through 5.31. Figure 5.28 exhibits the pyridine uptake in coal PSOC-791 as a function of normalized time at different temperature treatments. It can be seen that total equilibrium uptake is higher for the coals treated at 100°C and 150°C, and decreases for the the coal treated at 35°C. In the case of swelling in coal PSOC-247 (Figure 5.29), the initial diffusion rates and the total equilibrium pyridine uptake increases with temperature treatment. Some of the stresses within the network are removed by thermally treating the coal samples, which helps the penetrant to diffuse into the network. For the coal treated at 150°C case, there is an accelerated uptake at about 12.4 hours (7.5×10^3 h/cm^2). This indicates that the macromolecular chains have relaxed, and the network attains a new equilibrium uptake. Proceeding with the pyridine diffusion into coal PSOC-312 depicted in Figure 5.30, it can be seen that the highest temperature treated samples exhibit the higher equilibrium uptake and initial diffusion rates.

Figure 5.31 shows the pyridine uptake into coal PSOC-853. In this case, the 35°C study exhibits the higher equilibrium uptake followed by the 150°C and 100°C studies. With the exception of the lower temperature case, the total equilibrium uptake increases with temperature.

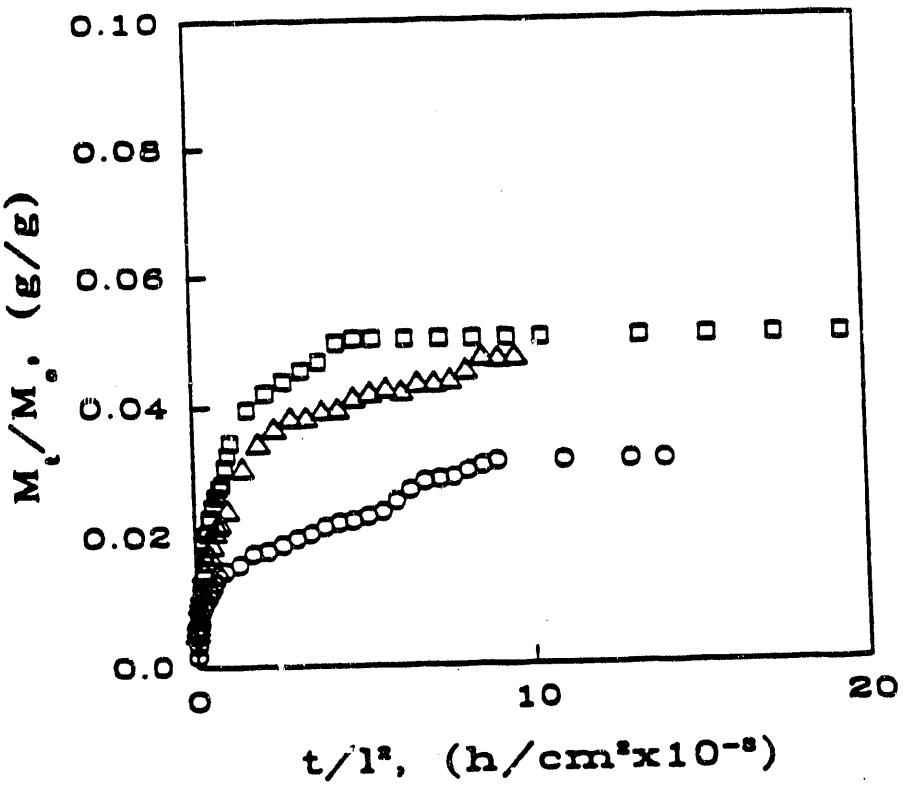

Figure 5.28 Phenomenological pyridine (penetrant activity < 0.04) uptake, M_t/M_e, as a function of normalized time, t/l^2, for coal PSOC-791 treated at: 35°C (O), 100°C (□) and 150°C (Δ).

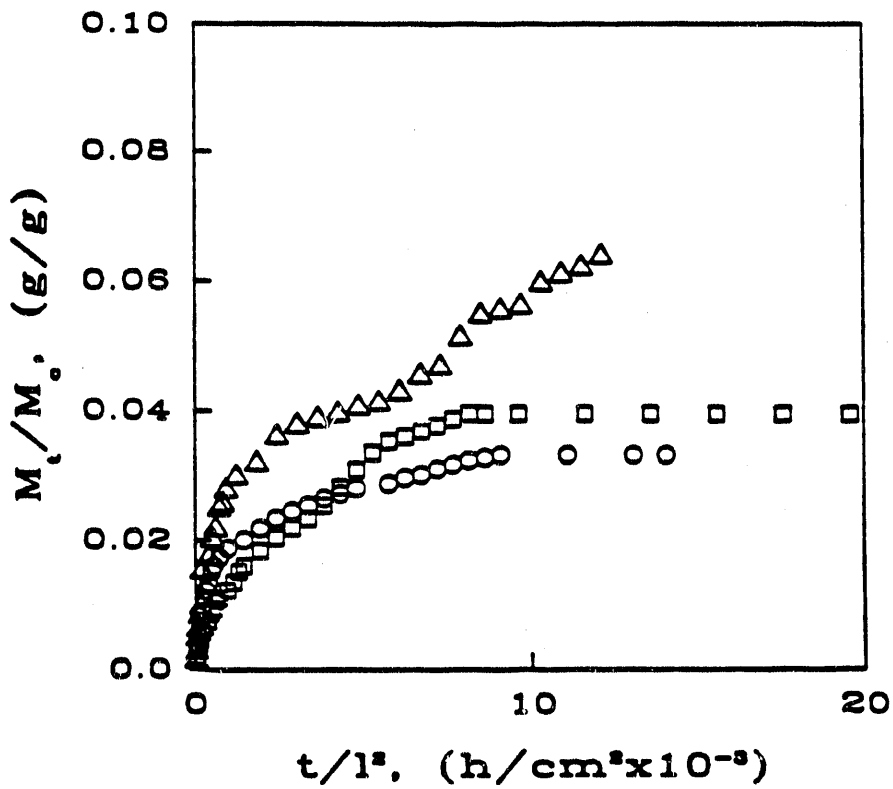

Figure 5.29 Phenomenological pyridine (penetrant activity < 0.04) uptake, M_t/M_c, as a function of normalized time, t/l^2, for coal PSOC-312 treated at: 35°C (O), 100°C (□) and 150°C (Δ).

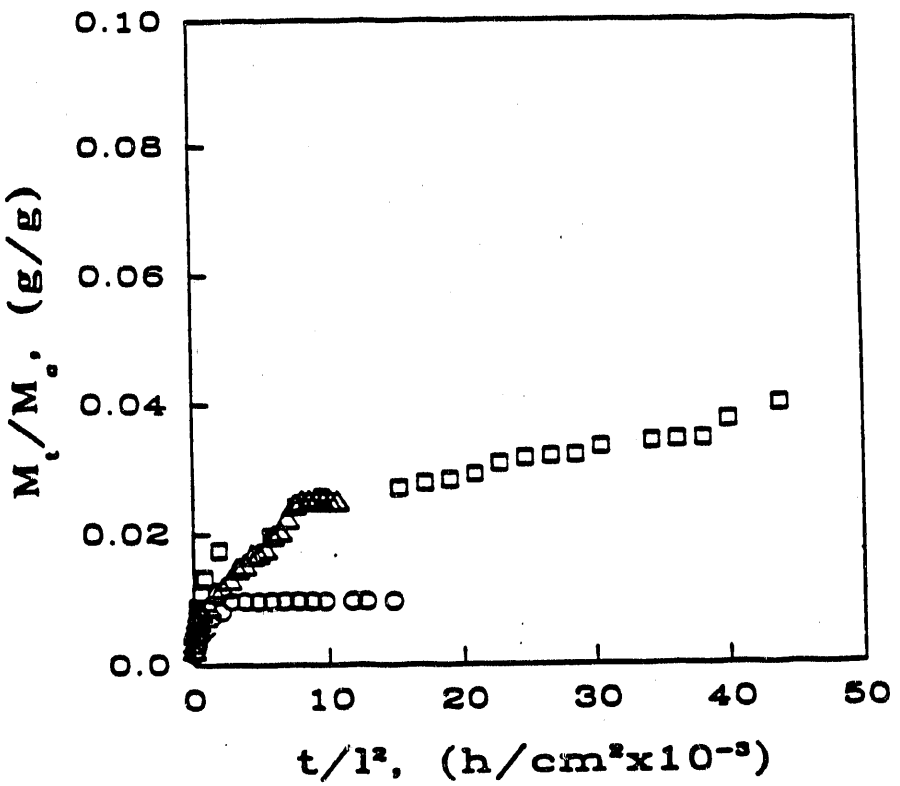

Figure 5.30 Phenomenological pyridine (penetrant activity < 0.04) uptake, M_t/M_e, as a function of normalized time, t/l^2, for coal PSOC-312 treated at: 35°C (○), 100°C (□) and 150°C (Δ).

Therefore, for the diffusion of pyridine into coals treated at different temperatures, the total equilibrium uptake and the initial diffusion rates increase with temperature treatments. The same phenomenon is observed in all four coals.

DMF diffusion into coals PSOC 791, 247, 312 and 853 at different temperature treatments is shown in Figures 5.32 through 5.35. In all four cases, it can be seen that the total equilibrium uptake is higher for coals treated at 35°C and decreases as the temperature treatment increases. Even the initial diffusion rates for some coals are higher at the lower temperature treatments (see Table 5.3). Contrary to the diffusion of pyridine into coals, the DMF diffusion into coals decreases as temperature treatment increases. An explanation to this phenomenon may be that by thermally treating the coal samples, some of the chemical sites which would originally form chemical bonds with DMF are destroyed. It was mentioned that the network density decreases when a coal-coal hydrogen-bond is replaced by a penetrant-coal hydrogen-bond.

The chloroform uptake in coals PSOC 791, 247, 312 and 853 at different temperature treatments is shown in Figures 5.36 through 5.39, respectively. In the case of chloroform diffusion into PSOC-791 depicted in Figure 5.36, it can be seen that the equilibrium uptake as well as the initial diffusion rates increases with temperature treatment; albeit by a very insignificant amount. On the contrary, the diffusion of chloroform into coal PSOC-247 depicted in Figure 5.37, shows that the initial diffusion rates and the equilibrium uptake decrease as the temperature treatment increases. Chemical sites available to chemically bond with chloroform are removed with a temperature treatment increase. Figure 5.38 exhibits the chloroform uptake as a function of normalized time for coal PSOC-312. In this case too, the equilibrium uptake as well as the initial diffusion rates decreases as the temperature treatment increases. Finally, Figure 5.39 exhibits the chloroform uptake as a function of normalized time for coal PSOC-853. The equilibrium penetrant uptake as well as the initial diffusion rates are

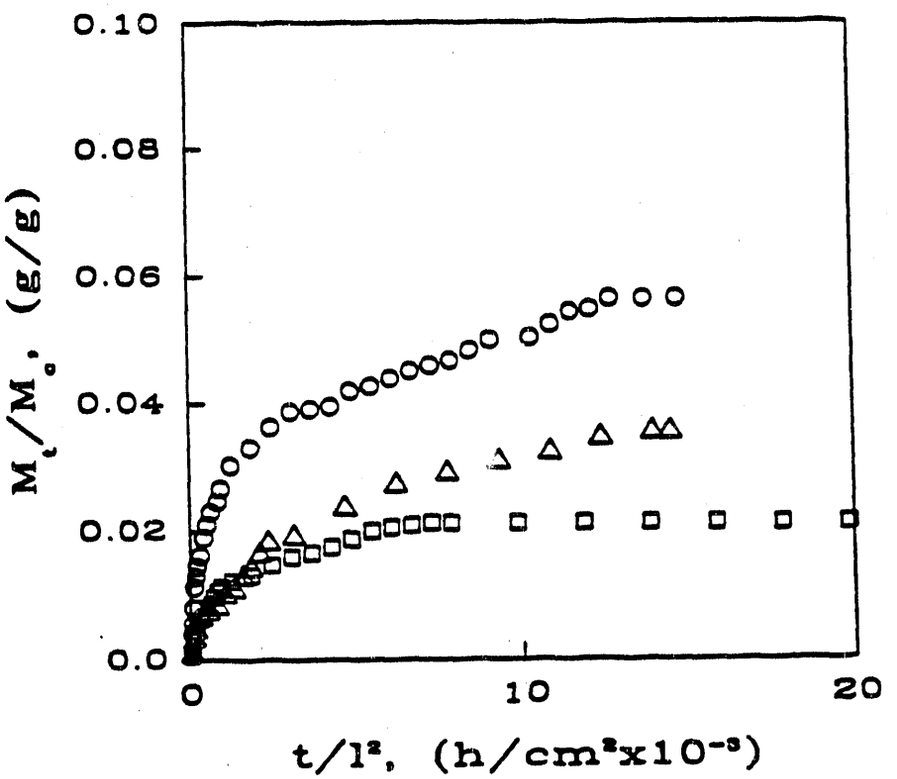

Figure 5.31 Phenomenological pyridine (penetrant activity < 0.04) uptake, M_t/M_c, as a function of normalized time, t/l^2, for coal PSOC-853 treated at: 35°C (○), 100°C (□) and 150°C (△).

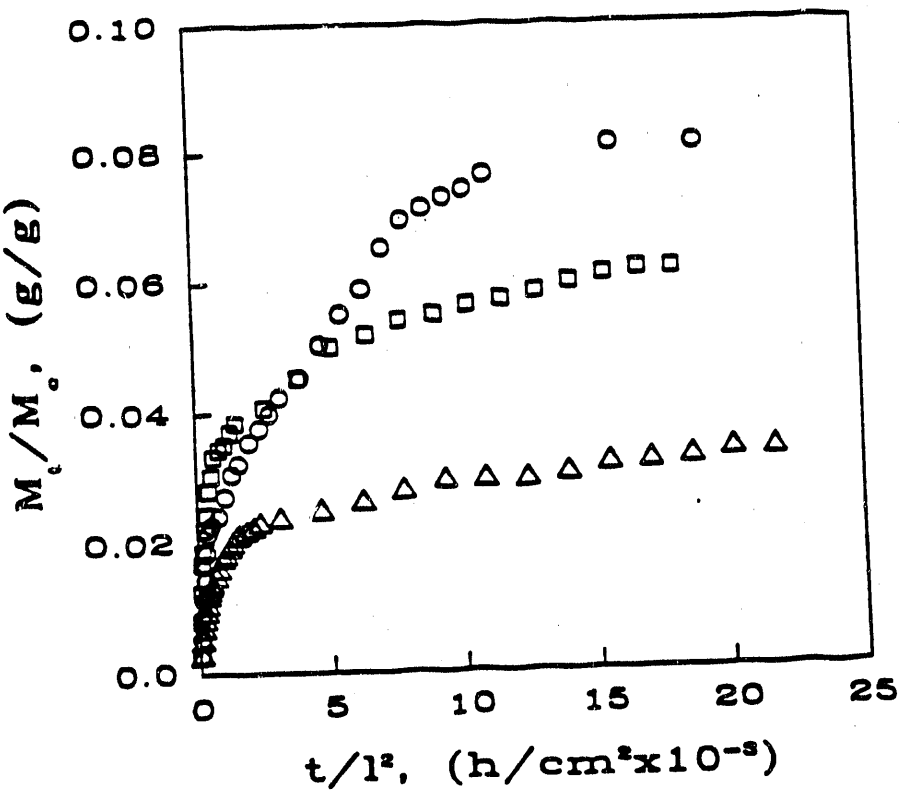

Figure 5.32 Phenomenological DMF (penetrant activity < 0.04) uptake, M_t/M_c, as a function of normalized time, t/l^2, for coal PSOC-791 treated at: 35°C (O), 100°C (□) and 150°C (Δ).

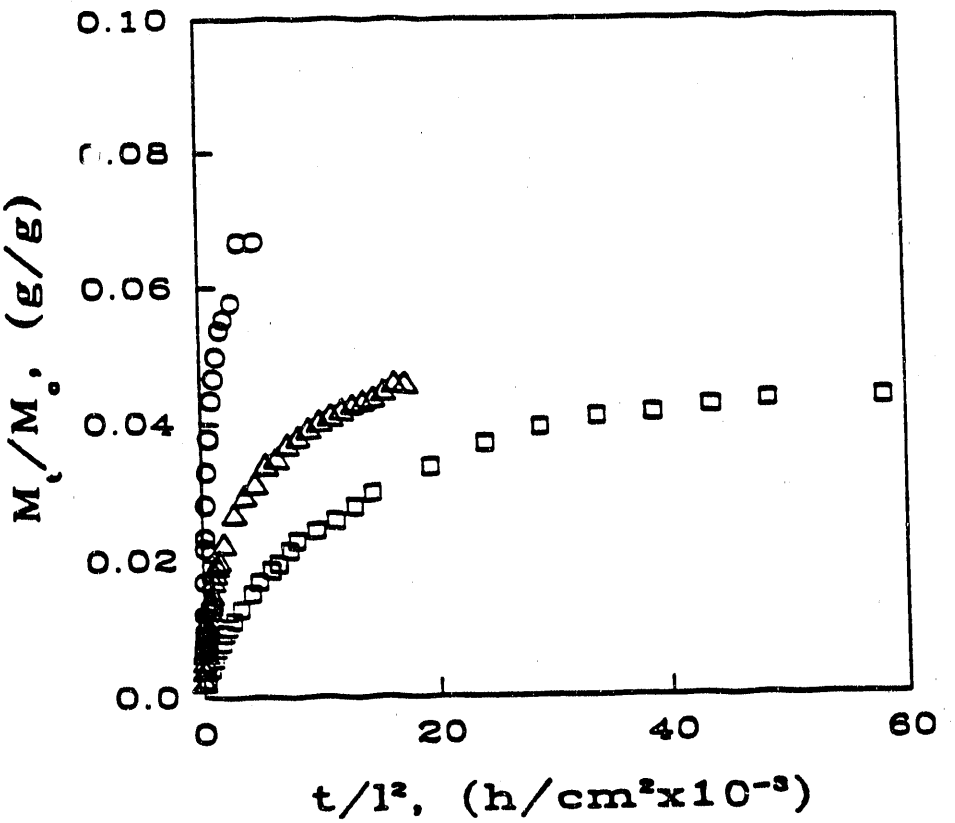

Figure 5.33 Phenomenological DMF (penetrant activity < 0.04) uptake, M_t/M_c, as a function of normalized time, t/l^2, for coal PSOC-247 treated at: 35°C (O), 100°C (□) and 150°C (Δ).

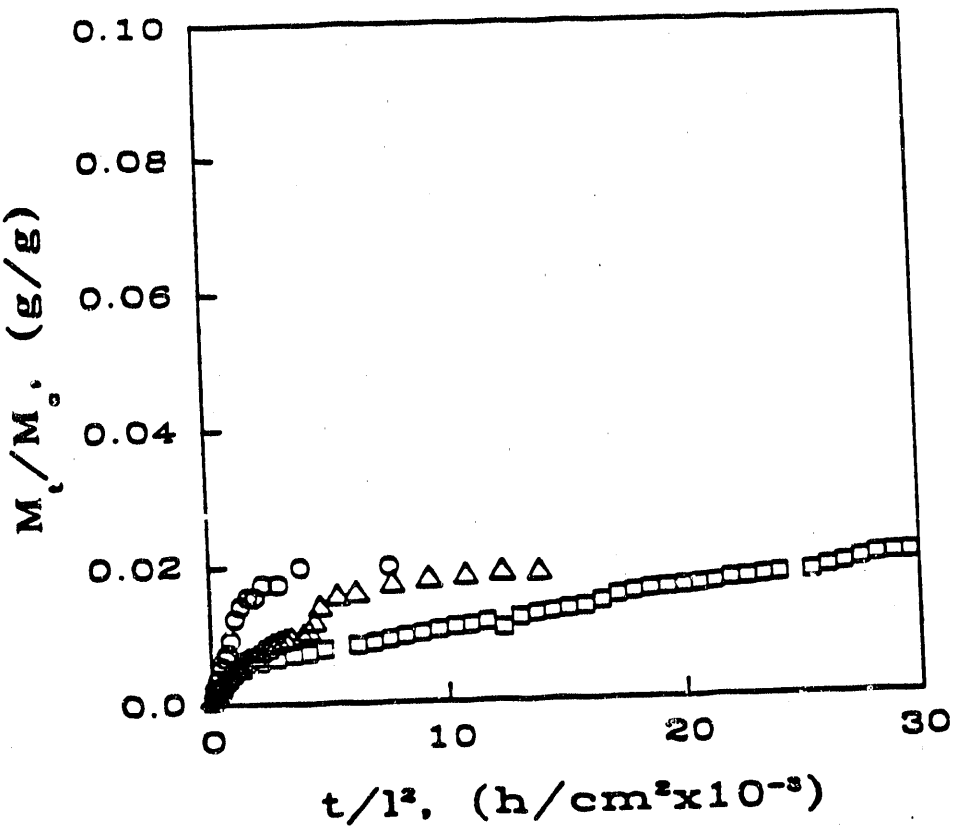

Figure 5.34 Phenomenological DMF (penetrant activity < 0.04) uptake, M_t/M_∞, as a function of normalized time, t/l^2, for coal PSOC-312 treated at: 35°C (O), 100°C (□) and 150°C (Δ).

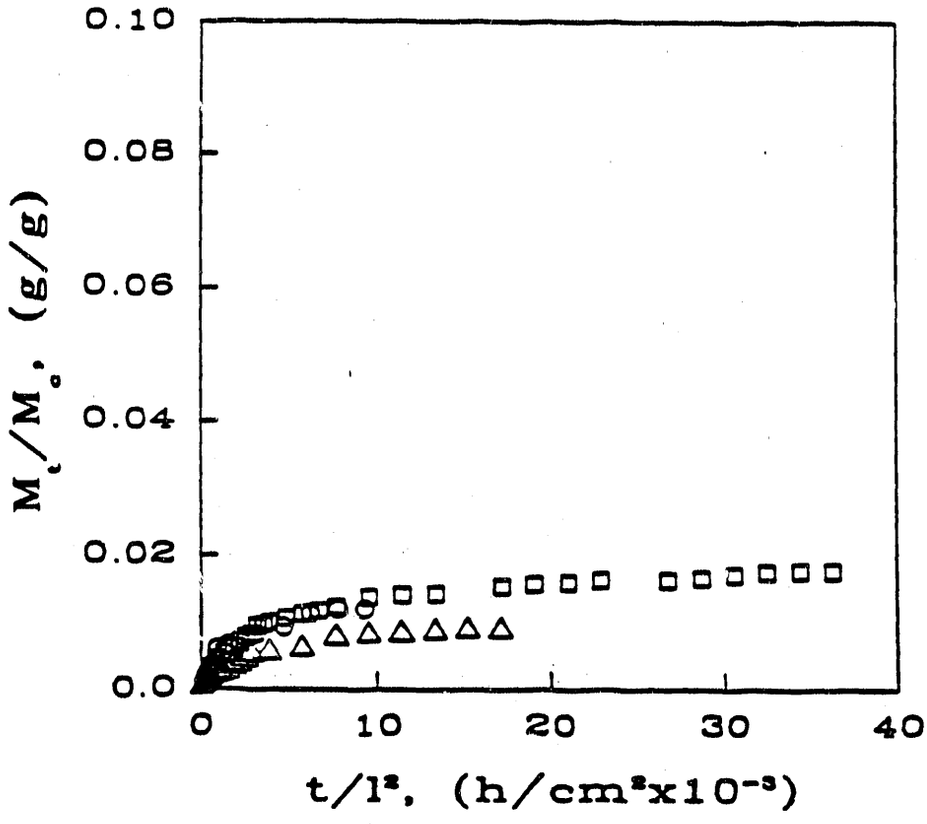

Figure 5.35 Phenomenological DMF (penetrant activity < 0.04) uptake, M_t/M_c, as a function of normalized time, t/l^2, for coal PSOC-853 treated at: 35°C (○), 100°C (□) and 150°C (△).

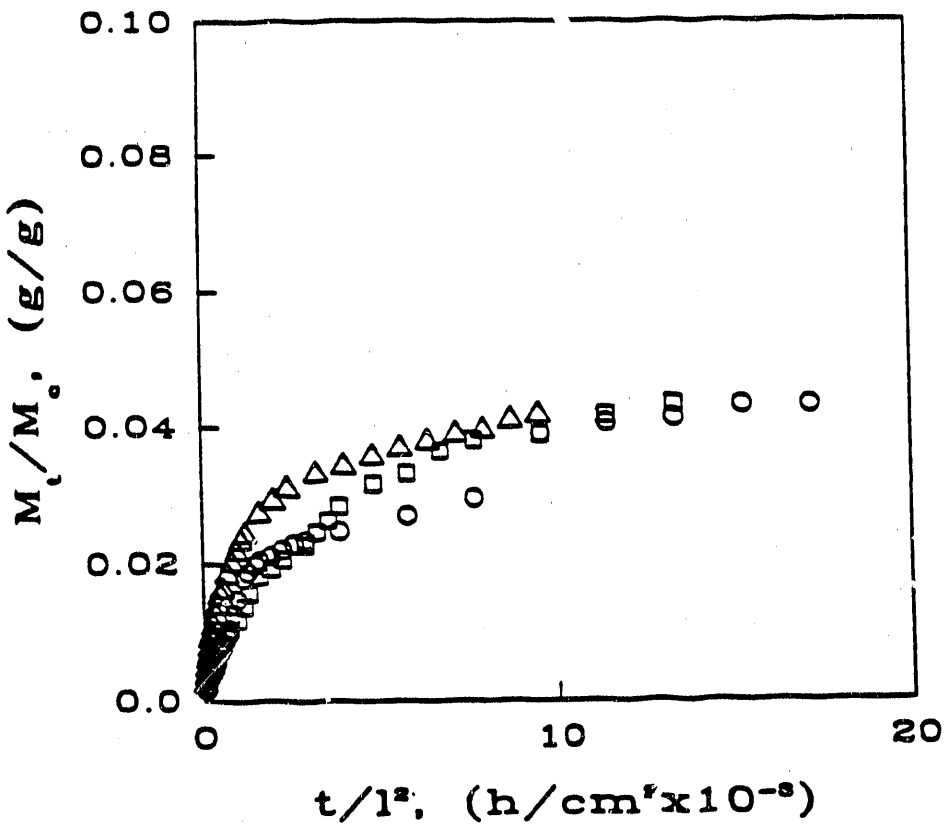

Figure 5.36 Phenomenological chloroform (penetrant activity = 0.04) uptake, M_t/M_c, as a function of normalized time, t/l^2, for coal PSOC-791 treated at: 35°C (O), 100°C (□) and 150°C (Δ).

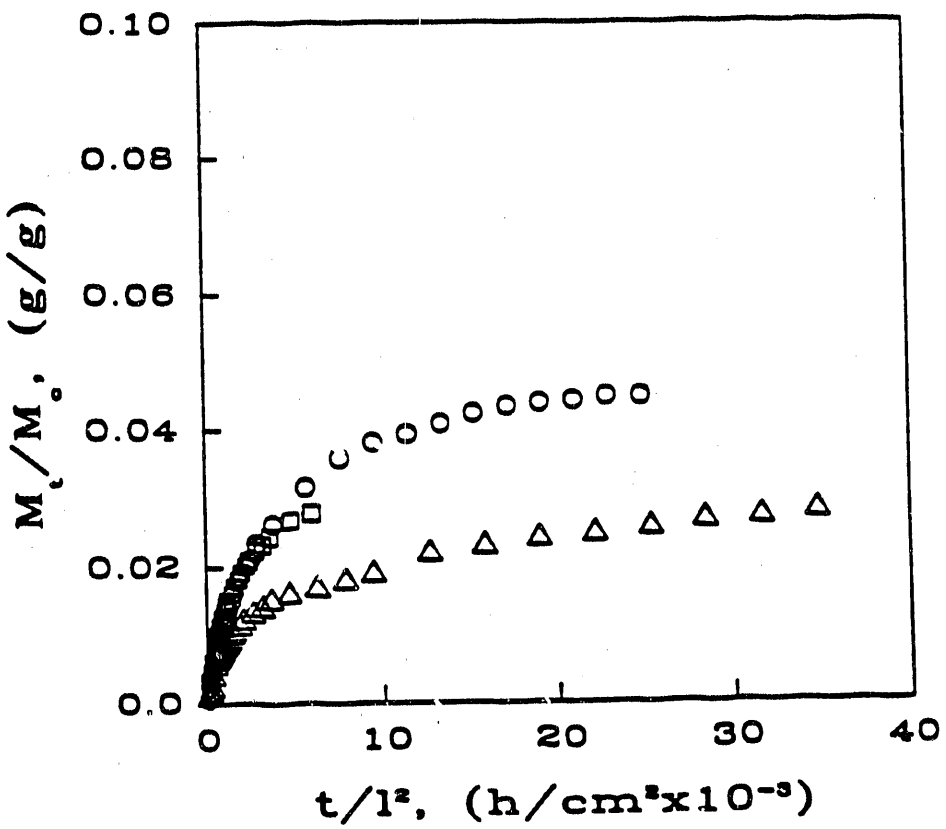

Figure 5.37 Phenomenological chloroform (penetrant activity = 0.04) uptake, M_t/M_c, as a function of normalized time, t/l^2, for coal PSOC-247 treated at: 35°C (O), 100°C (□) and 150°C (Δ).

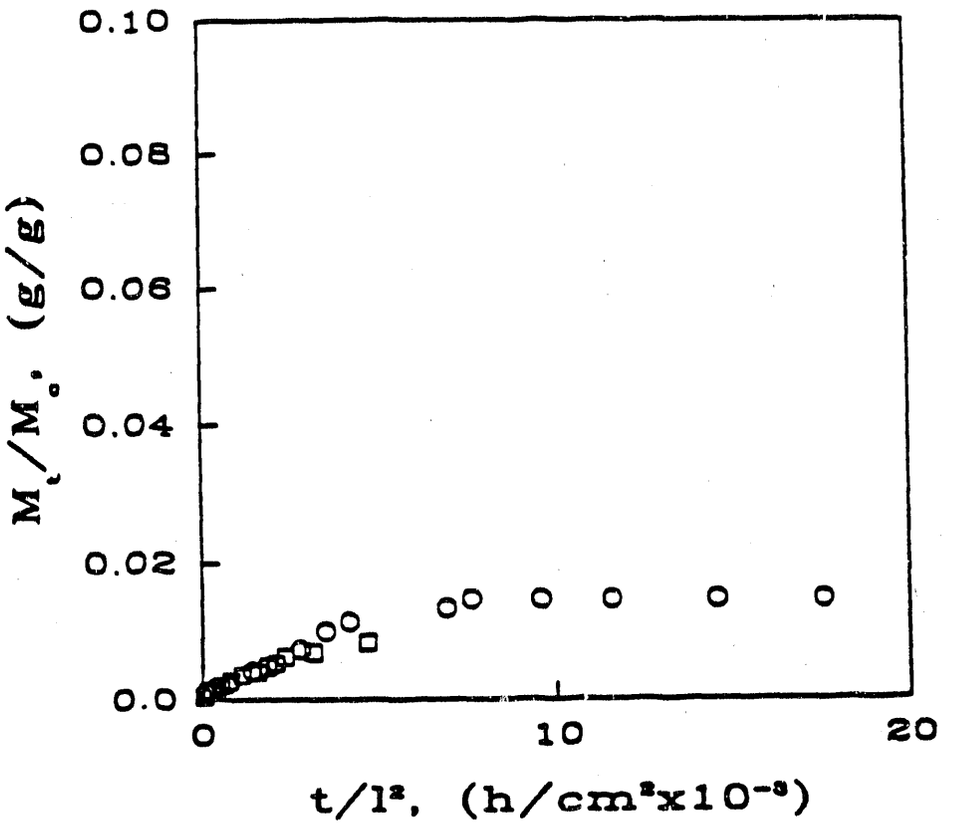

Figure 5.38 Phenomenological chloroform (penetrant activity = 0.04) uptake, M_t/M_c, as a function of normalized time, t/l^2, for coal PSOC-312 treated at: 35°C (O), 100°C (□) and 150°C (Δ).

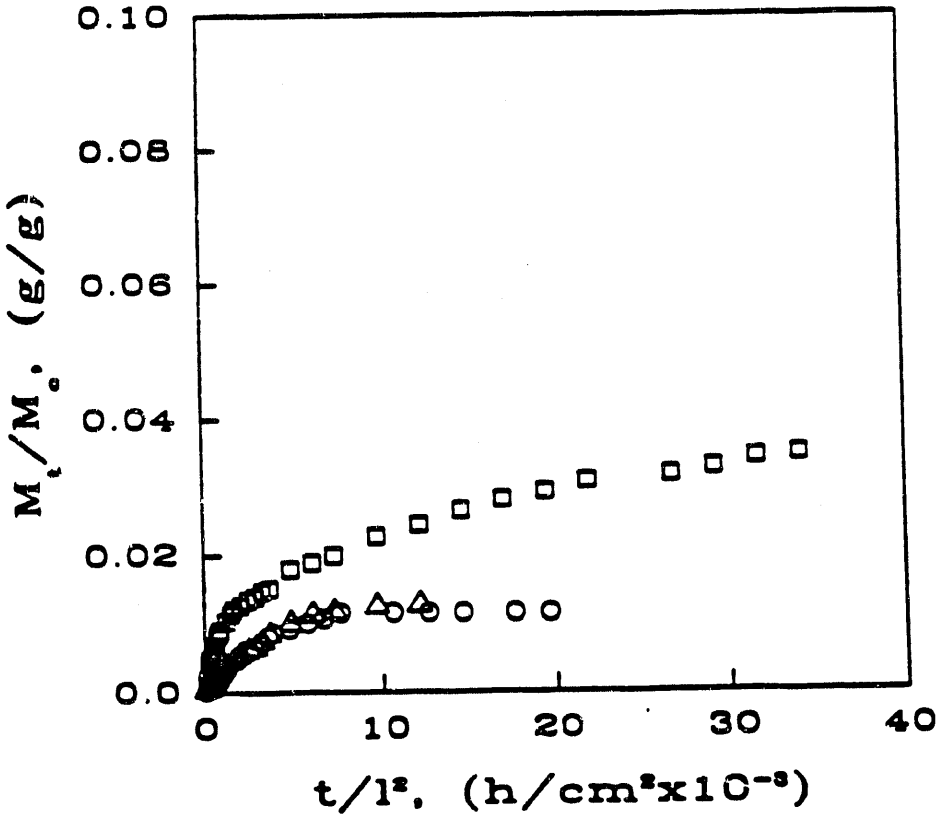

Figure 5.39 Phenomenological chloroform (penetrant activity = 0.04) uptake, M_t/M_c, as a function of normalized time, t/l^2, for coal PSOC-853 treated at: 35°C (○), 100°C (□) and 150°C (△).

highest for coals treated at 100°C followed by the values at 150°C. Therefore, the diffusion of chloroform into coals also decreases as temperature increases.

The conclusions for the penetrant uptake into coals as a function temperature treatment are:

i) for pyridine, the initial diffusion rates as well as the equilibrium penetrant uptakes increases with temperature treatment;

ii) for DMF and chloroform, the initial diffusion rates as well as the equilibrium penetrant uptakes decreases as temperature treatment increases;

iii) degradation may affect the diffusion process of DMF and chloroform into coals, but not the diffusion process of pyridine into coals.

5.2.3 Mechanistic Analysis of the Dynamic Swelling Data

The dynamic swelling data can be fitted to the semi-empirical equation (2.21) to elucidate the transport mechanisms governing penetrant diffusion into coals. The diffusional exponent n of the semi-empirical equation (2.21) can be related to the type of transport kinetics that is observed for a given macromolecule/penetrant pair. The diffusional exponent serves as a method by which actual sorption data can be analyzed in order to determine the mechanism of penetrant sorption.

The penetrant uptake behavior of pyridine, DMF and chloroform in coals can be described by fitting the initial 60% of the total penetrant uptake data to equation (2.21).

$$\frac{M_t}{M_c} = kt^n \qquad (2.21)$$

Here, k is a constant incorporating characteristics of the macromolecular network system and the penetrant, and n is the diffusional exponent which is indicative of the transport mechanism. Also,

incorporated in the constant k are the diffusion coefficient, D, and the relaxation constant, k, which describe the transport of penetrants into the macromolecular network. Possible values of the diffusional exponent for transport in films or slabs and their associated transport mechanisms are presented in Table 5.5.

Table 5.5. Diffusional Exponent n and its Associated Transport Mechanism for a One-Dimensional Diffusion Process.

Mechanism	n
Fickian	0.5
Case-II	1.0
Anomalous	$0.5 < n < 1.0$
Super Case-II	> 1.0

The phenomenological swelling data can be fitted to the semi-empirical equation to determine a phenomenological diffusional exponent, n_{phen}. The swelling data were analyzed using the semi-empirical equation (2.21). The temperature treatment, crosslinking and penetrant type effects were determined. The results of the analysis for the diffusion of pyridine, DMF and chloroform into coals PSOC 791, 247, 312 and 853 at different temperature treatments, are shown in Tables 5.6, 5.7 and 5.8, respectively. A 95% Confidence Interval (95% CI) for the diffusional exponent and the constant, k, is included.

From the results in Table 5.6, it can be seen that the transport mechanism for the diffusion of pyridine into coals treated at 35°C is Fickian diffusion. A small deviation from Fickian diffusion is observed for coal PSOC-853, indicating an anomalous transport for the higher carbon content coal. The constant k has no significance here, because it incorporates the Fickian diffusion and macromolecular relaxation contributions to the transport process which are unknown.

The results for pyridine diffusion into coals treated at 100°C show a Fickian diffusion mechanism for PSOC-791 and deviation to anomalous transport for PSOC 247 and 853. With the exception of PSOC-312 it can be seen that the transport mechanism deviates from Fickian diffusion to anomalous transport as the carbon content increases. Pyridine transport into coals treated at 150°C exhibits the same mechanistic characteristics.

Table 5.6. Analysis of Pyridine Transport by Equation (2.21)

Coal PSOC	Temperature Treatment (°C)	n	95% CI for n	k	95% CI for k
791	35	0.42	0.06	8.6×10^{-4}	2.3×10^{-4}
247	35	0.56	0.05	4.3×10^{-4}	1.1×10^{-4}
312	35	0.34	0.12	5.1×10^{-4}	2.6×10^{-4}
853	35	0.61	0.09	4.6×10^{-4}	2.0×10^{-4}
-	-	-	-	-	-
791	100	0.47	0.04	1.2×10^{-3}	2.4×10^{-4}
247	100	0.61	0.03	1.8×10^{-4}	3.3×10^{-5}
312	100	0.32	0.04	1.4×10^{-3}	3.5×10^{-4}
853	100	0.68	0.09	1.2×10^{-4}	4.4×10^{-5}
-	-	-	-	-	-
791	150	0.41	0.02	1.4×10^{-3}	1.4×10^{-4}
247	150	0.58	0.08	6.9×10^{-3}	2.8×10^{-3}
312	150	0.32	0.04	4.2×10^{-2}	9.1×10^{-3}
853	150	0.61	0.09	4.2×10^{-3}	2.0×10^{-3}

Table 5.7. Analysis of DMF Transport by Equation (2.21)

Coal PSOC	Temperature Treatment (°C)	n	95% CI for n	k	95% CI for k
791	35	0.49	0.05	8.8×10^{-4}	2.4×10^{-4}
247	35	0.51	0.04	1.5×10^{-3}	2.9×10^{-4}
312	35	0.74	0.13	6.5×10^{-5}	3.6×10^{-5}
853	35	0.62	0.29	6.6×10^{-5}	5.6×10^{-5}
-	-	-	-	-	-
791	100	0.47	0.07	1.6×10^{-3}	5.5×10^{-4}
247	100	0.67	0.03	5.7×10^{-5}	1.0×10^{-5}
312	100	0.52	0.03	9.6×10^{-5}	1.7×10^{-5}
853	100	0.70	0.04	3.3×10^{-5}	8.3×10^{-6}
-	-	-	-	-	-
791	150	0.59	0.06	3.2×10^{-4}	9.5×10^{-5}
247	150	0.55	0.03	3.9×10^{-4}	7.1×10^{-5}
312	150	0.61	0.02	6.7×10^{-5}	9.9×10^{-6}
853	150	0.65	0.04	2.4×10^{-5}	5.2×10^{-6}

Table 5.8. Analysis of Chloroform Transport by Equation (2.21)

Coal PSOC	Temperature Treatment (°C)	n	95% CI for n	k	95% CI for k
791	35	0.69	0.06	1.2×10^{-4}	3.8×10^{-5}
247	35	0.81	0.06	4.2×10^{-5}	1.4×10^{-5}
312	35	0.80	0.10	1.3×10^{-5}	7.3×10^{-6}
853	35	0.96	0.15	3.9×10^{-6}	2.5×10^{-6}
-	-	-	-	-	-
791	100	0.66	0.03	1.3×10^{-4}	2.1×10^{-5}
247	100	0.64	0.05	1.6×10^{-4}	1.2×10^{-4}
312	100	0.66	0.07	3.3×10^{-5}	2.1×10^{-5}
853	100	0.56	0.06	1.7×10^{-4}	5.8×10^{-5}
-	-	-	-	-	-
791	150	0.61	0.02	3.4×10^{-4}	3.8×10^{-5}
247	150	0.73	0.10	4.1×10^{-5}	2.1×10^{-5}
853	150	0.85	0.07	8.2×10^{-6}	3.3×10^{-6}

The transport mechanism deviates slightly from Fickian diffusion as the carbon content increases. This deviation accounts for the time it takes the macromolecular chains in the high density network coals to relax. This same mechanistic effect was observed by Hopfenberg and Frisch (1969), (see Figure 2.2). The diffusion process at low penetrant activities is concentration-independent and is described by Fickian diffusion.

Table 5.7 shows the diffusional exponent values, n, for the diffusion of DMF into coals PSOC 791, 247, 312 and 853 treated at 35°C. The lower carbon content coals show a Fickian diffusion mechanism; as the carbon content increases the mechanism becomes anomalous transport. It can be seen that as the temperature treatment increases the same mechanisms are observed. Thus, it is obvious that temperature treatments have no effect in the diffusion of low penetrant activity solvents into coals. The n values for the diffusion of pyridine and DMF into coals are very similar.

The diffusional exponent results for the diffusion of low penetrant activity chloroform into coals PSOC 791, 247, 312 and 853 are shown in Table 5.8. In this case the results for coals treated at 35°C indicate an anomalous transport for the lower carbon content coals and approach Case-II transport for the higher carbon content coals. As the temperature treatment increases, the transport mechanism remains anomalous. Therefore, contrary to the diffusion of pyridine and DMF into coals, the diffusion of chloroform vapors into coals is much faster.

Therefore, the diffusion of pyridine and DMF at low penetrant activities (<0.04) can be described by Fickian diffusion regardless of the temperature treatment (35°C-150°C). As the carbon content increases the mechanism deviates slightly to anomalous transport. The diffusion of chlororoform vapors (penetrant activity=0.04) into coals at different temperature treatments (35°C-150°C) can be described by anomalous transport.

5.2.4 Determination of Penetrant Diffusion Coefficients and Relaxation Constants from Dynamic Sorption Data

A mathematical model, first presented by Long and Richman (1960) for description of penetrant transport that results from a coupling of diffusional and relaxational phenomena has been used by several investigators to describe anomalous transport behavior in polymeric systems (Joshi and Astarita, 1979; Astarita and Nicolais, 1983). A simplified version of this mathematical model, which was proposed on the basis of heuristic arguments by Berens and Hopfenberg (1978), was utilized in this investigation to determine the relaxation constant and the penetrant diffusion coefficient for pyridine, DMF and chloroform transport in coals PSOC 791, 247, 312 and 853 at 35°C, 100°C and 150°C treatments.

The model proposed by Berens and Hopfenberg (1978) is a simple linear combination of Fickian diffusion and a first-order relaxation process. The sorption equation for this model can be written as:

$$\frac{M_t}{M_\infty} = \phi_F \left[1 - \sum_{n=0}^{n=\infty} \frac{8}{(2n+1)\pi^2} \exp\left[\frac{-D(2n+1)^2\pi^2}{l^2} t \right] \right] + \phi_R \left[1 - \exp(kt) \right] \qquad (5.1)$$

Here, M_t is defined as the mass of penetrant uptake at time t, M_∞ is the mass of penetrant uptake at infinite time, D is the penetrant diffusion coefficient for the Fickian portion of the penetrant transport, and k is a first-order relaxation constant. The terms ϕ_F and ϕ_R define the fractions of penetrant sorption which resulted from Fickian diffusion and the first-order relaxation process, respectively.

For a short time approximation, which is a reasonable assumption for the diffusion process of low penetrant activity solvents into coal, we obtain:

$$\frac{M_t}{M_\infty} = \phi_F \, 4 \left[\frac{Dt}{\pi l^2} \right]^{1/2} + \phi_R \left[1 - \exp(kt) \right] \qquad (5.2)$$

The sorption data up to the first point of equilibrium uptake were fitted to equation (5.2) using a non-linear regression analysis package (IMSL subroutines RNLIN-DRNLIN). Figure 5.40 presents the experimental results of the normalized pyridine uptake in coal PSOC-791 at 35°C as a function of time as well as the predicted values from equation (5.2). Though the model does not fit the experimental results very well, it can elucidate mechanistic changes due to temperature, carbon content and penetrant type effects.

The results of the diffusion coefficient, relaxation constant and the fraction due to Fickian diffusion, ϕ_F, for the diffusion of pyridine, DMF and chloroform into coals treated at different temperatures are tabulated in Tables 5.9, 5.10 and 5.11, respectively. Included in Tables 5.9 through 5.11 are the number of points analyzed and the sum of the squares of the error (SSE) which is minimized to predict the best unknown parameters.

It can be seen from Tables 5.9 through 5.11 that the diffusion coefficient for pyridine, DMF and chloroform diffusion in coals treated at 35° increases with carbon content to a maximum, then decreases as the carbon content increases. These results are represented graphically in Figure 5.41. An explanation to this phenomenon may be that the diffusion coefficient depends in the coal crosslink-density. The average molecular weight between crosslinks, $\overline{M}_c$, is shown as a function of carbon content in Figure 5.42. It can be seen that M_c reaches a maximum at about 78% carbon content where, one would expect the fastest diffusion rates (Barr-Howell, (1984); Lucht, (1983)).

No correlation of the diffusion coefficient with temperature treatment is observed. The diffusion studies in thermally treated coal samples were conducted at room temperature. This explains why the diffusion coefficients do not change with temperature treatment. The magnitude of the diffusion coefficients is between the range 4.0×10^{-8}-1.0×10^{-9} cm^2/s.

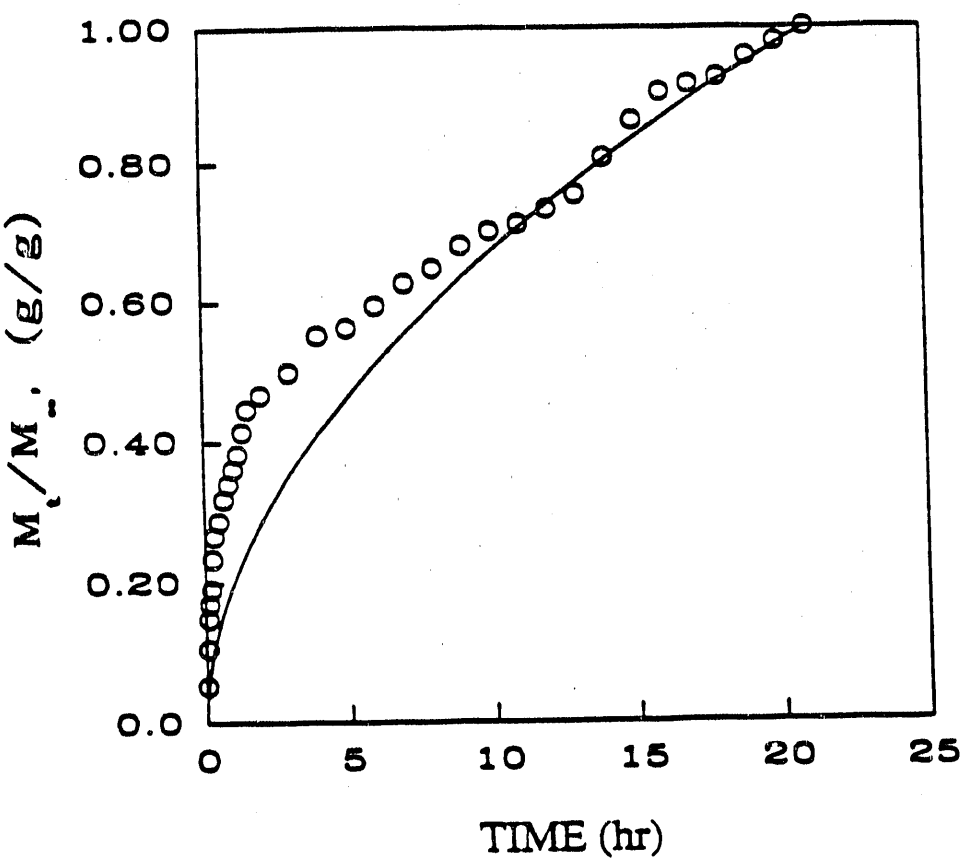

Figure 5.40 Normalized pyridine uptake, M_t/M_c, as a function of normalized time, t/l^2, for coal PSOC-791 treated at 35°C. Comparison of experimental sorption data, penetrant activity < 0.04 (O) and best fit curve from equation (5.1) (-).

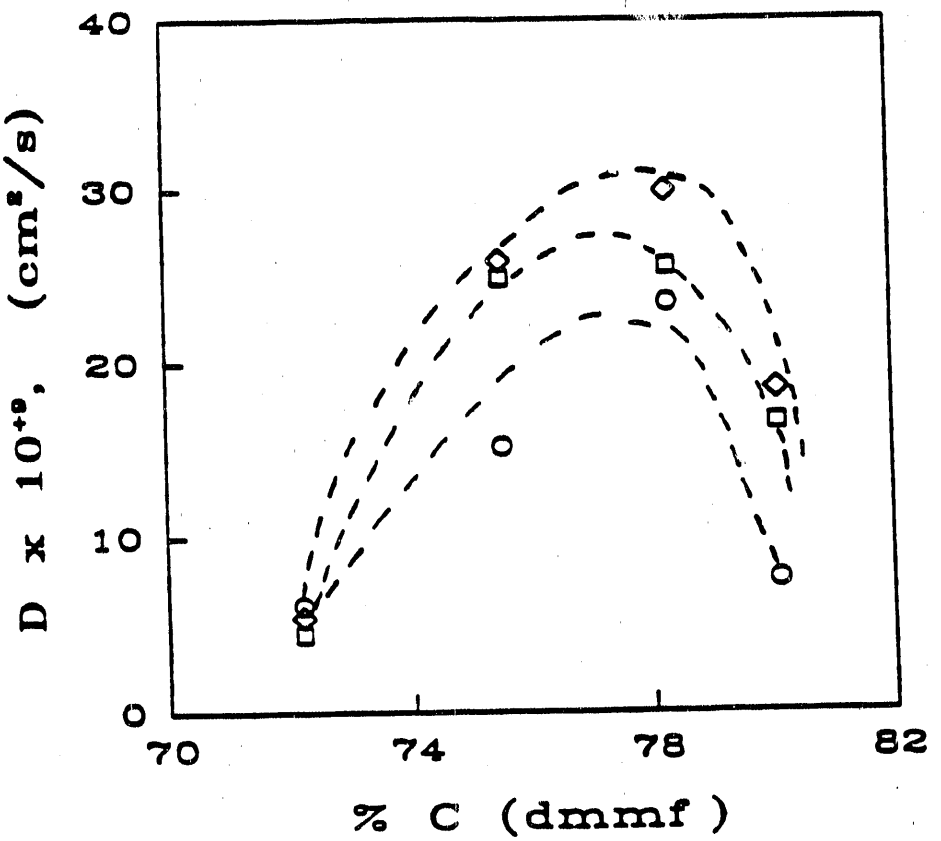

Figure 5.41 Diffusion coefficients, D, as a function of %C (dmmf.) in coals treated at 35°C for DMF (○), pyridine (□) and chloroform (◊).

Table 5.9 Diffusion Coefficients and Relaxation Constants for Pyridine Transport as Analyzed by Equation (5.2).

Coal PSOC	Temperature Treatment (°C)	D (cm^2/s)	k (s^{-1})	ϕ_P	No. Points Used	SSE
791	35	$6.1x10^{-9}$	$3.8x10^{-3}$	0.88	34	$4.7x10^{-2}$
247	35	$1.5x10^{-8}$	$1.3x10^{-6}$	0.69	30	$4.2x10^{-1}$
312	35	$2.4x10^{-8}$	$3.0x10^{-5}$	0.90	10	$2.2x10^{-2}$
853	35	$7.6x10^{-9}$	$6.4x10^{-6}$	0.77	32	$4.2x10^{-1}$
-	-	-	-	-	-	-
791	100	$1.3x10^{-8}$	$5.5x10^{-4}$	0.73	25	$2.7x10^{-2}$
247	100	$9.9x10^{-9}$	$2.0x10^{-5}$	0.62	30	$1.1x10^{-2}$
312	100	$1.0x10^{-9}$	$1.0x10^{-3}$	0.67	24	$2.5x10^{-2}$
853	100	$1.1x10^{-8}$	$1.7x10^{-5}$	0.88	25	$1.5x10^{-1}$
-	-	-	-	-	-	-
791	150	$8.6x10^{-9}$	-	1.00	31	$3.9x10^{-1}$
247	150	$1.1x10^{-8}$	$1.2x10^{-6}$	0.63	32	$1.9x10^{-1}$
312	150	$7.3x10^{-9}$	$9.5x10^{-6}$	0.87	23	$9.9x10^{-2}$
853	150	$7.7x10^{-9}$	$1.1x10^{-6}$	0.76	20	$2.7x10^{-2}$

Table 5.10 Diffusion Coefficients and Relaxation Constants for DMF Transport as Analyzed by Equation (5.2).

Coal PSOC	Temperature Treatment (°C)	D (cm^2/s)	k (s^{-1})	ϕ_F	No. Points Used	SSE
791	35	$4.5x10^{-9}$	$9.0x10^{-1}$	0.99	27	$4.5x10^{-2}$
247	35	$2.5x10^{-8}$	$2.9x10^{-3}$	0.86	17	$1.1x10^{-1}$
312	35	$2.6x10^{-8}$	$1.8x10^{-5}$	0.78	13	$6.8x10^{-2}$
853	35	$1.7x10^{-8}$	$9.1x10^{-6}$	0.66	8	$3.3x10^{-2}$
-	-	-	-	-	-	-
791	100	$1.2x10^{-8}$	$2.3x10^{-6}$	0.61	25	$9.7x10^{-1}$
247	100	$1.2x10^{-8}$	$1.0x10^{-6}$	0.33	27	$1.2x10^{-1}$
312	100	$4.5x10^{-9}$	$1.0x10^{-6}$	0.58	54	$4.5x10^{-2}$
853	100	$8.3x10^{-9}$	$4.0x10^{-6}$	0.47	34	$4.9x10^{-1}$
-	-	-	-	-	-	-
791	150	$6.6x10^{-9}$	$3.7x10^{-6}$	0.79	33	1.3
247	150	$6.6x10^{-9}$	$1.2x10^{-6}$	0.79	38	$2.1x10^{-1}$
312	150	$9.5x10^{-9}$	$3.7x10^{-6}$	0.70	34	$9.5x10^{-2}$
853	150	$7.7x10^{-9}$	$2.8x10^{-6}$	0.73	23	$6.7x10^{-2}$

Table 5.11 Diffusion Coefficients and Relaxation Constants for Chloroform Transport as Analyzed by Equation (5.2).

Coal PSOC	Temperature Treatment (°C)	D (cm^2/s)	k (s^{-1})	ϕ_F	No. Points Used	SSE
791	35	$5.5x10^{-9}$	$1.9x10^{-6}$	0.89	27	$1.2x10^{-1}$
247	35	$2.6x10^{-8}$	$2.7x10^{-7}$	0.34	34	$1.9x10^{-1}$
312	35	$3.0x10^{-8}$	$8.3x10^{-7}$	0.29	12	$2.5x10^{-1}$
853	35	$1.9x10^{-8}$	$3.5x10^{-7}$	0.75	20	$6.5x10^{-2}$
-	-	-	-	-	-	-
791	100	$1.0x10^{-8}$	$1.2x10^{-7}$	0.70	29	$5.5x10^{-2}$
247	100	$1.4x10^{-8}$	$1.7x10^{-6}$	0.89	26	$4.1x10^{-2}$
312	100	$4.0x10^{-8}$	$4.4x10^{-6}$	0.50	14	$4.5x10^{-2}$
853	100	$6.6x10^{-9}$	$5.1x10^{-7}$	0.55	32	$1.4x10^{-1}$
-	-	-	-	-	-	-
791	150	$9.8x10^{-9}$	$1.6x10^{-5}$	0.87	30	$3.8x10^{-1}$
247	150	$1.3x10^{-8}$	$8.5x10^{-7}$	0.39	32	$3.2x10^{-1}$
853	150	$8.7x10^{-9}$	$5.2x10^{-6}$	0.77	26	$1.3x10^{-1}$

5.3 In-Situ Diffusion Studies

The diffusion of liquids in materials is commonly studied by fluid uptake and/or desorption as a function of time. For simple and well characterized materials this approach is effective, but for coal, which is a heterogeneous material that varies from micro region to micro region within each sample, this technique can only give approximate results. A technique utilized with polymers is to observe the movement of the advancing penetrant front; for coal this method becomes a difficult task due to the high opacity of coals and the preparation of satisfactory samples.

Brenner (1985) was the first to observe in-situ the pyridine diffusion into coal Illinois No.6. He reported some qualitative observations of the diffusion of penetrants into coal, but not much quantitative results. In this section, in-situ studies in coals as a function of temperature, carbon content of coals, and penetrant type are reported for the first time.

5.3.1 Quantitative In-Situ Penetrant Diffusion Studies

N,N-Dimethylformamide diffusion studies in coal PSOC-853 were conducted at 25°C, 40°C, 70°C and 100°C to elucidate the temperature effects in the diffusion process. These results are presented in Figure 5.43, where the transition layer thickness (μm), is plotted as a function of time. The transition layer thickness is the distance of the advancing penetrant front from a fixed point in space at time t=0. It can be seen from this plot that the equilibrium transition layer thickness and the initial rate of change in the transition layer thickness increase with temperature (see Table 5.12). Also, the higher temperature studies reached equilibrium much faster. These results show that a temperature increase helps the macromolecular chains to relax; the relaxation time decreases and the rate of change in the transition layer thickness increases.

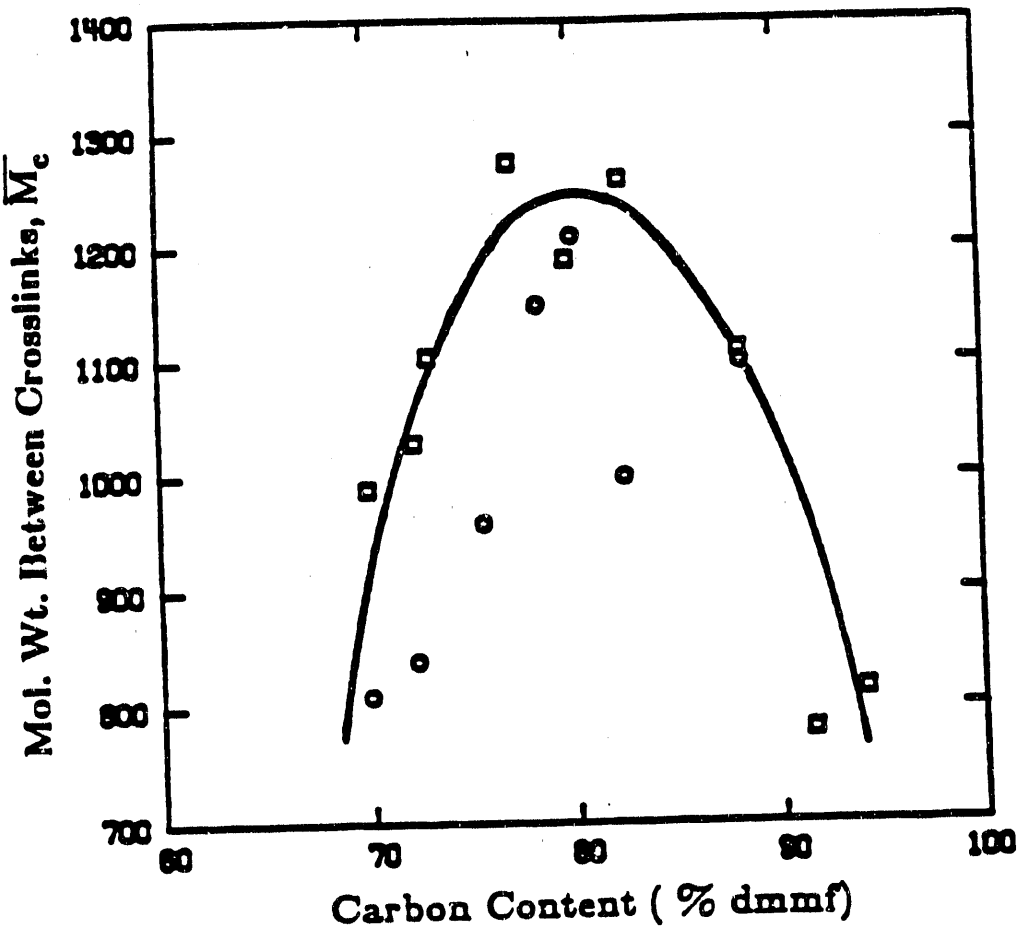

Figure 5.42 Molecular weight between crosslinks as a function of carbon content for 600-850 μm coal particles. Values of M_c obtained from equilibrium pyridine swelling studies at 35°C by Barr-Howell (1984) (○), and Lucht (1983) (□).

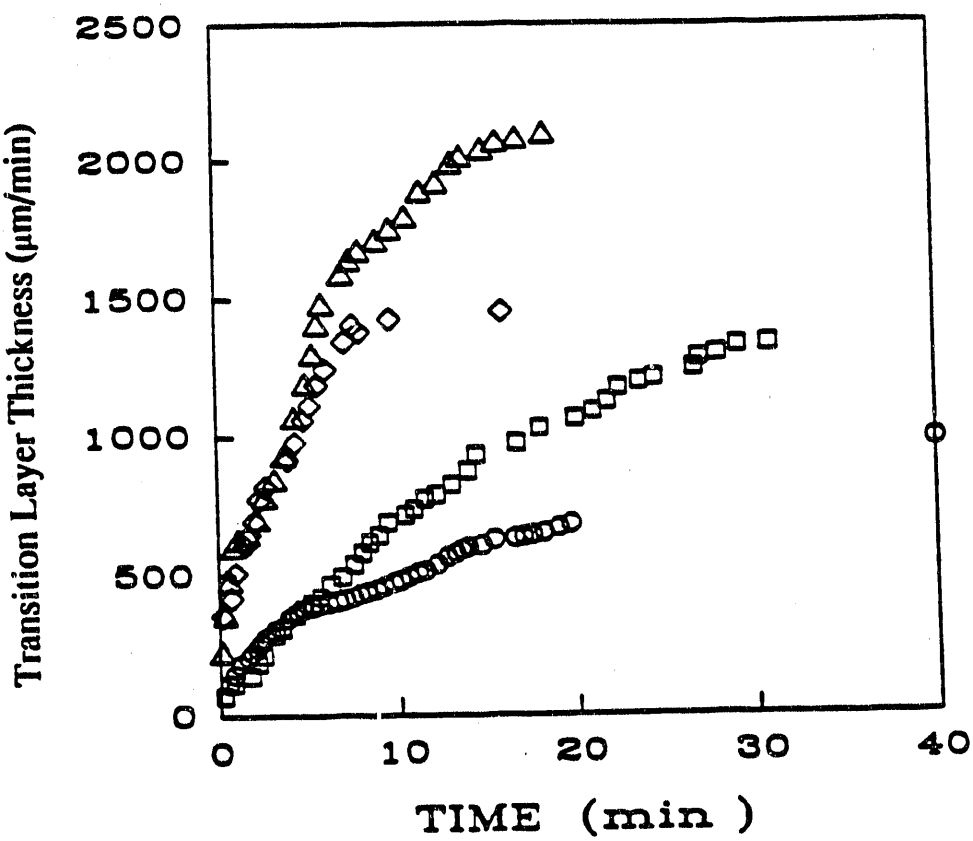

Figure 5.43 Transition layer thickness as a function of time for the diffusion of DMF into coal PSOC-853 at 25°C (O), 40°C (□), 70°C (◊) and 100°C (Δ).

Table 5.12 Rate of Change in the Transition Layer thickness, dX/dt, and the Equilibrium Transition Layer Thickness for the Diffusion of DMF in coal PSOC-853 at Various Temperatures.

Temperature (°C)	dX/dt (μm/min)	Equilibrium Transition Layer Thickness (μm)
25	34	986
40	73	1334
70	195	1453
100	216	2085

In-situ studies were also conducted as a function of carbon content of coals. Figure 5.44 depicts these results at 25°C. In this case, even though an equilibrium transition layer thickness is not well defined, the rates of change of these layers are clearly defined. The initial rate of change is higher for PSOC-247 followed by PSOC 312 and 853, respectively (see Table 5.13). It was discussed before in Section 5.1 and 5.2 why coal PSOC-247 exhibits the highest initial diffusion rates (dM_c/dt). This phenomenon can be better understood by comparing the initial diffusion rates to the average molecular weight between crosslinks as a function of carbon content of coal (see Figure 5.42). Coal PSOC-247 exhibits the highest average molecular weight between crosslinks as well as the highest initial diffusion rates.

Finally, in-situ studies were conducted in coal PSOC-853 with various solvents to elucidate the penetrant type effect in the diffusion process. The results for the diffusion of DMF, chloroform, methylene chloride, THF and pyridine into coal PSOC-853 are shown in Figures 5.45 through 5.49, respectively. In the case of methylene chloride, the diffusion process could not be continued to an equilibrium, because the solvent cracks and dissolves the coal samples. However, the initial penetrant front velocity for methylene chloride were recorded before cracking and dissolution took place (see Table 5.14). Therefore, only the initial transition layer thicknesses for all 5 penetrants will be discussed here.

From Figures 5.45 through 5.49, the transition layer thicknesses for all five penetrants will be compared after 3 minutes of exposure to the solvent. It can be seen from these figures that chloroform and methylene chloride exhibit a transition layer thickness equal to 400 μm at 3 minutes. Pyridine exhibits the next highest transition layer thickness (330 μm), followed by THF (300 μm) and DMF (250 μm). This phenomenon was also observed in the equilibrium penetrant studies as a function of solubility parameters, Section 5.1. The chlorinated solvents are more compatible with PSOC coals.

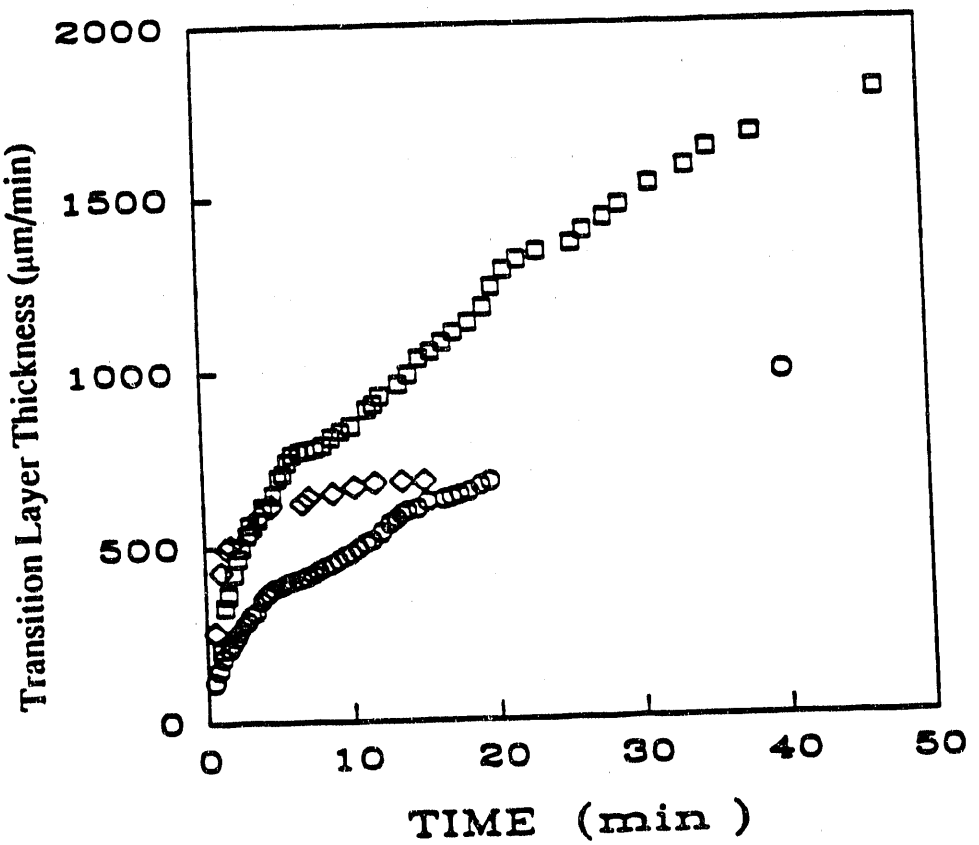

Figure 5.44 Transition layer thickness as a function of time for the diffusion of DMF at 25°C into coals PSOC-853 (O), PSOC-312 (□) and PSOC-247 (◊).

Table 5.13 Rate of Change in the Transition Layer thickness, dX/dt, for the Diffusion of DMF in PSOC coals at 25°C.

Coal PSOC	dX/dt (μm/min)
247	62
312	53
853	34

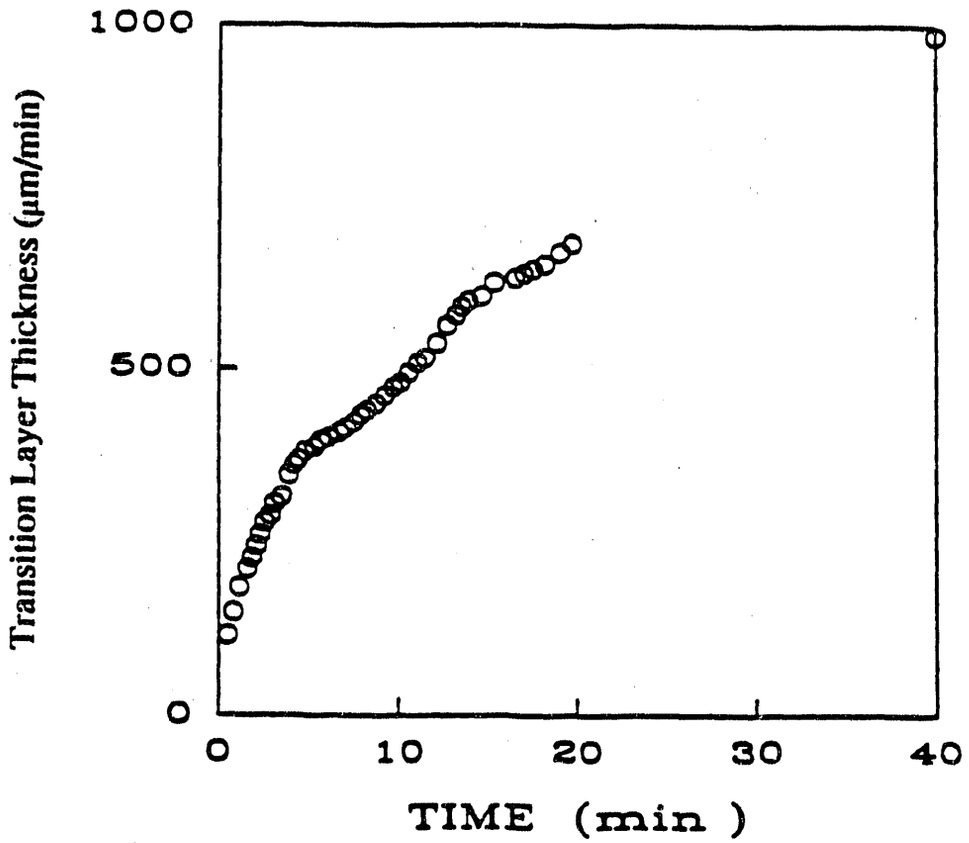

Figure 5.45 Transition layer thickness as a function of time for the diffusion of DMF into coal PSOC-853 at 25°C.

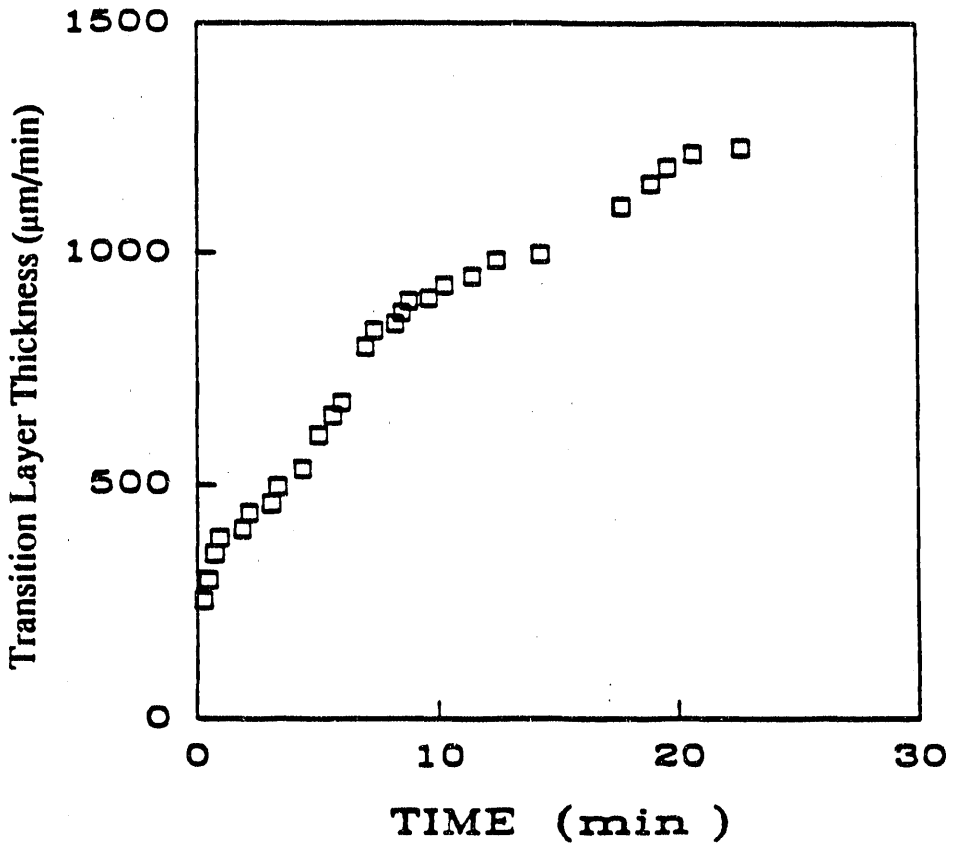

Figure 5.46 Transition layer thickness as a function of time for the diffusion of chloroform into coal PSOC-853 at 25°C.

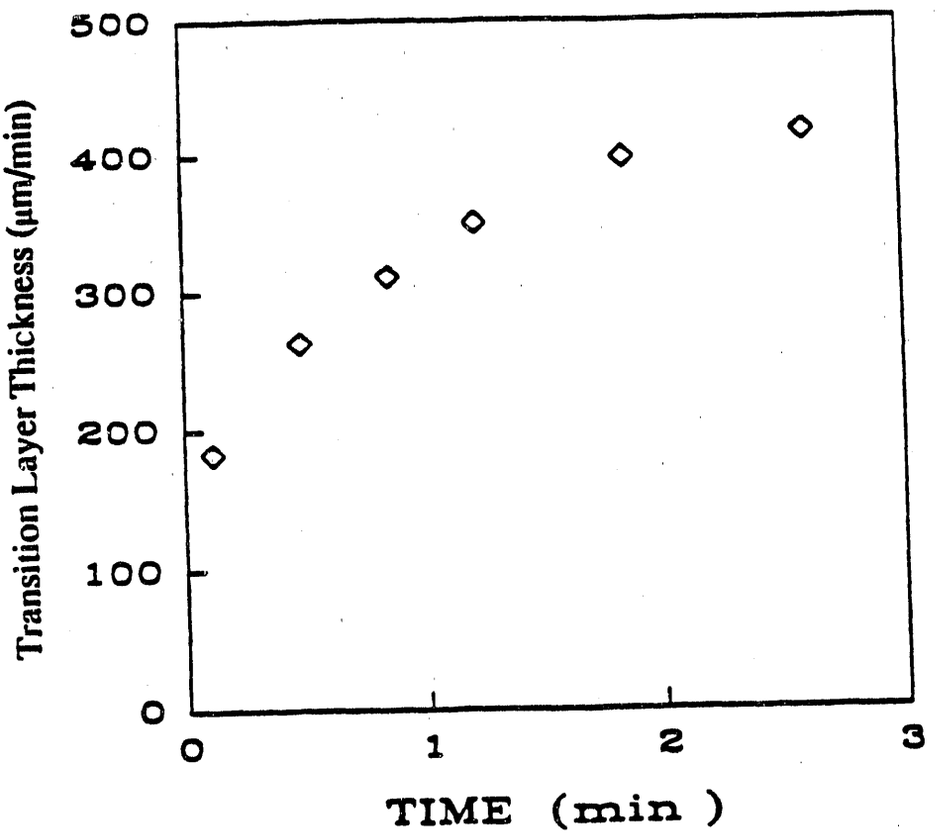

Figure 5.47 Transition layer thickness as a function of time for the diffusion of methylene chloride into coal PSOC-853 at 25°C.

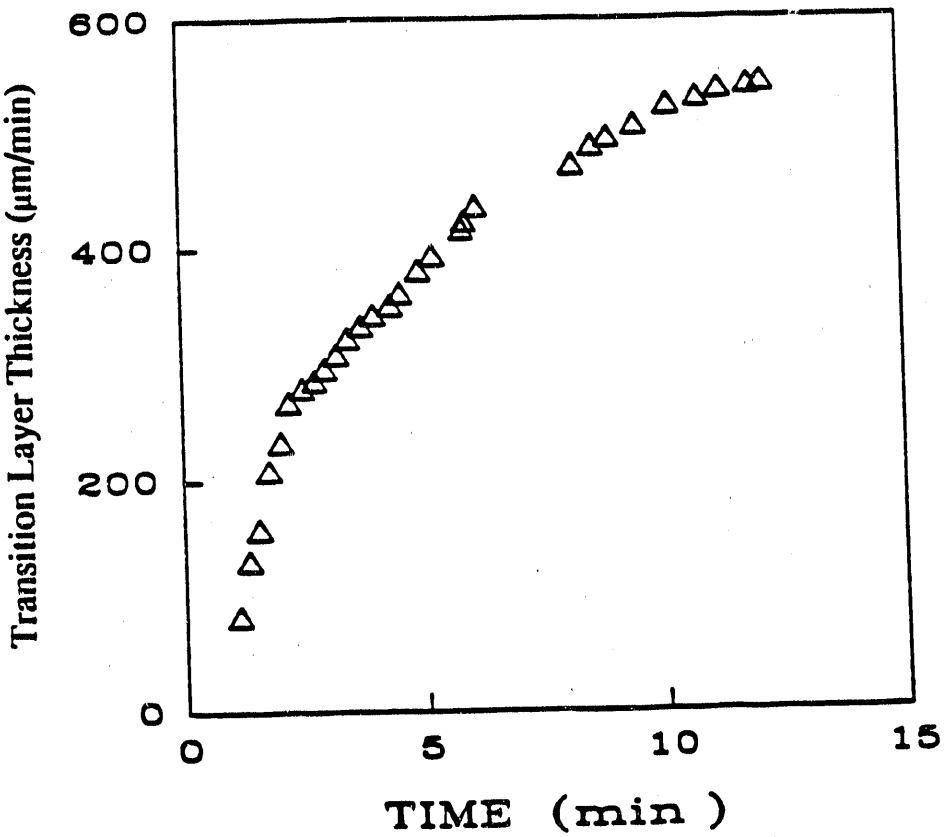

Figure 5.48 Transition layer thickness as a function of time for the diffusion of THF into coal PSOC-853 at 25°C.

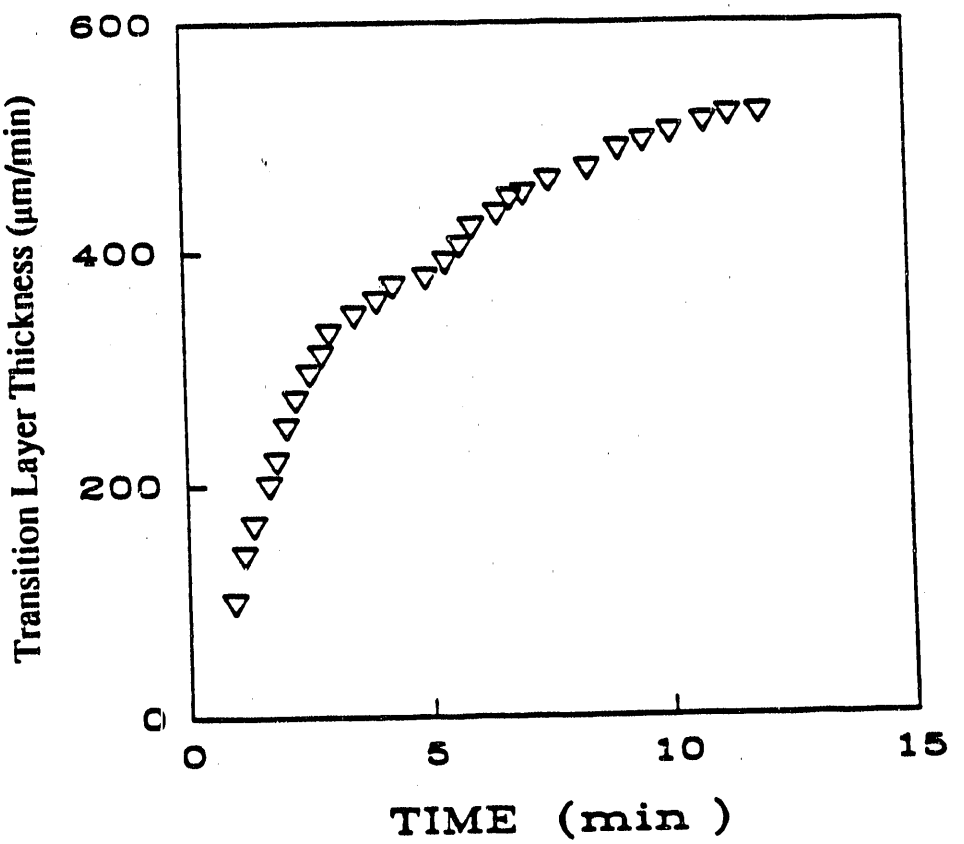

Figure 5.49 Transition layer thickness as a function of time for the diffusion of pyridine into coal PSOC-853 at 25°C.

The in-situ diffusion data were fitted to the second order polynomial:

$$X = \alpha t^2 + \beta t + \gamma \tag{5.3}$$

where X is the penetrant front position in μm, t is the time in minutes, α, β and γ are constants. A linear regression analysis can be used to solve for the three constant and to find the best fit of the data. Figure 5.50 exhibits the experimental data for the diffusion of DMF into coal PSOC-853 at 25°C, and the predicted values from the model. It can be seen that the model fits the experimental values well.

Table 5.14 Rate of Change in the Transition Layer thickness, dX/dt, for the Diffusion of Various Penetrants in coal PSOC-853 at 25°C.

Penetrant	dX/dt (μm/min)
Methylene chloride	206
Chloroform	82
THF	80
DMF	34
Pyridine	80

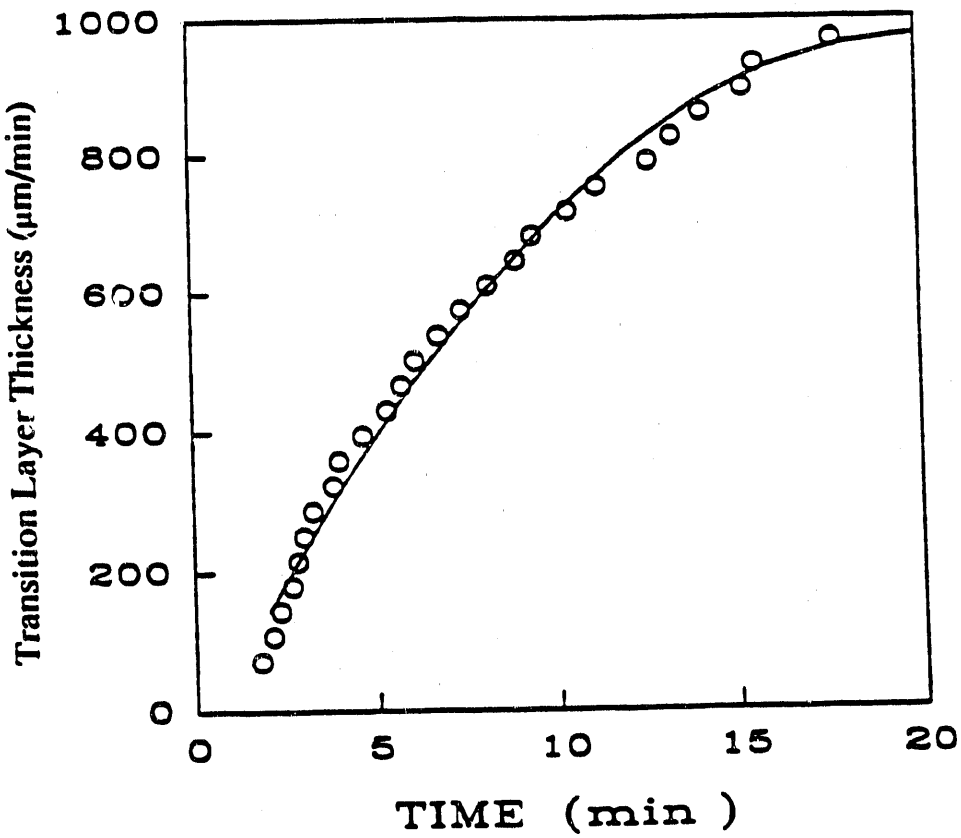

Figure 5.50 Transition layer thickness as a function of time for the diffusion of DMF into coal PSOC-853 at 25°C (O), and the best fit curve from equation (5.3) (-).

Taking the first derivative of X with respect to time, one gets an expression for the penetrant front velocity (V) in μm/min

$$V = 2\alpha t + \beta \tag{5.4}$$

The penetrant front velocities as a function of time for different temperature studies are exhibited in Figure 5.51. It can be seen that the initial velocity increases with temperature. Also, the higher temperature diffusion cases exhibit a faster equilibrium transition layer thickness. This indicates that the relaxation time decreases as temperature increases, and the rates of change in the transition layer thickness increases.

The diffusion of DMF into coal PSOC-853 is depicted in Figure 5.52 in terms of penetrant front velocity as a function of time. It can be seen, that the initial velocity is higher for coal PSOC-247, as expected, followed by coal PSOC 312 and 853, respectively. Finally, Figure 5.53 exhibits the penetrant front velocity as a function of time for the diffusion of chloroform, DMF, methylene chloride, pyridine and THF into coal PSOC-853. The initial penetrant front velocity is higher for the diffusion of methylene chloride followed by that of chloroform, pyridine, THF and DMF, respectively. This phenomenon proves once more the compatibility of chlorinated solvents with PSOC coals.

The conclusions to the in-situ diffusion studies are:

i) the diffusion of penetrants into PSOC coals increases with temperature;

ii) equilibrium transition layer thickness is attained much faster at high temperatures;

iii) coal PSOC-247 exhibits the highest rates of change in the transition layer thickness, indicating that it is the lowest crosslinked coal;

iv) chlorinated solvents exhibit the higher penetrant front velocities in coal PSOC-853.

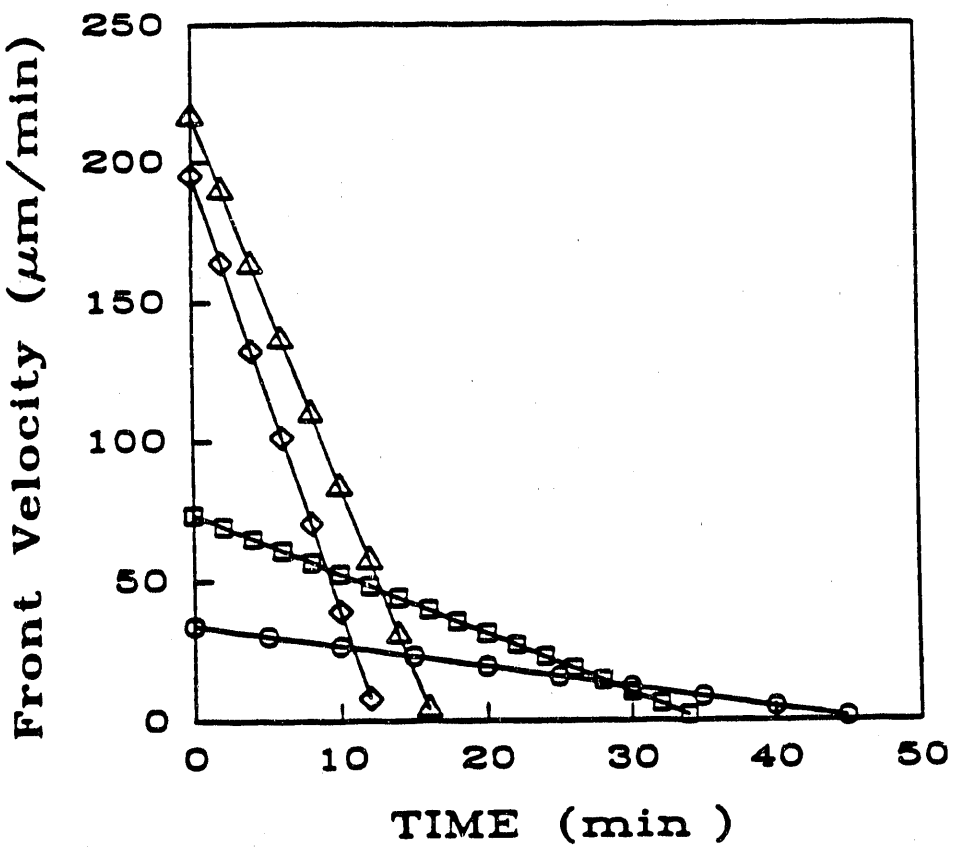

Figure 5.51 Penetrant front velocity, V, as a function of time for the diffusion of DMF into coal PSOC-853 at 25°C (○), 40°C (□), 70°C (◇) and 100°C (△).

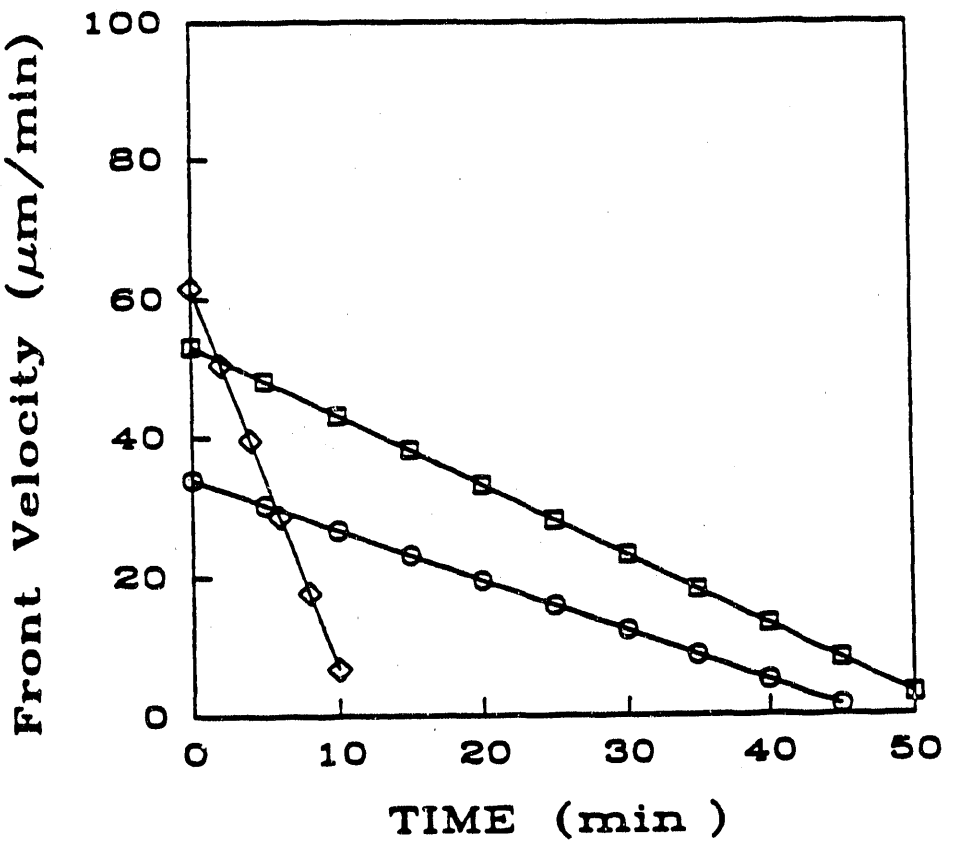

Figure 5.52 Penetrant front velocity, V, as a function of time for the diffusion of DMF at 25°C into coals PSOC-853 (○), PSOC-312 (□) and PSOC-247 (◇).

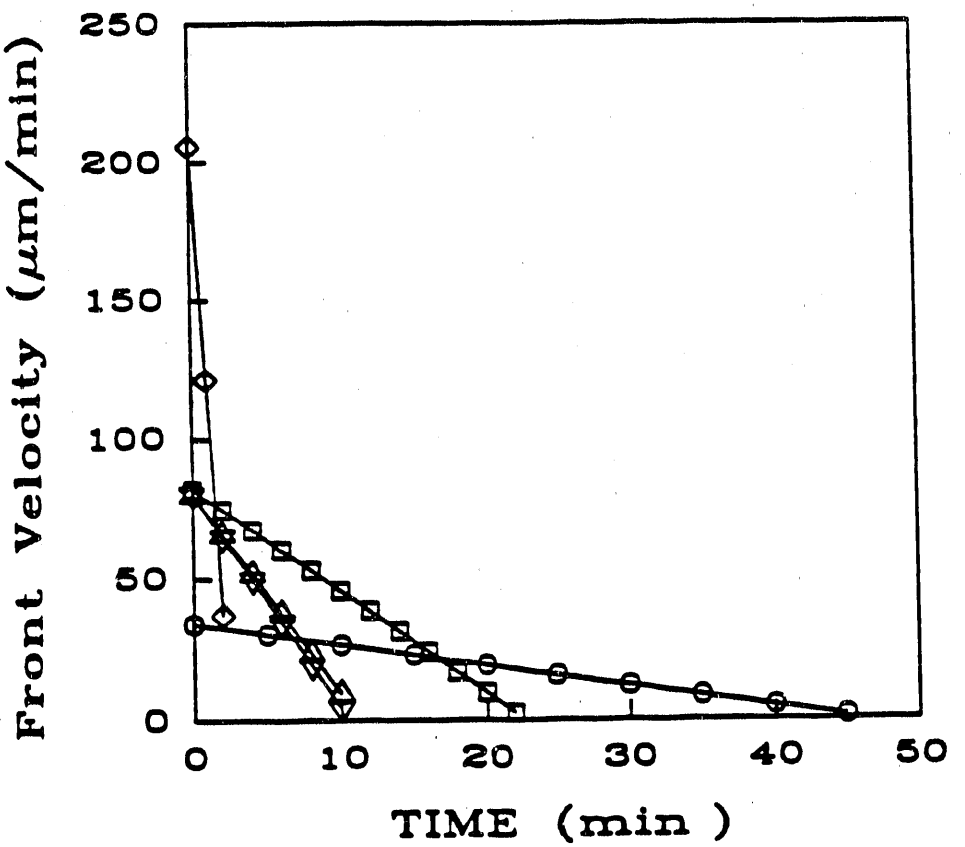

Figure 5.53 Penetrant front velocity, V, as a function of time for the diffusion of penetrants into coal PSOC-853 at 25°C. DMF (○), chloroform (□), methylene chloride (◊), THF (△) and pyridine (▽).

5.3.2 Qualitative Discussion of In-Situ Studies

In this section the in-situ observations of the penetrant diffusion into coal are discussed qualitatively. The observations were taken from a monitor that was connected to a polarized microscope. Photographs were taken from the monitor with a 35 mm camera (NikonFM, Garden City, NY) to elucidate the in-situ diffusion process. Coal under transmitted polarized light has a dark red color. When the penetrant is introduced into the coal network, swelling takes place, and the color changes from the dark red of the unswollen coal to a light orange color of the expanded coal network. This change in color positioned at swollen region is caused by the orientation of the coal structure. The expanding coal behind the diffusion front is constrained by the unswollen coal ahead of the diffusion front. This constraint leads to the stretching and alignment of the macromolecular network in this region. Such partially oriented macromolecular chains cause a significant difference in the index of refraction parallel and perpendicular to the direction of orientation (Brenner, 1985). This causes a rotation in the direction of polarization of light passing through the specimen, and the result is a higher index of refraction for the swollen area.

The swollen and unswollen areas in coal are separated by a sharp advancing penetrant front. This separation is evident in Figure 5.54, for the diffusion of DMF into coal PSOC-853 at 25°C. In this case, DMF is diffusing in from the left side and advancing in through the glassy region. It can be seen that behind the advancing penetrant front, the coal specimen begins to craze, and this crazing progresses as the penetrant concentration increases. Crazing of coal is due to the stresses formed by the penetrant concentration gradient. The direction of the crazed lines gives the impression that the macromolecular chains rearrange and orient in the direction of the diffusing penetrant. It also gives the impression that coal becomes rubbery behind the advancing front. This indicates that the glass transition temperature, T_g, decreases as the penetrant concentration increases. Therefore, it is possible to lower the glass

transition temperature of coal to room temperature, by attaining a certain penetrant concentration.

The diffusion of DMF into coal PSOC-853 at 25°C is shown in Figures 5.55 through 5.63. The transition layer thickness is given as a function of time. The coal sample PSOC-853 before penetrant diffusion is shown in Figure 5.55a. The unexposed coal sample has a very sharp edge; thus diffusion occurs uniformly.

Coal exposed to DMF after 19 seconds (Figure 5.55b) shows an edge exposed to the DMF which starts to deform. This is due to the stresses formed from the DMF concentration gradient. It can also be observed that the light blue section of the figure gets darker when the DMF is introduced. This indicates that DMF has adsorbed some of the polarized light. The diffusion process after 80 seconds is shown in Figure 5.56a. The initial boundary has moved outwards, indicating that coal expands anisotropically (parallel and perpendicular to the direction of the bedding plane). A change in color is observed, indicating that there is a swollen and a glassy state present.

As the penetrant concentration gradient increases, the stresses increase and the coal begins to craze (Figure 5.56b). In this case, coal PSOC-853 has been exposed to DMF for 122 seconds. A sharp penetrant front begins to form, leaving behind a crazed coal material. A sharp front can be observed with a transition layer thickness of 947 μm after 166 seconds (Figure 5.57a). It is observed also that the crazed material starts to crack forming holes within the coal specimen. This indicates that a chemical reaction may be taking place. The holes formed within the coal have different areas, and are not randomly spaced apart. This phenomenon is due to the heterogeneity of the network.

Figures 5.57b through 5.62b show the transition layer thickness of DMF into the same coal specimen at 25°C from 976 μm to 1427 μm. Coal PSOC-853 obtains an equilibrium transition layer thickness after 17.5 minutes of exposure to DMF. The advancing penetrant front as a function of time

can be observed from the photographs; also the moving boundary can be observed, which indicates swelling in a direction parallel to the bedding plane. Finally Figure 5.63, shows the same diffusion process after 17.5 minutes. In this case the frame of reference is shifted to the right to elucidate the equilibrated penetrant front.

The diffusion of methylene chloride into coal PSOC-853 at 35°C is shown in figures 5.64a through 5.66b as a function of time. Figure 5.64a shows the diffusion process after 14 seconds. It can observed that the coal specimen starts to crack immediately. This phenomenon is due to the strong stresses formed from the methylene chloride concentration gradient. It was mentioned before in this chapter that chlorinated compounds and PSOC coals are very compatible. Figure 5.65a, shows how the cracks start to propagate through the coal. Finally in Figures 5.65b and 5.66a, it is observed that methylene chloride starts to dissolve some of the coal. This indicates that strong chemical reactions are occurring during the diffusion process, and that chemical reaction rates are much faster than the diffusion rates. This is an indication of Case-II and Super Case-II transport. Finally, Figure 5.66b exhibits the methylene chloride diffusion process into the coal specimen after 5 minutes.

The diffusion of chloroform into coal PSOC-853 at 25°C is exhibited in Figures 5.67a through 5.68b as a function of time. A similar phenomenon of cracking in the coal specimen as in the methylene chloride diffusion process is observed. In this case the cracks observed are much smaller than those caused by methylene chloride. Also, less dissolution is observed for the chloroform diffusion process. This indicates that the stresses due to the concentration gradient of methylene chloride are much stronger than those caused by chloroform.

The diffusion of THF into coal PSOC-853 at 25°C is exhibited in Figure 5.69a. It is observed that THF crazes coal, but to a lesser extent. In this case the index of refraction for the swollen region is smaller than that of DMF.

The diffusion of DMF into coal PSOC-853 at 40°C, 70°C, and 100°C is exhibited in Figures 5.69b, 5.70a, and 5.70b, respectively. The dark circle around the sample comes from the hot plate source, which has an opening of about 1 mm. in diameter for the transmission of light. The dark bubbles observed are from the movement of silicone grease as temperature increases. It can be seen that as temperature increases, the amount of crazing in coal increases. This is expected, because an increase in temperature as well as concentration increases the movement of the macromolecular chains.

Diffusion into coal as a function of temperature, crosslink, and penetrant type has been observed in-situ at the microscopic level for the first time. For the diffusion of DMF, pyridine, and THF a sharp penetrant front was observed, and the diffusive flow was highly concentration dependent. The movement of the front slowed with depth of penetration into the coal. When the coal samples are exposed to a penetrant, the index of refraction for the swollen portion of the coal sample increases. This indicates that the orientation of the macromolecular network occurs as a result of the stresses of the penetrant concentration gradient. Swelling of coals with chlorinated solvents, induces cracking and possible dissolution of coal. This is an indication of the compatibility of coals with chlorinated penetrants.

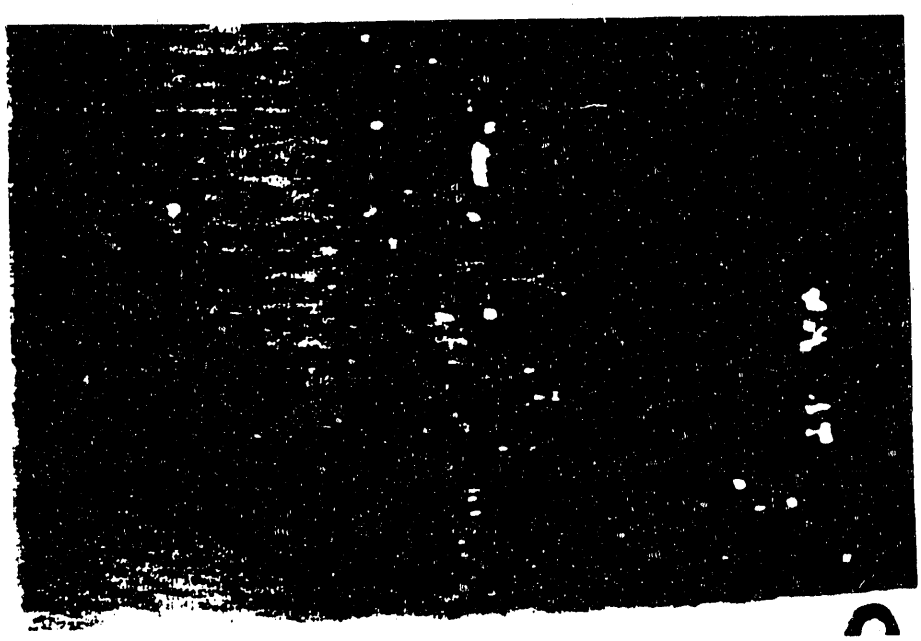

Figure 5.54 DMF diffusion into coal PSOC-853 at 25°C.

(a)

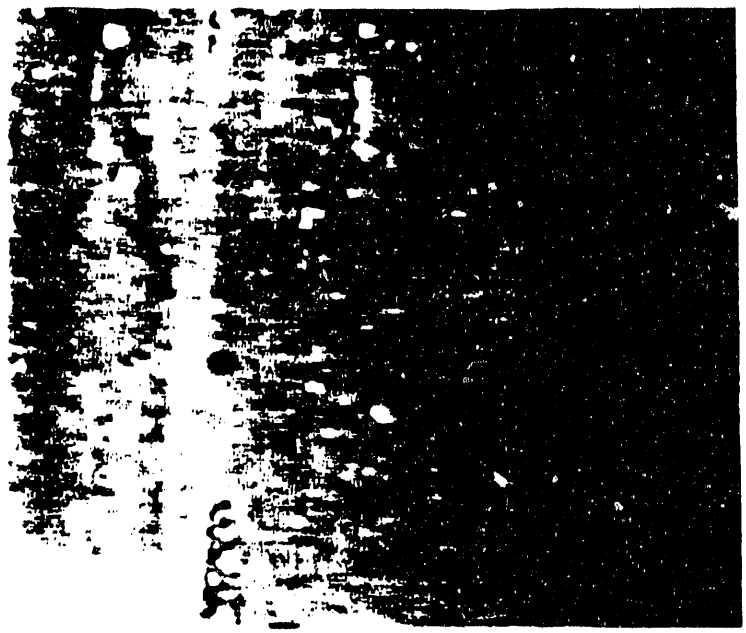

(b)

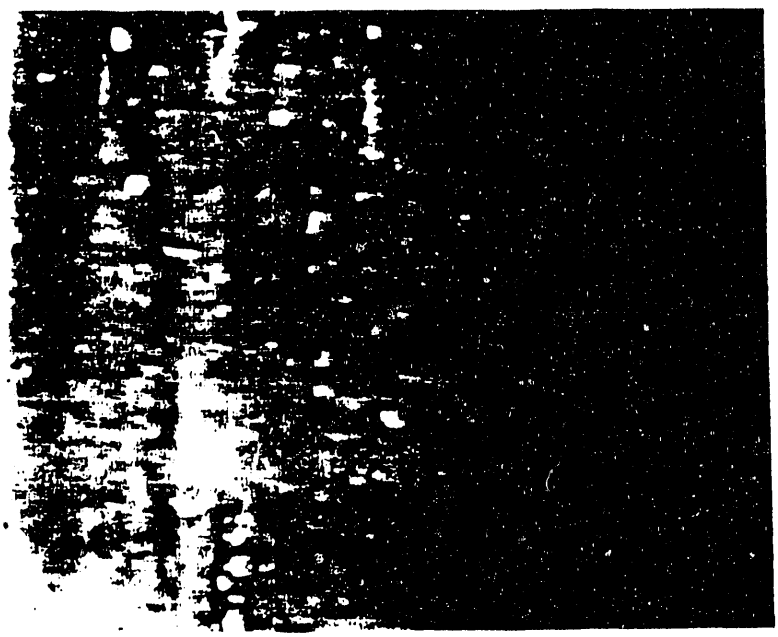

Figure 5.55 Diffusion of DMF in coal PSOC-853 at 25°C, thickness: 7.6 μm; (a) before DMF diffusion and (b) after 0.32 minutes (transition layer thickness: 83.2 μm).

(a)

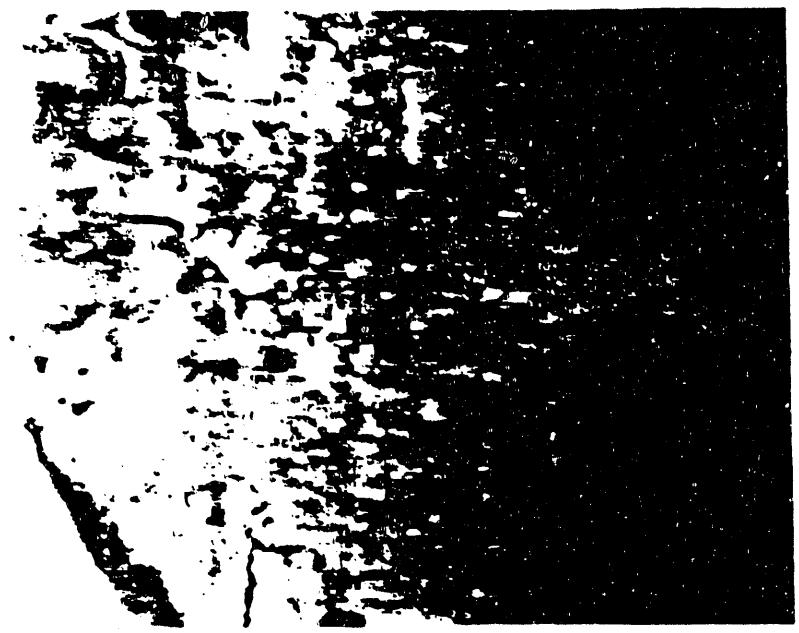

(b)

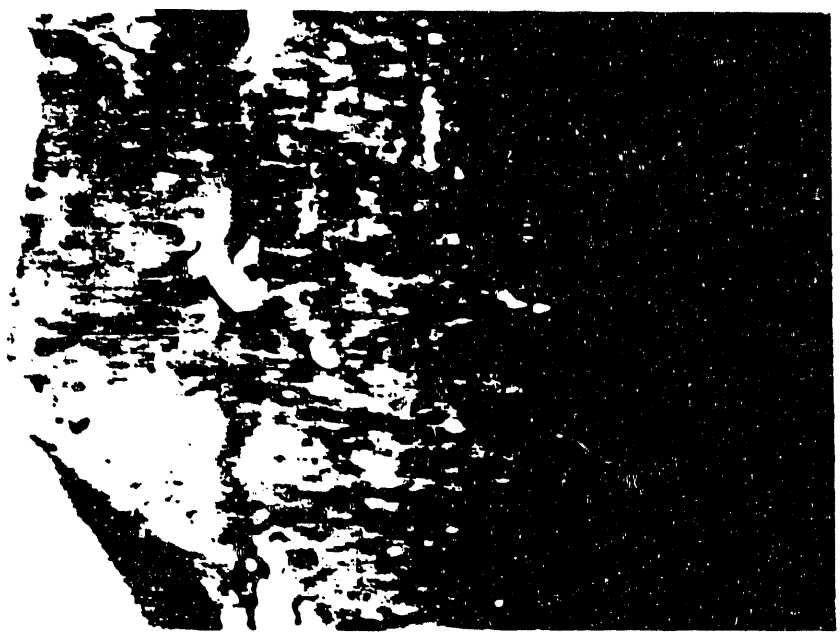

Figure 5.56 Diffusion of DMF in coal PSOC-853 at 25°C, thickness: 7.6 μm; (a) after 1.33 minutes (transition layer thickness: 614.0 μm) and (b) after 2.03 minutes (transition layer thickness: 865.8 μm).

(a)

(b)

Figure 5.57 Diffusion of DMF in coal PSOC-853 at 25°C, thickness: 7.6 μm; (a) after 2.80 minutes (transition layer thickness: 946.8 μm) and (b) after 3.25 minutes (transition layer thickness: 975.5 μm).

(a)

(b)

Figure 5.58 Diffusion of DMF in coal PSOC-853 at 25°C, thickness: 7.6 μm; (a) after 3.73 minutes (transition layer thickness: 997.0 μm) and (b) after 4.50 minutes (transition layer thickness: 1018.6 μm).

(a)

(b)

Figure 5.59 Diffusion of DMF in coal PSOC-853 at 25°C, thickness: 7.6 μm; (a) after 5.80 minutes (transition layer thickness: 1068.8 μm) and (b) after 6.67 minutes (transition layer thickness: 1111.8 μm).

(a)

(b)

Figure 5.60 Diffusion of DMF in coal PSOC-853 at 25°C, thickness: 7.6 μm; (a) after 7.72 minutes (transition layer thickness: 1140.5 μm) and (b) after 9.05 minutes (transition layer thickness: 1162.0 μm).

(a)

(b)

Figure 5.61 Diffusion of DMF in coal PSOC-853 at 25°C, thickness: 7.6 μm; (a) after 10.48 minutes (transition layer thickness: 1212.2 μm) and (b) after 12.05 minutes (transition layer thickness: 1269.6 μm).

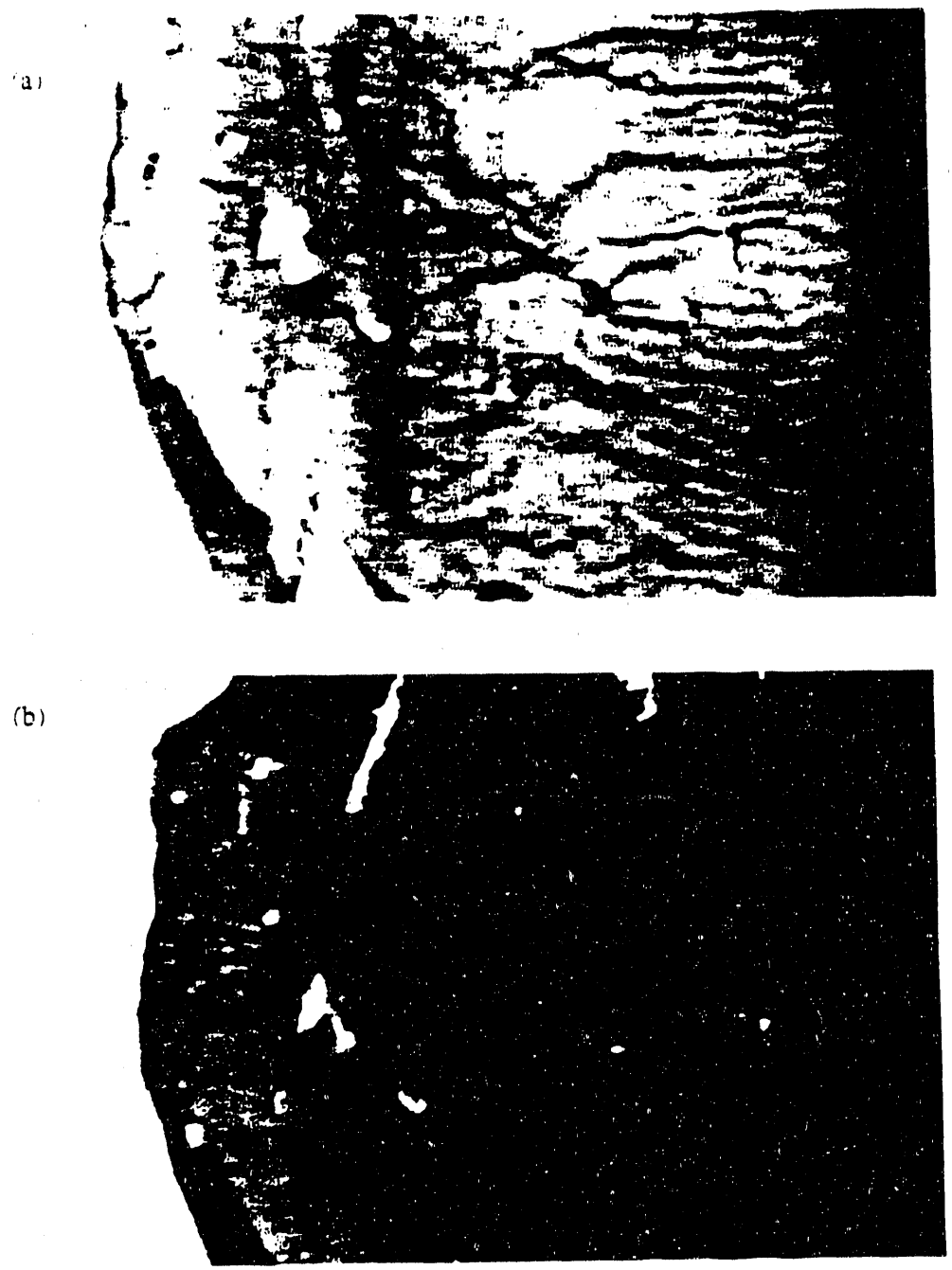

Figure 5.62 Diffusion of DMF in coal PSOC-853 at 25°C, thickness: 7.6 μm; (a) after 14.10 minutes (transition layer thickness: 1334.2 μm) and (b) after 16.80 minutes (transition layer thickness: 1427.4 μm).

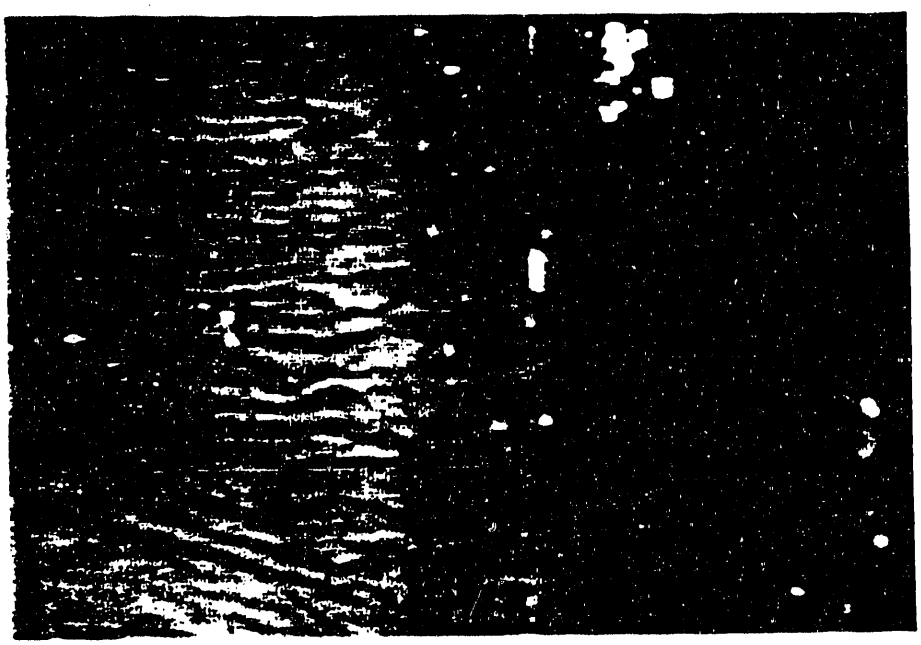

Figure 5.63 Equilibrium DMF front in coal PSOC-853 at 25°C separating the glassy and the swollen regions, 17.35 minutes.

(a)

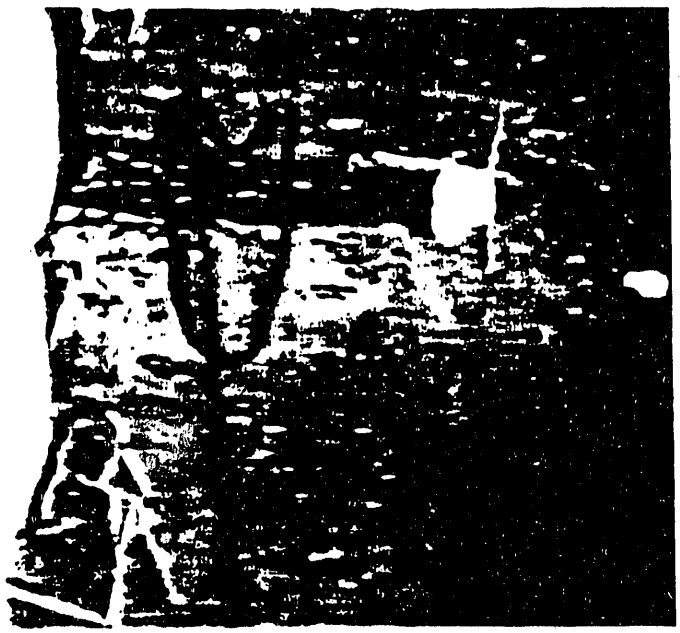

(b)

Figure 5.64 Diffusion of methylene chloride in coal PSOC-853 at 25°C, thickness: 7.6 μm: (a) after 0.23 minutes and (b) after 0.70 minutes.

(a)

(b)

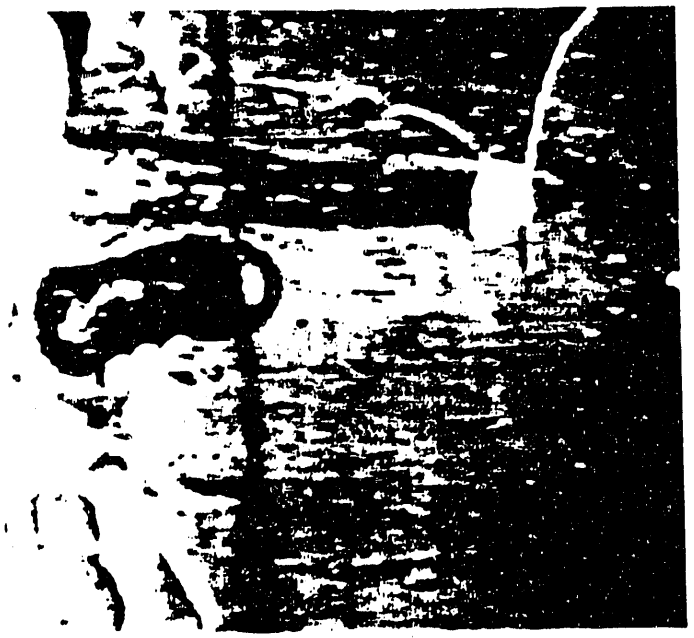

Figure 5.65 Diffusion of methylene chloride in coal PSOC-853 at 25°C, thickness: 7.6 μm; (a) after 1.05 minutes and (b) after 1.50 minutes.

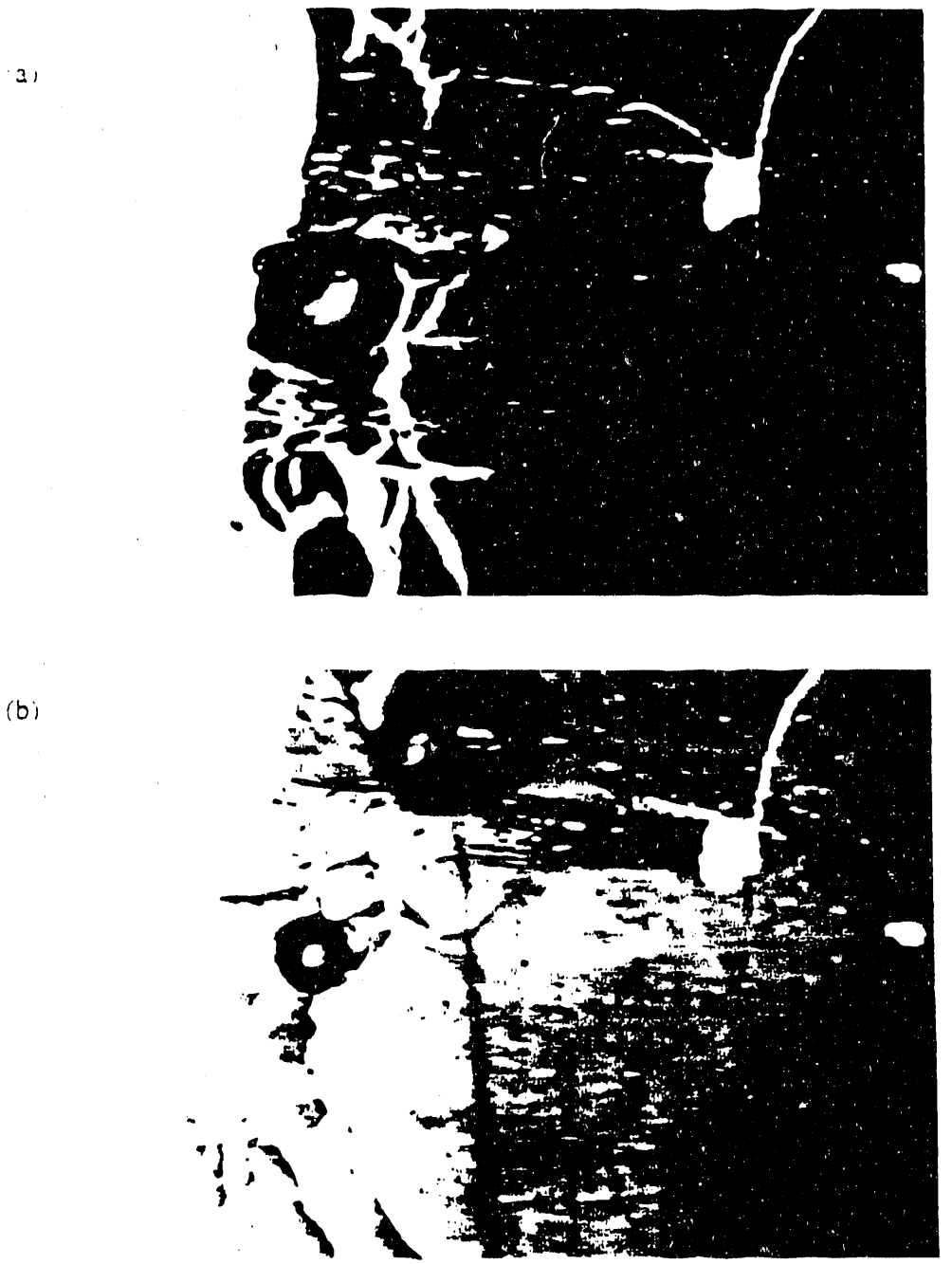

Figure 5.66 Diffusion of methylene chloride in coal PSOC-853 at 25°C, thickness: 7.6 μm; (a) after 2.60 minutes and (b) after 5.00 minutes.

(a)

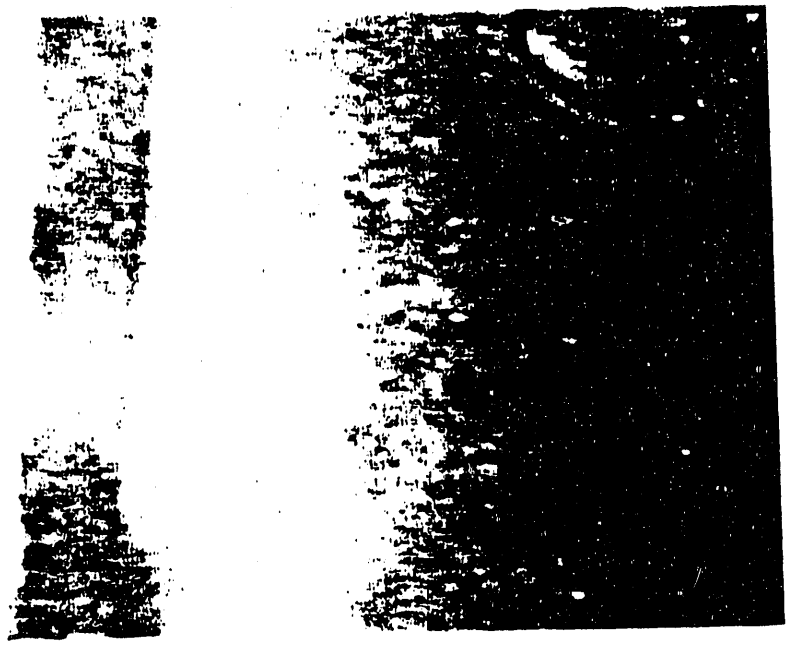

(b)

Figure 5.67 Diffusion of chloroform in coal PSOC-853 at 25°C, thickness: 7.6 μm; (a) before chloroform diffusion and (b) after 0.97 minutes.

(a)

(b)

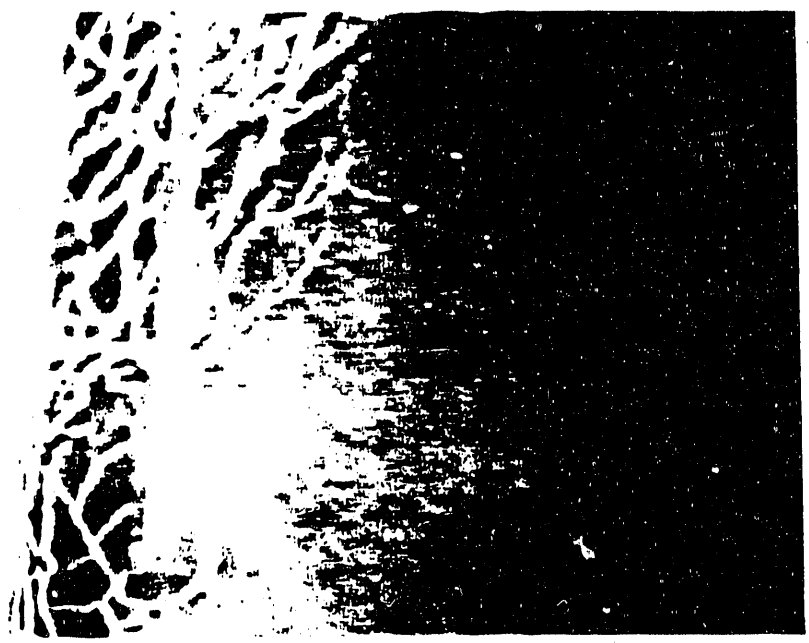

Figure 5.68 Diffusion of chloroform in coal PSOC-853 at 25°C, thickness: 7.6 μm; (a) after 3.28 minutes and (b) after 3.68 minutes.

(a)

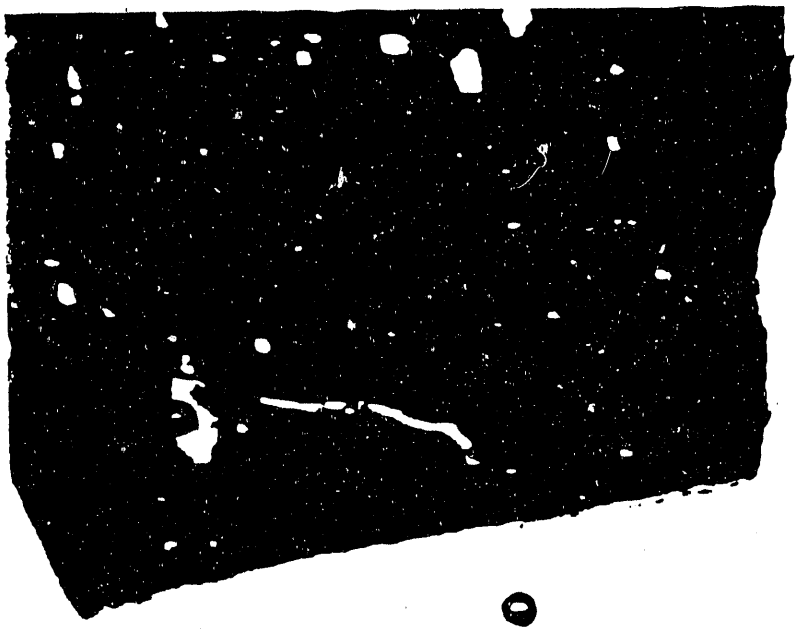

(b)

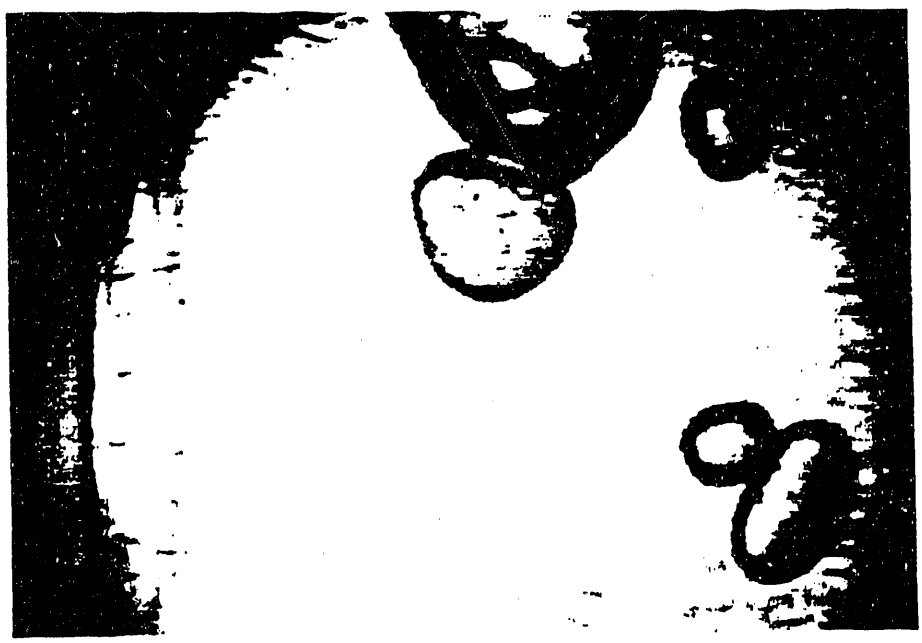

Figure 5.69 (a) Diffusion of THF in coal PSOC-853 at 25°C, thickness: 7.6 μm and (b) diffusion of DMF in coal PSOC-853 at 40°, thickness: 7.6 μm.

(a)

(b)

Figure 5.70 Diffusion of DMF in coal PSOC-853, thickness: 7.6 μm at: (a) 70°C and (b) 100°C.

6. CONCLUSIONS AND RECOMMENDATIONS

Penetrant transport studies were conducted in PSOC coals as a function of temperature treatment, crosslinking and penetrant type. The effects of these three parameters on the diffusion of penetrants into coals were analyzed phenomenologically and with mechanisms. In-situ microscopic diffusion studies in coals at different temperatures were obtained for the first time. This research is a continuation to previous work in our laboratory.

In the earliest work, Lucht (Lucht, 1983; Peppas et al., 1983) investigated the diffusion of pyridine in pre-extracted and unextracted coal samples for particles of two different sizes, 150-180 μm and 600-850 μm, and for coal chunks (1-2 cm^3). A general conclusion to their work was that the pyridine transport changes from non-Fickian to Fickian diffusion as the particle size decreases. These conclusions were based on the analysis of the sorption data using the diffusional exponent of equation (2.21).

Subsequently, Barr-Howell (Barr-Howell, 1984; Barr-Howell and Peppas, 1985; Barr-Howell et al., 1986b) conducted swelling studies in thin coal sections with various amines, and various temperatures (up to °C). They also conducted swelling studies on well characterized stiff-chain polymers that simulate coal structures. Many conclusions were made on their work in coals, one of them been the elucidation of an anomalous penetrant transport mechanism. An effort was made to obtained high temperature diffusion studies. However, degradation of coal was a problem. They observed negative penetrant uptakes (loss of weight) for the diffusion studies at 100° C or higher.

Ritger (Ritger and Peppas, 1987a; Ritger and Peppas, 1987b) continued the work by conducting high penetrant activity swelling studies in thin coal sections of different thicknesses. The studies were also conducted as a function of temperature (up to 65°C). Their conclusions were that, within a

thickness rage of 150 μm to 1500 μm the transport mechanism of pyridine in the macromolecular structure of coal is purely relaxation-controlled. At 65°C, coal is well below its glass transition temperature, and the penetrant transport mechanism remains Case-II transport or relaxation controlled.

Even though the work in the diffusion of penetrants into coals seemed to be completed, there were many questions generated from previous work that needed to be answered. At that time (1988), this research was initiated with the purpose to answer these questions:

i) is it possible to obtain dynamic swelling data at high temperatures and account for degradation?

ii) how can the diffusional and relaxational processes be decoupled?

iii) what are the effects of temperature, crosslinking and penetrant type on the diffusion of penetrants into coal?

Thermogravimetric swelling studies in coal were conducted in order to answer these questions.

i) In previous work (Barr-Howell et al., 1987), a thermogravimetric analyzer was used to obtain dynamic swelling data at high temperatures. A problem with this technique is that there is a temperature gradient between the micro-furnace which contains the coal sample and the sourrounding atmosphere. Therefore, the penetrant activity changes as the penetrant approaches the high temperature micro-furnace. Also, if any penetrant diffusion occurs at high temperatures, one has to account for simulataneous coal degradation. A convenient way to elucidate the temperature effects on the diffusion of penetrants into coal, is to conduct swelling studies at room temperature in thermally treated coal samples. By thermally treating coal samples, we are accounting for coal degradation and rearrangement of the macromolecular chains.

ii) Berens and Hopfenberg (1978) proposed an mathematical expression for the diffusion of penetrants into glassy polymers which incorporates the Fickian and macromolecular relaxation

contributions to the diffusion process. Dynamic swelling data for coal were fitted to this model before (Ritger and Peppas, 1987b); however, no elucidation of the diffusion coefficient could be made. Ritger and Peppas (1987b) concluded that the diffusion of high activity pyridine vapors into PSOC coals is purely relaxation controlled. This indicates that the Fickian term in equation (5.1) is zero. In order to elucidate the diffusional and relaxational contributions to the transport process, the transport mechanism must be anomalous transport. This can be accomplished by lowering the penetrant activity of the diffusion process (Hopfenberg and Frisch; 1969). In this work, we were able to elucidate changes in the diffusion coefficient and the relaxation constant when the penetrant activity equal 0.04.

iii) The equilibrium penetrant uptake studies in coal as a function of solubility parameter, indicate that penetrants with a solubility parameter equal to 9.5 $cal^{1/2}/cm^{3/2}$ exhibit the highest swelling to PSOC coals. In terms of cohesive energy contributions, it was found that solvents with dispersive interaction contributions, δ_d, equal to 9.0 $cal^{1/2}/cm^{3/2}$, polar δ_p, and hydrogen-bond δ_h, interaction contributions equal to 3.0 $cal^{1/2}/cm^{3/2}$ exhibit the highest swelling to PSOC coals. The methylene chloride equilibrium uptake increases with the average molecular weight between crosslinks. In this case, coal PSOC-247 (75.5% C dmmf) showed the highest penetrant uptakes.

Thermogravimetric swelling studies as a function of carbon content in coals treated thermally at 35°C, showed that the initial diffusion rates and the equilibrium uptakes of pyridine, DMF and chloroform into PSOC coals increase with the average molecular weight between crosslinks. At high thermal treatment temperatures (100°C-150°C), the diffusion of these three penetrants into coal decreases as the carbon content in coals increases. All three penetrants showed similar phenomenological swelling observations.

The penetrant uptake into thermally treated coals as a function of temperature studies showed that the initial diffusion rates and the equilibrium pyridine uptakes increase with temperature treatment. Contrary, for DMF and chloroform, the initial diffusion rates and equilibrium penetrant uptakes decrease as temperature treatment increases. This indicates that a chemical reaction may take place during the diffusion process; and by increasing the temperature, the reactive sites within the coal network are destroyed.

Analysis of the semi-empirical equation (2.21), indicates that the diffusion of pyridine and DMF at low penetrant activities (<0.04) can be described by Fickian diffusion regardless of the temperature treatment (35°C-150°C). As the carbon content increases the transport mechanism deviates slightly to anomalous transport. The diffusion of chloroform vapors (penetrant activity=0.04) into coals at different temperatures (35°C-150°C) can be described by anomalous transport.

Equation (5.1) was solved to determine diffusion coefficients, D, and relaxation constants, k, for the diffusion of penetrants into coal. It was found that at 35°C the diffusion coefficient for pyridine, DMF and chloroform increases with the average molecular weight between crosslinks. The magnitude of the diffusion coefficients is between the range 4.0×10^{-8}-1.0×10^{-9} cm^2/s. At 35°C, the macromolecular relaxation time increases as the carbon content increases. The same mechanistic effect was obtained from the semi-empirical equation (2.21), where the transport mechanism deviates from Fickian diffusion to anomalous transport as the carbon content increases. The magnitude for the relaxation times is between 0.0-1.2×10^{6} s. These results at low penetrant activities compare very well to the results for the diffusion of low activity penetrants into poly(1,4-dimethylnaphthaleno-2,5-dihydroxybenzene). This model which simulates the structure of coal was proposed by Barr-Howell et al. (1986a).

The penetrant transport in coal has been elucidated by means of gravimetric swelling studies. A more accurate way of elucidating the penetrant transport is to follow the diffusion of penetrants in-situ at the microscopic level. Brenner (Brenner, 1982; Brenner and Hagan, 1985) was the first to observe in-situ the diffusion of pyridine into coal Illinois No. 6 using uncontamined thin sections of coal (15 μm thick). He reported qualitative observations; but not quantitative results from the penetrant transport in coals. In this work, we used Brenner's method (Brenner, 1982) to study the diffusion of various penetrants into PSOC coals. We report for the first time quantitative and qualitative results for the diffusion of penetrants into PSOC coals at various temperatures (25°C-100°C).

The in-situ diffusion studies in coal, show that the transition layer thickness and the initial penetrant front velocity increase with temperature. This indicates that the diffusion coefficient for the diffusion process increases with temperature. It was also found that an equilibrium transition layer thickness is attained much faster at high temperatures. At high temperatures the macromolecular chains relax; the relaxation time decreases and so does the total diffusion time. This method also confirmed that coal PSOC-247 exhibits highest average molecular weight between crosslinks, and that chlorinated penetrants are compatible with PSOC coals.

The stresses due to the penetrant concentration gradients cause the coal to swell. When exposed to a penetrant, coal starts to craze; and when the stresses are very strong, cracking and coal dissolution results. From the direction of the craze lines, it was concluded that the macromolecular chains orient and rearrange in the direction of the diffusing penetrant. This partial macromolecular chain orientation increases the index of refraction in the swollen region.

7. LIST OF REFERENCES

Alfrey, T., E.F. Gurnee, and W.G. Lloyd, "Anomalous Transport in Polymers", *J. Polym. Sci., C12*, 249 (1966).

Astarita, G., and L. Nicolais, "Physics and Mathematics of Heat and Mass Transfer in Polymers:, *Pure and Appl. Chem., 55*, 727, (1983).

Barr-Howell, B.D., "Characteristics of Diffusion in Highly Crosslinked Macromolecular Networks", M.S. Thesis, School of Chemical Engineering, Purdue University, West Lafayette, IN, 1984.

Barr-Howell, B.D., J.M. Howell, and N.A. Peppas, "Thermoplastic and Viscoelastic Properties of Coals", *Fuel Chem. Prepr., 30(1)*, 64 (1985).

Barr-Howell, B.D., N.A. Peppas, "Mechanisms of Amine Transport in Coal Particles", *Fuel Chem. Prepr., 30(1)*, 108 (1985).

Barr-Howell, B.D., N.A. Peppas, and T.G. Squires, "Transport of Penetrants in the Macromolecular Structure of Coals. II. Dynamic Swelling of Stiff Polymer Networks That Simulate the Coal Structure" *J. Appl. Polym. Sci., 31*, 39 (1986a).

Barr-Howell, B.D., N.A. Peppas, and D.N. Winslow, "Transport of Penetrants in the Macromolecular Structure of Coals. II. Effects of Porous Structure on Pyridine Transport Mechanism," *Chem. Eng. Commun.*, 43, 301 (1986b).

Barr-Howell, B.D., J.M. Howell, and N.A. Peppas, "Transport of Penetrants in the Macromolecular Structure of Coals. VIII. Transport Mechanism as a Function of Temperature", *Thermochimica Acta*, 116, 153 (1987).

Berens, A.R., and H.B. Hopfenberg, "Diffusion and Relaxation in Glassy Polymer Powders: 2. Separation of Diffusion and Relaxation Parameters", *Polymer, 19*, 489 (1978).

Brenner, D., "In-Situ Microscopic Studies of the Solvent-Swelling of Coal", *Proceedings of the International Conference of Coal Science*, Verlag Gluckauf, Essen, 163 (1981).

Brenner, D., and P.S. Hagan, "Diffusive Uptake of Fluids by Coal Particles. Effects of Particle Shape and Particle Size Distribution", *Fuel Chem. Prepr., 30(1)*, 71 (1985).

Brenner, D., "In Situ Observations of Liquid Diffusion in Thin Sections of Coal", *Fuel Chem, Prepr., 30(1)*, 83 (1985).

Brenner, D., "Solvent-Induced Swelling of Thin Sections of Coal", *Fuel Chem, Prepr., 27(3)*, 244 (1982).

Crank, J., and G.S. Park, "Methods and Measurement" in *Diffusion in Polymers*,J. Crank and G.S. Park, eds., Academic Press, New York, N.Y., 21 1968.

Davidson, R.M., *Molecular Structure of Coal*, Report Number ICTIS/TR 08, IEA Coal Research, London, 1980.

Dryden, I.G.C., "Action of Solvents on Coal at Lower Temperatures I.", *Fuel, 30*, 39 (1951a).

Dryden, I.G.C., "Action of Solvents on Coal at Lower Temperatures II.", *Fuel, 30*, 145 (1951b).

Dryden, I.G.C., "Action of Solvents on Coal at Lower Temperatures III.", *Fuel, 30*, 176 (1951c).

Dryden, I.G.C., "Action of Solvents on Coal at Lower Temperatures VI.", *Fuel, 30*, 217 (1951d).

Enscore, D.J., H.B. Hopfenberg, and V.T. Stannett, "Effect of Particle Size on the Mechanism Controlling n-Hexane Sorption in Glassy Polystyrene Microspheres", *Polymer, 18*, 793 (1977).

Evans, D.J., and R.J. Hooper, "Deduction of the Structure of Brown Coal by Reaction with Phenol", in *Coal Structure*, M.L. Gorbaty and K. Ouchi, eds., ACS Advances in Chemistry Series, 192, Washington, D.C., 191, 1981.

Gardon, J.L., and J.P. Teas, "Solubility Parameters", *Treatise on Coatings*, R.R. Myers, and J.S. Long, eds., Dekker, New York, N.Y., 2, (1976).

Gerstein, B.C., L.M. Lyan, and P. Dubois Murphy, "An Estimation of Average Polynuclear Aromatic Ring Size in a Iowa Vitrin and a Virginia Vitrain", in *Coal Structure*, M.L. Gorbaty and K. Ouchi, eds., ACS Advances in Chemistry Series, 192, Washington, D.C., 15, 1981.

Given, P.H., "The Distribution of Hydrogen in Coals and its Relation to Coal Structure", *Fuel, 39*, 147 (1960).

Green, T., J. Kovac, D. Brenner, and J.W. Larsen, "The Macromolecular Structure of Coals", in *Coal Structure*, R.A. Meyers, ed., Academic Press, New York, N.Y., 199, 1982.

Hall, P.J., H. Marsh, and M. Thomas, "Solvent Induced Swelling of Coals to Study Macromolecular Structure", *Fuel, 67*, 863 (1988).

Hansen, C.M., *J. Paint Technol., 39*, 104 (1967).

Hayatsu, R., R.G. Scott, R.L. McBeth, and R.E. Winans, "Lignite Coal: Its Chemical Structure and Origen", *Org. Chem. Coat., 43(2)*, 401 (1980).

Hayatsu, R., R.E. Winans, R.L. McBeth, R.G. Scott, L.P. Moore, and M.H. Studier, "Structural Characterization of Coal: Lignin-Like Polymers in Coals", in *Coal Structure*, M.L. Gorbaty and K. Ouchi, eds., ACS Advances in Chemistry Series, 192, Washington, D.C., 133, 1981.

Hayatsu, R., R.E. Winans, R.G. Scott, L.P. Moore, and M.H. Studier, "Trapped Organic Compounds and Aromatic Units in Coals", *Fuel, 57*, 541 (1978).

Heredy, L.A., and I. Wender, "Model Structure for a Bituminous Coal", *Fuel Chem. Prepr., 25(3)*, 38 (1980).

Hildebrand, J.H., and R.L. Scott, "Regular Solutions", *Prentice-Hall*, Englewood Cliffs, N.J., 1962.

Hopfenberg, H.B., and H.L. Frisch, "Transport of Organic Micromolecules in Amorphous Polymers", *J. Polym. Sci., Polym. Letters, 7*, 405 (1969).

Hopfenberg, H.B., R.H. Holley, and V.T. Stannett, "The Effect of Penetrant Activity and Temperature on the Anomalous Diffusion of Hydrocarbons and Solvent Crazing in Polystyrene, Part 1: Biaxially Oriented Polystyrene", *Polymer Engineering and Science, 9*, 242 (1969).

Hopfenberg, H.B., and V.T. Stannett, "The Physics of Glassy Polymers", *(Ed. R. N. Haward)*, Wiley, New York, Ch. 9, (1973).

Howell, J.M., and N.A. Peppas, "Viscoelastic Properties of Bituminous Coals", /fIFuel Chem. Prepr., 29(1), 207 (1984).

Hsieh, S.T., "The Penetration of Solvent Vapor into Coal Particles", Ph.D. Thesis, School of Chemical Engineering, Pennsylvania State University, University Park, PA, 1984.

Jacques, C.H.M., H.B. Hopfenberg, and V. Stannett, "Super Case II Transport of Organic Vapors in Glassy Polymers", in *Permeability of Plastic Films and Coatings to Gases, Vapors, and Liquids*, H.B. Hopfenberg, ed., Plenum Press, New York, N.Y., 73, 1974.

Joshi, S., and G. Astarita, "Diffusion-Relaxation Coupling in Polymers Which Show Two-Stage Sorption Phenomena", *Polymer, 20* 455 (1979).

Larsen, J.W., T.K. Green, and J. Kovac, "The Nature of the Macromolecular Network Structure of Bituminous Coals", *J. Org. Chem., 50*, 4729 (1985).

Larsen, J.W., and J. Kovac, "Polymer Structure of Bituminous Coals", in *Organic Chemistry of Coal*, J.W. Larsen, ed., ACS Symposium Series, 71, Washington, D.C., 36, 1978.

Long, F.A., and D. Richman, "Concentration Gradients for Diffusion of Vapors in Glassy Polymers and Their Relation to Time Dependent Diffusion Phenomena", *J. Amer. Chem. Soc., 82*, 513, (1960).

Lucht, L.M., and N.A. Peppas, "Crosslinked Macromolecular Structures in Bituminous Coals: Theoretical and Experimental Considerations", in *Chemistry and Physics of Coal Utilization*, B.R. Cooper and L. Petrakis, eds., Amer. Inst. Phys., New York, N.Y., 28, 1981.a.

Lucht, L.M., and N.A. Peppas, "Cross-Linked Structures in Coals: Models and Preliminary Experimental Data", in *New Approches in Coal Chemistry*, B.d. Blaustein, B.C. Bockrath, and S.

Friedman, eds., ACS Symposium Series 169, Washington, D.C., 43, 1981.b.

Lucht, L.M., "Macromolecular Network Structure of Coals: Interpretation of Equilibrium and Dynamic Swelling Experiments", Ph.D. Thesis, School of Chemical Engineering, Purdue University, West Lafayette, IN, 1983.

Michaels, A.S., H.J. Bixler, and H.B. Hopfenberg, *J. Appl. Polym. Sci.*, 12, 991 (1968).

Nelson, J.R., "Determination of Molecular Weight between Crosslinks of Coals from Solvent-Swelling Studies", *Fuel*, *62*, 112 (1983).

Peppas, N.A., and L.M. Lucht, "Macromolecular Structure of Coals. I. The Organic Phase of Bituminous Coals as a Macromolecular Network", *Chem. Eng. Commun.*, 30, 291 (1984).

Peppas, N.A., and L.M. Lucht, "Transport of Penetrants in the Macromolecular Structure of Coals. I. Anomalous Transport in Untreated and Pyridine Extracted Coals", *Chem. Eng. Commun.*, 37, 333 (1985).

Peppas, N.A., L.M. Lucht, J.M. Larson, and G.W. Sinclair, "Analysis of Solvent Transport Mechanisms in Macromolecular Coal Networks", *Proceed. Intern. Coal Conference*, *2*, 280 (1983).

Peppas, N.A., and J.L. Sinclair, "Anomalous Trasnport of Penetrants in Glassy Polymers", *Colloid and Polymer Sci.*, 261, 404 (1983).

Quinga, M.Y. and J.W. Larsen, "Solvent Swelling of Coals", Y. Yurum (ed.), *New Trends in Coal Science*, Kluwer, 85 (1987).

Ritger, P.L., and N.A. Peppas, "Transport of Penetrants in the Macromolecular Structure of Coals 4. Models for Analysis of Dynamic Penetrant Transport", *Fuel*, *66*, 815 (1987a).

Ritger, P.L., and N.A. Peppas, "Transport of Penetrants in the Macromolecular Structure of Coals 7. Transport in Thin Coal Sections", *Fuel*, *66*, 1379 (1987b).

Sanada, Y., and H. Honda, "Swelling Equilibrium of Coal by Pyridine at 25°C", *Fuel*, *45*, 295 (1966).

Sanada, Y., and H. Honda, "Swelling Equilibrium of Coal by Various Solvents", *Fuel*, *46*, 451 (1967).

Sanada, Y., and H. Honda, "Creep in Coal over the Temperature Range 200 to 370°C", *Fuel*, *42*, 479 (1963).

Schlosberg, R.H., T.R. Ashe, R.J. Pancirov, and M. Donaldson, *Fuel*, *60*, 155 (1981).

Sinclair, G.W., and N.A. Peppas, "Analysis of Non-Fickian Transport in Polymers using Simplified Exponential Expressions", *J. Membr. Sci.*, *17*, 329 (1984).

Szeliga, J., and A. Marzec, "Swelling of Coal in Relation to Solvent Electron-Donor Numbers", *Fuel*,

62, 1229 (1983).

Solomon, P.R., "Coal Structure and Thermal Decomposition", in *New Approaches in Coal Chemistry*, B.D. Blaustein, B.C. Bockrath, and S. Friedman, eds., ACS Symposium Series, 169, Washington, D.C., 61 1981.

Speight, J.G., "The Chemistry and Technology of Coal", *Chemical Industries*, *12*, 1983.

Squires, T.G., B.F. Smith, R.E. Winans, R.G Scott, and R. Hayatsu, *Proc. Intern. Conf. Coal Sci.*, *2*, 292 (1983).

Szeliga, J., and A. Marzec, "Swelling of Coal in Relation to Solvent Electron-Donor Numbers", *Fuel*, *62*, 1229 (1983).

van Krevelen, D.W., "Chemical Structure and Properties of Coal XXVIII-Coal Constitution and Solvent Extraction", *Fuel*, *44*, 229 (1965).

van Krevelen, D.W., *Coal*, Elsevier, New York, N.Y., 1981.

Vernon, L.W., *Fuel*, *59*, 102 (1980).

Vrentas, J.S., and J.L. Duda, "Diffusion in Polymer-Solvent Systems. III. Construction of Deborah Number Diagrams", *J. Polym. Sci., Polym. Phys. Ed.*, *15*, 441 (1977).

Vrentas, J.S., C.M. Jarzebski, and J.L. Duda, "A Deborah Number for Diffusion in Polymer-Solvent Systems", *AICHE J.*, *21*, 894 (1975).

Wender, I., L.A. Heredy, M.B. Neuworth, and I.G.C. Dryden, "Chemical Reactions and the Constitution of Coal", in *Chemistry of Coal Utilization*, M.A. Elliott, ed., Second Supplementary Volume, Wiley, New York, N.Y., 425, 1981.

Wiser, W., *Fuel Chem. Prepr.*, *20(2)*, 122 (1975).

APPENDICES

Appendix A

Computer Programs Used to Solve for Equation (2.32)

and to Simulate Data for Equation (2.31).

```
c     This program will solve a short time approximation of the
c     Berens-Hopfenberg equation (equation (2.32)).
c     The IMSL subroutines are R2LIN/DR2LIN from the STAT/LIBRARY pp.239
c
      integer ldr, nobs, nparm, iparam(6)
      integer ideriv, irank, nout
c     Indicate the number of observations (nobs); number of unknown
c     parameters (nparm), in this case the diffusion coefficient,
c     the relaxation constant, and the fraction contribution due to
c     Fickian diffusion.
      parameter(nobs=32 ,nparm=3, ldr=nparm)
.....dimension wk(11*nparm+4), iwk(nparm)
      real dfe, exampl, r(ldr,nparm), sse, theta(nparm),
     $     xdata(nobs), ydata(nobs),rparam(7), m
      common /xydata/ xdata, ydata
.....external exampl, r2lin, umach, wrrrn
c     Read x-y data as time (hr) - penetrant uptake (g.)
c     Write time in seconds and penetrant uptake as a fraction
c     of the total penetrant uptake at infinite times
.....open(7,file='datafile')
.....rewind (7)
c     m is the penetrant uptake at infinite time (in grams)
      m=0.1553
      do 10 i=1,nobs
      read(7,*)x, y
      xdata(i)=x*3600
      ydata(i)=y/m
   10 continue
c     Open a file which will indicate the initial guesses for the
c     three unknown constants (Diff. coeff., Relaxation constant,
c     and the fraction constant due to fickian diffusion)
.....open(8,file='guess')
..... .....rewind(8)
.....read(8,*) (theta(n),n=1,nparm)
.....call umach (2, nout)
.....iparam(1)=0
.....ideriv=0
.....call r2lin (exampl, nparm, ideriv, theta, r, ldr, irank,
     $          dfe, sse, iparam, rparam, scale, iwk, wk)
.....write (nout,*) 'theta=',theta
.....write (nout,*) 'irank=', irank, 'dfe=', dfe, 'sse=', sse
      write (nout,*) 'iterations=',iparam(3),'sse evals=',iparam(4)
.....call wrrrn ('r', nparm, nparm, r, ldr, 0)
      stop
.....end
c
```

```
      Subroutine exampl (nparm, theta, iopt, iobs, frq, wt, e, de,
     $                   iend)
      integer nparm, iopt, iobs, iend
      real theta(nparm), frq, wt, e, de(1)
      integer nobs
      parameter (nobs=32)
      real alog, xdata(nobs), ydata(nobs), l
      common /xydata/ xdata, ydata
      intrinsic alog
c     Use the Berens-Hopfenber equation to determine the three unknowns
c
      if (iobs .le. nobs) then
         wt=1.0e0
         frq=1.0e0
         iend=0
         l=0.0381
         e=ydata(iobs)-(theta(2)*4*(theta(1)*xdata(iobs)/(3.141592654*
     $     l**2))**0.5 + (1-theta(2))*(1-exp(-theta(3)*xdata(iobs))))
      else
         iend=1
      end if
      return
      end
```

```
c     This program will simulate the normalized penetrant uptake, M_t/M_∞,
c     as a function of time from equation (2.31) given the diffusion
c     coefficient, the relaxation constant and the
c     fractional contribution due to Fickian diffusion.
      parameter (n=34)
      dimension xx(n), yy(n)
      real d, f, k, sum, fick, l, p
c     Open a data file containing time in seconds.
      open (5, file='datafile')
c     Open a file to store the results for M_t/M_∞ and time.
      open (8, file='x-ydata')
      rewind(8)
      rewind(5)
c     d = Diffusion coefficient (cm^2/s).
      d = 6.12e-09
c     f = Fractional contribution due to Fickian diffusion.
      f = 0.88
c     k = Relaxation constant (s^-1).
      k = 3.79e-06
c     l = Sample thickness (cm).
      l = 0.0483
      p = 3.141592654
      do 100 j=1,n
..... read (5,*) xx(j)
 100  continue
      do 20 i=1,n
        sum = 0.0
        fick = 0.0
        c = 0.0
 30       fick=(8/((2*c+1)*p)**2)*exp((-d*(2*c+1)**2*xx(i))/l**2)
          diff = (sum + fick) - sum
          err=1.0e-82
          if(diff.le.err) then
            sum=sum+fick
..... else
            sum=sum+fick
            c=c+1
            goto 30
..... endif
        yy(i) = f*(1-sum)+(1-f)*(1-exp(-k*xx(i)))
        write (8, *) xx(i), yy(i)
 20   continue
      stop
      end
```

Appendix B

Equilibrium and Dynamic Penetrant Uptake Data.

Microscopy Data.

Equilibrium Uptake
Coal Type: PSOC 418
Penetrant: Acetone Vapor
Mass of Coal (dmmf), M_c: 10.8 mg
Temperature: 35°C

t/l^2 (h/cm^2 X 10^{-3})	M_t/M_c (g/g)
0.0000	0.0000
2.5640	0.1760
6.4050	0.1020
18.2550	0.0000
25.6210	0.1300
30.7450	0.1570
37.1510	0.1300
50.6020	0.1200
56.3670	0.0926
64.3730	0.0926
84.5500	0.0926

Equilibrium Uptake
Coal Type: PSOC 418
Penetrant: Cyclohexane Vapor
Mass of Coal (dmmf), M_c: 15.1 mg
Temperature: 35°C

t/l^2 (h/cm^2 X 10^{-3})	M_t/M_c (g/g)
0.0000	0.0000
1.3770	0.0331
3.4430	0.0927
9.8140	0.0464
13.7740	0.0861
16.5290	0.0464
19.9720	0.0927
27.2030	0.0662
30.3030	0.0728
34.6070	0.0728
45.4550	0.0861

Equilibrium Uptake
Coal Type: PSOC 418
Penetrant: Methanol Vapor
Mass of Coal (dmmf), M_c: 13.3 mg
Temperature: 35°C

t/l^2 (h/cm^2 X 10^{-3})	M_t/M_c (g/g)
0.0000	0.0000
0.9560	0.1053
2.3920	0.0977
6.8180	0.0376
9.5690	0.0752
11.4830	0.0376
13.8760	0.0827

Equilibrium Uptake
Coal Type: PSOC 418
Penetrant: Methyl Ethyl Ketone Vapor
Mass of Coal (dmmf), M_c: 6.7 mg
Temperature: 35°C

t/l^2 (h/cm^2 X 10^{-3})	M_t M_c (g/g)
0.0000	0.0000
0.9560	0.0367
2.3920	0.0110
6.8180	0.0147
9.5690	0.0171
11.4830	0.0159
13.8760	0.0159
18.9000	0.0147
21.0530	0.0184
24.0430	0.0147
31.5790	0.0171

Equilibrium Uptake
Coal Type: PSOC 418
Penetrant: Toluene Vapor
Mass of Coal (dmmf), M_c: 11.2 mg
Temperature: 35°C

t/l^2 (h/cm^2 X 10^{-3})	M_t/M_c (g/g)
0.0000	0.0000
2.5130	0.0000
5.3820	0.0714
15.6080	0.0804
21.5280	0.0804
25.8340	0.0714
31.2160	0.0982
42.5190	0.1070
47.3630	0.1340
54.0900	0.0536
71.0440	0.1160

Equilibrium Uptake
Coal Type: PSOC 418
Penetrant: Methylene Chloride Vapor
Mass of Coal (dmmf), M_c: 10.6 mg
Temperature: 35°C

t/l^2 (h/cm^2 X 10^{-3})	M_t/M_c (g/g)
0.0000	0.0000
1.3770	0.7075
3.4430	0.7358
9.8140	0.5470
13.7740	0.5189
16.5290	0.6890
19.9700	0.6130
27.2030	0.5090
30.3030	0.5940
34.6070	0.5940
45.4550	0.5940

Equilibrium Uptake
Coal Type: PSOC 853
Penetrant: Acetone Vapor
Mass of Coal (dmmf), M_c: 58.3 mg
Temperature: 35°C

t/l^2 (h/cm^2 X 10^{-3})	M_t/M_c (g/g)
0.0000	0.0000
0.1938	0.0952
0.4840	0.0278
1.3810	0.0469
1.9380	0.0688
2.3250	0.0717
2.8100	0.0791
3.8270	0.0805
4.2630	0.0747
4.8690	0.0805
6.3950	0.0805

Equilibrium Uptake
Coal Type: PSOC 853
Penetrant: Cyclohexane Vapor
Mass of Coal (dmmf), M_c: 42.4 mg
Temperature: 35°C

t/l^2 (h/cm^2 X 10^{-3})	M_t/M_c (g/g)
0.0000	0.0000
0.2480	0.0000
0.7110	0.0094
2.0280	0.0142
2.8470	0.0425
3.4160	0.0377
4.1280	0.0519
5.6220	0.0425
6.2620	0.0401
7.1520	0.0448
9.3940	0.0495

Equilibrium Uptake
Coal Type: PSOC 853
Penetrant: methanol Vapor
Mass of Coal (dmmf), M_c: 15.5 mg
Temperature: 35°C

t/l^2 (h/cm^2 X 10^{-3})	M_t/M_c (g/g)
0.0000	0.0000
1.3770	0.1806
3.4440	0.1097
9.8140	0.1032
13.7740	0.1161
16.5290	0.0774
19.9720	0.1484

Equilibrium Uptake
Coal Type: PSOC 853
Penetrant: Methyl Ethyl Ketone Vapor
Mass of Coal (dmmf), M_c: 38.0 mg
Temperature: 35°C

t/l^2 (h/cm^2 X 10^{-3})	M_t/M_c (g/g)
0.0000	0.0000
0.2030	0.1420
0.5090	0.0526
1.4520	0.1450
2.0380	0.1740
2.4460	0.1840
2.9550	0.1870
4.0250	0.1970
4.4485	0.2080
5.1200	0.2050
6.7260	0.2130

Equilibrium Uptake
Coal Type: PSOC 853
Penetrant: Toluene Vapor
Mass of Coal (dmmf), M_c: 7.5 mg
Temperature: 35°C

t/l^2 (h/cm^2 X 10^{-3})	M_t/M_c (g/g)
0.0000	0.0000
0.9560	0.3570
2.3920	0.4380
6.8180	0.4830
9.5690	0.4380
11.4830	0.5340
13.8760	0.4940
18.9000	0.4260
21.0530	0.4770
24.0430	0.5450
31.5790	0.4940

Equilibrium Uptake
Coal Type: PSOC 384
Penetrant: Acetone Vapor
Mass of Coal (dmmf), M_c: 10.8 mg
Temperature: 35°C

t/l^2 (h/cm^2 X 10^{-3})	M_t/M_c (g/g)
0.0000	0.0000
8.6096	0.1110
21.5230	0.1570
61.3430	0.0926
86.0960	0.3330
103.3140	0.2410
124.8390	0.1110
170.0380	0.1850
189.4100	0.0463
216.3150	0.1480
284.1150	0.1380

Equilibrium Uptake
Coal Type: PSOC 384
Penetrant: Cyclohexane Vapor
Mass of Coal (dmmf), M_c: 46.5 mg
Temperature: 35°C

t/l^2 (h/cm^2 X 10^{-3})	M_t/M_c (g/g)
0.0000	0.0000
0.9560	0.0215
2.3920	0.0215
6.8180	0.0237
9.5690	0.0280
11.4830	0.0280
13.8760	0.0473
18.9000	0.0409
21.0530	0.0430
24.0430	0.0323
31.5790	0.0452

Equilibrium Uptake
Coal Type: PSOC 384
Penetrant: Methanol Vapor
Mass of Coal (dmmf), M_c: 81.7 mg
Temperature: 35°C

t/l^2 $(h/cm^2 \times 10^{-3})$	M_t/M_c (g/g)
0.0000	0.0000
0.3690	0.0416
0.9120	0.0122
2.6260	0.0122
3.6860	0.0147
4.4230	0.0098
5.3470	0.0220

Equilibrium Uptake
Coal Type: PSOC 384
Penetrant: Methyl Ethyl Ketone Vapor
Mass of Coal (dmmf), M_c: 29.0 mg
Temperature: 35°C

t/l^2 $(h/cm^2 \times 10^{-3})$	M_t/M_c (g/g)
0.0000	0.0000
1.5810	0.0310
3.9530	0.0207
11.2600	0.0138
15.8100	0.0172
18.9720	0.0172
22.9250	0.0207
31.2220	0.0103
34.7830	0.0276
39.7000	0.0138
52.1740	0.0241

Equilibrium Uptake
Coal Type: PSOC 384
Penetrant: Toluene Vapor
Mass of Coal (dmmf), M_c: 8.3 mg
Temperature: 35°C

t/l^2 (h/cm^2 X 10^{-3})	M_t/M_c (g/g)
0.0000	0.0000
12.4220	0.0000
31.0560	0.0480
90.0620	0.0120
124.2000	0.0480
149.0700	0.0241
180.1240	0.0843
245.3000	0.0120
273.3000	0.0964
312.0000	0.0000
409.8999	0.0602

Equilibrium Uptake
Coal Type: PSOC 384
Penetrant: Methylene Chloride Vapor
Mass of Coal (dmmf), M_c: 14.4 mg
Temperature: 35°C

t/l^2 (h/cm^2 X 10^{-3})	M_t/M_c (g/g)
0.0000	0.0000
4.8430	0.5070
12.1000	0.5560
35.1000	0.3610
48.4260	0.3260
58.1110	0.4440
70.2180	0.3680
95.6420	0.2920
106.5000	0.3680
121.6700	0.3820
159.8060	0.3960

Equilibrium Uptake
Coal Type: PSOC 418
Penetrant: Methylene Chloride Vapor
Mass of Coal (dmmf), M_c: 10.2 mg
Temperature: 35°C

t/l^2 $(h/cm^2 \times 10^{-3})$	M_t/M_c (g/g)
0.5667	0.9418
1.1340	0.8630
1.7000	0.9110
2.2670	0.9863
2.8360	1.0205
4.5360	0.9110
6.2360	0.9897
10.7710	0.9315
12.3300	0.9486
15.0220	1.0000

Equilibrium Uptake
Coal Type: PSOC 853
Penetrant: Methylene Chloride Vapor
Mass of Coal (dmmf), M_c: 6.3 mg
Temperature: 35°C

t/l^2 (h/cm^2 X 10^{-3})	M_t/M_c (g/g)
1.1560	0.7620
2.2670	0.9680
3.3870	1.0800
4.4890	1.0300
5.6000	1.0000
8.9330	0.9680
21.1560	1.0200
24.2110	1.0300
29.4890	1.0000

Equilibrium Uptake
Coal Type: PSOC 384
Penetrant: Methylene Chloride Vapor
Mass of Coal (dmmf), M_c: 9.4 mg
Temperature: 35°C

t/l^2 (h/cm^2 X 10^{-3})	M_t/M_c (g/g)
2.4490	0.4680
4.7170	0.6170
6.9840	0.6280
9.2520	0.7450
11.5190	0.6380
18.3220	0.5420
43.2650	0.6170
49.5010	0.6280
60.2720	0.6170

Equilibrium Uptake
Coal Type: PSOC 312
Penetrant: Methylene Chloride Vapor
Mass of Coal (dmmf), M_c: 16.9 mg
Temperature: 35°C

t/l^2 (h/cm^2 X 10^{-3})	M_t/M_c (g/g)
0.5530	0.3430
1.0460	0.5680
1.5410	0.4260
2.0350	0.5330
2.5280	0.5800
4.0090	0.4320
5.4910	0.4440
9.4420	0.4730
10.8000	0.4790
13.1450	0.4910

Equilibrium Uptake
Coal Type: PSOC 341
Penetrant: Methylene Chloride Vapor
Mass of Coal (dmmf), M_c: 10.5 mg
Temperature: 35°C

t/l^2 $(h/cm^2 \times 10^{-3})$	M_t/M_c (g/g)
1.3330	1.7000
2.4440	1.5200
3.5550	1.4600
4.6660	1.2000
5.7770	1.1000
9.1110	0.6380
12.4440	0.6380
21.3330	0.6570
24.3880	0.7900
29.6670	0.6480

Equilibrium Uptake
Coal Type: PSOC 247
Penetrant: Methylene Chloride Vapor
Mass of Coal (dmmf), M_c: 3.8 mg
Temperature: 35°C

t/l^2 (h/cm^2 X 10^{-3})	M_t/M_c (g/g)
2.1280	3.8400
3.7280	3.8600
5.3280	3.0800
6.9280	2.2100
8.5280	2.9200
13.3280	1.2100
18.1280	1.2100
30.9280	1.2100
35.3120	1.4700
42.9120	1.5800

Equilibrium Uptake in PMMA
Crosslinking Degree: 1.0 wt%
Penetrant: Methylene Chloride Vapor
Mass of Crosslinked PMMA, M_c: 13.6 mg
Temperature: 35°C

t/l^2 (h/cm^2 X 10^{-3})	M_t/M_c (g/g)
2.2970	1.8600
4.4620	2.0500
6.5290	1.4300
10.6610	2.6000
16.8600	2.0500
23.0580	2.0100
39.5870	1.6900
45.2690	2.0700
55.0830	2.1300

Equilibrium Uptake in PMMA
Crosslinking Degree: 2.0 wt%
Penetrant: Methylene Chloride Vapor
Mass of Crosslinked PMMA, M_c: 14.4 mg
Temperature: 35°C

t/l^2 (h/cm^2 X 10^{-3})	M_t/M_c (g/g)
2.2680	1.9100
4.5350	1.7500
6.8020	1.8500
9.0700	2.0000
11.3370	2.0700
18.1410	1.8500
24.9430	2.0100
43.0840	1.8900
49.3190	1.9200
60.0900	2.0200

Equilibrium Uptake in PMMA
Crosslinking Degree: 5.0 wt%
Penetrant: Methylene Chloride Vapor
Mass of Crosslinked PMMA, M_c: 16.4 mg
Temperature: 35°C

t/l^2 (h/cm^2 X 10^{-3})	M_t/M_c (g/g)
1.6000	1.5200
3.2000	1.4600
4.8000	1.5200
6.4000	1.6000
8.0000	1.6900
12.8000	1.5200
17.6000	1.5800
30.4000	1.5300
34.8000	1.5700
42.4000	1.6300

Dynamic Uptake
Coal Type: PSOC 791
Penetrant: Pyridine Vapor
Penetrant Activity < 0.04
Sample Thickness: 483 μm
Mass of Coal (dmmf), M_c: 5.47 mg
Treatment Temperature: 35°C

Time (hr)	M_c *(g)*	*Time (hr)*	M_c *(g)*
0.0333	0.0091	12.000	0.1255
0.0667	0.0182	13.000	0.1291
0.1000	0.0255	14.000	0.1382
0.1333	0.0291	15.000	0.1473
0.2000	0.0327	16.000	0.1545
0.2667	0.0400	17.000	0.1564
0.3333	0.0455	18.000	0.1582
0.5000	0.0491	19.000	0.1636
0.6667	0.0545	20.000	0.1673
0.8333	0.0582	21.000	0.1709
1.0000	0.0618		
1.1667	0.0655		
1.3333	0.0709		
1.5000	0.0764		
2.0000	0.0800		
3.0000	0.0855		
4.0000	0.0945		
5.0000	0.0964		
6.0000	0.1018		
7.0000	0.1073		
8.0000	0.1109		
9.0000	0.1164		
10.000	0.1200		
11.000	0.1218		

Dynamic Uptake
Coal Type: PSOC 247
Penetrant: Pyridine Vapor
Penetrant Activity < 0.04
Sample Thickness: 457 μm
Mass of Coal (dmmf), M_c: 8.17 mg
Treatment Temperature: 35°C

Time (hr)	M_c *(g)*
0.0333	0.0145
0.0667	0.0236
0.1000	0.0291
0.1333	0.0400
0.2000	0.0455
0.2667	0.0527
0.3333	0.0727
0.5000	0.0873
0.6667	0.1000
0.8333	0.1091
1.0000	0.1236
1.1667	0.1309
1.5000	0.1418
2.0000	0.1527
3.0000	0.1636
4.0000	0.1782
5.0000	0.1909
6.0000	0.2000
7.0000	0.2073
8.0000	0.2164
9.0000	0.2218
10.000	0.2291
12.000	0.2345
13.000	0.2418
14.000	0.2455
15.000	0.2527
16.000	0.2582
17.000	0.2636
18.000	0.2673
19.000	0.2709

Dynamic Uptake
Coal Type: PSOC 312

Penetrant: Pyridine Vapor
Penetrant Activity < 0.04
Sample Thickness: 381 μm
Mass of Coal (dmmf), M_c: 5.73 mg
Treatment Temperature: 35°C

Time (hr)	M_c *(g)*
0.0333	0.0093
0.2667	0.0139
0.3333	0.0186
0.5000	0.0186
0.6667	0.0279
1.0000	0.0279
1.5000	0.0325
2.0000	0.0418
3.0000	0.0465
4.0000	0.0558

Dynamic Uptake
Coal Type: PSOC 853
Penetrant: Pyridine Vapor
Penetrant Activity < 0.04
Sample Thickness: 406 μm
Mass of Coal (dmmf), M_c: 4.52 mg
Treatment Temperature: 35°C

Time (hr)	M_c *(g)*	*Time (hr)*	M_c *(g)*
0.0333	0.0075	18.0000	0.2365
0.0667	0.0184	19.0000	0.2456
0.1000	0.0256	20.0000	0.2475
0.1330	0.0365	21.0000	0.2547
0.2000	0.0511		
0.2661	0.0584		
0.3330	0.0656		
0.5000	0.0729		
0.6660	0.0856		
0.8330	0.0946		
1.0000	0.1038		
1.3300	0.1111		
1.5000	0.1202		
2.0000	0.1365		
3.0000	0.1493		
4.0000	0.1638		
5.0000	0.1747		
6.0000	0.1765		
7.0000	0.1784		
8.0000	0.1893		
9.0000	0.1929		
10.0000	0.1984		
11.0000	0.2038		
12.0000	0.2075		
13.0000	0.2111		
14.0000	0.2184		
15.0000	0.2256		
17.0000	0.2275		

Dynamic Uptake
Coal Type: PSOC 791
Penetrant: Pyridine Vapor
Penetrant Activity < 0.04
Sample Thickness: 432 μm
Mass of Coal (dmmf), M_c: 5.71 mg
Treatment Temperature: 100°C

Time (hr)	M_c *(g)*
0.0333	0.0327
0.0667	0.0400
0.1000	0.0436
0.1300	0.0473
0.2000	0.0545
0.2667	0.0655
0.3333	0.0709
0.5000	0.0982
0.6667	0.1164
0.8300	0.1309
1.0000	0.1400
1.1667	0.1491
1.3333	0.1564
1.5000	0.1600
1.6667	0.1745
1.8333	0.1855
2.0000	0.1964
3.0000	0.2255
4.0000	0.2400
5.0000	0.2500
6.0000	0.2600
7.0000	0.2673
8.0000	0.2836
9.0000	0.2873
10.000	0.2873

Dynamic Uptake
Coal Type: PSOC 247
Penetrant: Pyridine Vapor
Penetrant Activity < 0.04
Sample Thickness: 457 μm
Mass of Coal (dmmf), M_c: 8.90 mg
Treatment Temperature: 100°C

Time (hr)	M_c *(g)*	*Time (hr)*	M_c *(g)*
0.0667	0.0109	16.000	0.3436
0.1333	0.0182	17.000	0.3509
0.2000	0.0255		
0.2667	0.0327		
0.3333	0.0400		
0.5000	0.0509		
0.6667	0.0582		
0.8333	0.0655		
1.0000	0.0764		
1.1667	0.0836		
1.3333	0.0945		
1.5000	0.0982		
2.0000	0.1091		
2.3333	0.1200		
2.6667	0.1345		
3.0000	0.1418		
4.0000	0.1636		
5.0000	0.1818		
6.0000	0.1945		
7.0000	0.2073		
8.0000	0.2255		
9.0000	0.2509		
10.000	0.2745		
11.000	0.2982		
12.000	0.3127		
13.000	0.3200		
14.000	0.3273		
15.000	0.3345		

Dynamic Uptake
Coal Type: PSOC 312
Penetrant: Pyridine Vapor
Penetrant Activity < 0.04
Sample Thickness: 229 μm
Mass of Coal (dmmf), M_c: 4.36 mg
Treatment Temperature: 100° C

Time (hr)	M_c *(g)*
0.0333	0.0218
0.0667	0.0273
0.1000	0.0327
0.1333	0.0382
0.2667	0.0473
0.4333	0.0582
1.0000	0.0764
3.0000	0.0855
4.0000	0.1055
5.0000	0.1127
8.0000	0.1182
9.0000	0.1213
10.000	0.1236
11.000	0.1273
12.000	0.1345
13.000	0.1381
14.000	0.1394
15.000	0.1400
16.000	0.1455
18.000	0.1495
19.000	0.1503
20.000	0.1509
21.000	0.1636
23.000	0.1745

Dynamic Uptake
Coal Type: PSOC 853
Penetrant: Pyridine Vapor
Penetrant Activity < 0.04
Sample Thickness: 406 μm
Mass of Coal (dmmf), M_c: 5.84 mg
Treatment Temperature: 100°C

Time (hr)	M_c *(g)*
0.0333	0.0035
0.0666	0.0071
0.1000	0.0126
0.1333	0.0181
0.2000	0.0217
0.2667	0.0254
0.3333	0.0308
0.5000	0.0363
0.6667	0.0399
0.8333	0.0472
1.0000	0.0508
1.1660	0.0563
1.3330	0.0617
1.5000	0.0654
2.0000	0.0708
3.0000	0.0763
4.0000	0.0854
5.0000	0.0926
6.0000	0.0963
7.0000	0.1017
8.0000	0.1090
9.0000	0.1163
10.000	0.1199
11.000	0.1217
12.000	0.1235

Dynamic Uptake
Coal Type: PSOC 791
Penetrant: Pyridine Vapor
Penetrant Activity < 0.04
Sample Thickness: 457 μm
Mass of Coal (dmmf), M_c: 7.34 mg
Treatment Temperature: 150°C

Time (hr)	M_c *(g)*	*Time (hr)*	M_c *(g)*
0.0333	0.0364	16.000	0.3200
0.0667	0.0436	17.000	0.3309
0.1000	0.0509	18.000	0.3455
0.1333	0.0545	19.000	0.3436
0.2000	0.0691	20.000	0.3455
0.2667	0.0764		
0.3333	0.0836		
0.5000	0.1055		
0.6667	0.1164		
0.8333	0.1236		
1.0000	0.1345		
1.1667	0.1491		
1.3333	0.1564		
1.5000	0.1600		
2.0000	0.1745		
3.0000	0.2218		
4.0000	0.2491		
5.0000	0.2655		
6.0000	0.2782		
7.0000	0.2782		
8.0000	0.2855		
9.0000	0.2873		
10.000	0.3000		
11.000	0.3055		
12.000	0.3105		
13.000	0.3073		
14.000	0.3164		
15.000	0.3164		

Dynamic Uptake
Coal Type: PSOC 247
Penetrant: Pyridine Vapor
Penetrant Activity < 0.04
Sample Thickness: 406 μm
Mass of Coal (dmmf), M_c: 5.26 mg
Treatment Temperature: 150°C

Time (hr)	M_c *(g)*	*Time (hr)*	M_c *(g)*
0.0333	0.0073	17.000	0.3127
0.0667	0.0146	18.000	0.3200
0.1000	0.0255	19.000	0.3255
0.1333	0.0327	20.000	0.3345
0.2000	0.0436		
0.2667	0.0509		
0.3333	0.0800		
0.6667	0.0909		
0.8333	0.1055		
1.0000	0.1145		
1.1667	0.1309		
1.3333	0.1345		
1.5000	0.1455		
2.0000	0.1564		
3.0000	0.1673		
4.0000	0.1891		
5.0000	0.1982		
6.0000	0.2036		
7.0000	0.2073		
8.0000	0.2127		
9.0000	0.2164		
10.000	0.2245		
11.000	0.2382		
12.000	0.2455		
13.000	0.2691		
14.000	0.2873		
15.000	0.2909		
16.000	0.2945		

Dynamic Uptake
Coal Type: PSOC 312
Penetrant: Pyridine Vapor
Penetrant Activity < 0.04
Sample Thickness: 432 μm
Mass of Coal (dmmf), M_c: 5.45 mg
Treatment Temperature: 150°C

Time (hr)	M_c *(g)*
0.0333	0.0109
0.0667	0.0164
0.1000	0.0236
0.1333	0.0273
0.2600	0.0291
0.3333	0.0309
0.5000	0.0364
0.6667	0.0418
1.0000	0.0436
2.0000	0.0473
3.0000	0.0582
4.0000	0.0618
5.0000	0.0691
6.0000	0.0782
7.0000	0.0818
8.0000	0.0891
9.0000	0.0909
10.000	0.0945
11.000	0.1055
12.000	0.1091
13.000	0.1200
14.000	0.1309
15.000	0.1345

Dynamic Uptake
Coal Type: PSOC 853
Penetrant: Pyridine Vapor
Penetrant Activity < 0.04
Sample Thickness: 254 μm
Mass of Coal (dmmf), M_c: 4.03 mg
Treatment Temperature: 150°C

Time (hr)	M_c *(g)*	*Time (hr)*	M_c *(g)*
0.0333	0.0036	16.000	0.1418
0.0667	0.0127	17.000	0.1418
0.1000	0.0182	18.000	0.1418
0.2000	0.0254	19.000	0.1418
0.3333	0.0291	20.000	0.1418
0.5000	0.0327		
0.6667	0.0400		
0.8333	0.0436		
1.0000	0.0509		
1.1667	0.0564		
1.3333	0.0655		
1.5000	0.0727		
2.0000	0.0764		
3.0000	0.0945		
4.0000	0.1091		
5.0000	0.1164		
6.0000	0.1236		
7.0000	0.1291		
8.0000	0.1382		
9.0000	0.1418		
10.000	0.1418		
11.000	0.1418		
12.000	0.1418		
13.000	0.1418		
14.000	0.1418		
15.000	0.1418		

Dynamic Uptake
Coal Type: PSOC 791
Penetrant: DMF Vapor
Penetrant Activity < 0.04
Sample Thickness: 356 μm
Mass of Coal (dmmf), M_c: 8.60 mg
Treatment Temperature: 35°C

Time (hr)	M_c *(g)*	*Time (hr)*	M_c *(g)*
0.0333	0.0257	12.000	0.6258
0.0666	0.0472	12.999	0.6361
0.1333	0.0760	14.000	0.6542
0.1999	0.0979	19.999	0.6937
0.2999	0.1237		
0.3999	0.1598		
0.4999	0.1856		
0.6666	0.1959		
0.9999	0.2071		
1.3333	0.2329		
1.6667	0.2630		
2.0000	0.2767		
2.4999	0.3051		
2.9999	0.3232		
3.4999	0.3421		
4.0000	0.3636		
4.9999	0.3894		
6.0000	0.4323		
7.0000	0.4728		
7.9999	0.5054		
9.0000	0.5596		
9.9999	0.5966		
11.000	0.6112		

Dynamic Uptake
Coal Type: PSOC 247
Penetrant: DMF Vapor
Penetrant Activity < 0.04
Sample Thickness: 381 μm
Mass of Coal (dmmf), M_c: 4.49 mg
Treatment Temperature: 35°C

Time (hr)	M_c *(g)*
0.0333	0.0359
0.0667	0.0431
0.1000	0.0538
0.1666	0.0758
0.2667	0.0974
0.3333	0.1046
0.4333	0.1261
0.5999	0.1477
0.8333	0.1697
1.0000	0.1697
1.3333	0.1948
1.6667	0.2092
2.0000	0.2236
2.4999	0.2415
3.0000	0.2487
4.0000	0.2595
5.0000	0.2994

Dynamic Uptake
Coal Type: PSOC 312
Penetrant: DMF Vapor
Penetrant Activity < 0.04
Sample Thickness: 229 μm
Mass of Coal (dmmf), M_c: 5.83 mg
Treatment Temperature: 35°C

Time (hr)	M_c *(g)*
0.0666	0.0145
0.1333	0.0215
0.2333	0.0326
0.3000	0.0396
0.3666	0.0431
0.4333	0.0542
0.5333	0.0722
0 6666	0.0827
0.8333	0.0903
0.9999	0.0903
1.1666	0.1008
1.5000	0.1008
1.9999	0.1154

Dynamic Uptake
Coal Type: PSOC 853
Penetrant: DMF Vapor
Penetrant Activity < 0.04
Sample Thickness: 254 μm
Mass of Coal (dmmf), M_c: 6.75 mg
Treatment Temperature: 35°C

Time (hr)	M_c *(g)*
0.1333	0.01080
0.2666	0.01822
0.5999	0.03982
0.9999	0.04387
1.9999	0.05460
2.9999	0.06200
3.9999	0.07620
4.9999	0.08030

Dynamic Uptake
Coal Type: PSOC 791
Penetrant: DMF Vapor
Penetrant Activity < 0.04
Sample Thickness: 279 μm
Mass of Coal (dmmf), M_c: 4.92 mg
Treatment Temperature: 100°C

Time (hr)	M_c *(g)*
0.0333	0.0400
0.0667	0.0618
0.1000	0.0836
0.1333	0.0927
0.2000	0.1091
0.2667	0.1200
0.3333	0.1382
0.4333	0.1491
0.5000	0.1636
0.6667	0.1691
0.8333	0.1727
1.0000	0.1818
1.1667	0.1891
2.0000	0.2000
3.0000	0.2218
4.0000	0.2455
5.0000	0.2545
6.0000	0.2655
7.0000	0.2691
8.0000	0.2764
9.0000	0.2800
10.000	0.2855
11.000	0.2927
12.000	0.2982
13.000	0.3018

Dynamic Uptake
Coal Type: PSOC 247
Penetrant: DMF Vapor
Penetrant Activity < 0.04
Sample Thickness: 101 μm
Mass of Coal (dmmf), M_c: 2.06 mg
Treatment Temperature: 100°C

Time (hr)	M_c *(g)*
0.0333	0.0051
0.0667	0.0084
0.1000	0.0116
0.1333	0.0145
0.1667	0.0164
0.2000	0.0193
0.2333	0.0211
0.2667	0.0231
0.3333	0.0265
0.4333	0.0313
0.5000	0.0349
0.6000	0.0385
0.6667	0.0404
0.7667	0.0444
0.8333	0.0473
1.0000	0.0504
1.1667	0.0535
1.3333	0.0578
1.5000	0.0618
2.0000	0.0698
2.5000	0.0767
3.0000	0.0815
3.5000	0.0847
4.0000	0.0858
4.5000	0.0878
5.0000	0.0895
6.0000	0.0902

Dynamic Uptake
Coal Type: PSOC 312
Penetrant: DMF Vapor
Penetrant Activity < 0.04
Sample Thickness: 381 μm
Mass of Coal (dmmf), M_c: 6.35 mg
Treatment Temperature: 100°C

Time (hr)	M_c *(g)*	*Time (hr)*	M_c *(g)*
0.0333	0.0025	17 000	0.0727
0.0667	0.0033	18.000	0.0665
0.1000	0.0047	19.000	0.0764
0.1333	0.0058	20.000	0.0797
0.2000	0.0084	21.000	0.0810
0.2667	0.0091	22.000	0.0830
0.3333	0.0109	23.000	0.0851
0.5000	0.0138	24.000	0.0902
0.6667	0.0153	25.000	0.0953
0.8333	0.0182	26.000	0.0982
1.0000	0.0207	27.000	0.1004
1.1667	0.0233	28.000	0.1014
1.3333	0.0260	29.000	0.1030
1.5000	0.0280	30.000	0.1040
2.0000	0.0316	31.000	0.1051
3.0000	0.0378	32.000	0.1076
4.0000	0.0418	33.000	0.1097
5.0000	0.0447	34.000	0.1112
6.0000	0.0464	35.000	0.1123
7.0000	0.0498	37.000	0.1137
9.0000	0.0535	38.000	0.1181
10.000	0.0560	39.000	0.1210
11.000	0.0585	40.000	0.1250
12.000	0.0611	41.000	0.1278
13.000	0.0633	42.000	0.1293
14.000	0.0658	43.000	0.1304
15.000	0.0687		
16.000	0.0698		

Dynamic Uptake
Coal Type: PSOC 853
Penetrant: DMF Vapor
Penetrant Activity < 0.04
Sample Thickness: 229 μm
Mass of Coal (dmmf), M_c: 5.36 mg
Treatment Temperature: 100°C

Time (hr)	M_c *(g)*	*Time (hr)*	M_c *(g)*
0.0333	0.0025	12.000	0.0869
0.0667	0.0051	14.000	0.0869
0.1000	0.0069	15.000	0.0887
0.1333	0.0091	16.000	0.0916
0.2000	0.0124	17.000	0.0935
0.2667	0.0153	18.000	0.0945
0.3333	0.0178		
0.4333	0.0225		
0.5000	0.0244		
0.6667	0.0284		
0.8333	0.0324		
1.0000	0.0335		
1.1667	0.0378		
1.3333	0.0411		
1.5000	0.0436		
1.6667	0.0496		
1.8333	0.0513		
2.0000	0.0531		
2.5000	0.0564		
3.0000	0.0600		
3.5000	0.0625		
4.0000	0.0658		
5.0000	0.0731		
6.0000	0.0751		
7.0000	0.0760		
9.0000	0.0818		
10.000	0.0836		
11.000	0.0851		

Dynamic Uptake
Coal Type: PSOC 791
Penetrant: DMF Vapor
Penetrant Activity < 0.04
Sample Thickness: 254 μm
Mass of Coal (dmmf), M_c: 2.09 mg
Treatment Temperature: 150°C

Time (hr)	M_c *(g)*	*Time (hr)*	M_c *(g)*
0.0333	0.0055	9.0000	0.0629
0.0667	0.0102	10.000	0.0658
0.1000	0.0138	11.000	0.0665
0.1333	0.0167	12.000	0.0676
0.1667	0.0193	13.000	0.0698
0.2000	0.0215		
0.2333	0.0244		
0.2667	0.0258		
0.3000	0.0273		
0.3333	0.0284		
0.4333	0.0305		
0.5000	0.0331		
0.6000	0.0364		
0.6667	0.0378		
0.7667	0.0400		
0.8333	0.0415		
0.9333	0.0433		
1.0000	0.0440		
1.1667	0.0451		
1.3333	0.0462		
1.5000	0.0476		
2.0000	0.0491		
3.0000	0.0516		
4.0000	0.0542		
5.0000	0.0578		
6.0000	0.0611		
7.0000	0.0611		
8.0000	0.0611		

Dynamic Uptake
Coal Type: PSOC 247
Penetrant: DMF Vapor
Penetrant Activity < 0.04
Sample Thickness: 330 μm
Mass of Coal (dmmf), M_c: 2.93 mg
Treatment Temperature: 150°C

Time (hr)	M_c *(g)*	*Time (hr)*	M_c *(g)*
0.0333	0.0055	9.0000	0.1102
0.0667	0.0105	10.000	0.1138
0.1000	0.0142	11.000	0.1167
0.1333	0.0178	12.000	0.1193
0.1667	0.0193	13.000	0.1218
0.2000	0.0211	14.000	0.1240
0.2333	0.0229	15.000	0.1255
0.2667	0.0244	16.000	0.1269
0.3000	0.0258	17.000	0.1298
0.3333	0.0273	18.000	0.1331
0.3667	0.0284		
0.4000	0.0298		
0.5000	0.0327		
0.6000	0.0364		
0.6667	0.0385		
0.7667	0.0404		
0.8333	0.0429		
1.0000	0.0487		
1.1667	0.0520		
1.3333	0.0553		
1.5000	0.0575		
2.0000	0.0647		
3.0000	0.0775		
4.0000	0.0851		
5.0000	0.0902		
6.0000	0.0982		
7.0000	0.1011		
8.0000	0.1069		

Dynamic Uptake
Coal Type: PSOC 312
Penetrant: DMF Vapor
Penetrant Activity < 0.04
Sample Thickness: 254 μm
Mass of Coal (dmmf), M_c: 3.73 mg
Treatment Temperature: 150°C

Time (hr)	M_c *(g)*	*Time (hr)*	M_c *(g)*
0.0333	0.0033	3.5000	0.0571
0.0667	0.0042	4.0000	0.0589
0.1000	0.0047	5.0000	0.0636
0.1333	0.0058	6.0000	0.0658
0.1667	0.0069	7.0000	0.0673
0.2000	0.0080	8.0000	0.0687
0.2300	0.0091		
0.2667	0.0102		
0.3000	0.0113		
0.4000	0.0127		
0.5000	0.0149		
0.5667	0.0160		
0.6667	0.0178		
0.7333	0.0196		
0.8000	0.0211		
0.9000	0.0222		
1.0000	0.0236		
1.1667	0.0247		
1.3333	0.0273		
1.5000	0.0291		
1.6667	0.0313		
1.8333	0.0327		
2.0000	0.0336		
2.1667	0.0345		
2.5000	0.0360		
2.6667	0.0382		
2.8333	0.0433		
3.0000	0.0513		

Dynamic Uptake
Coal Type: PSOC 853
Penetrant: DMF Vapor
Penetrant Activity < 0.04
Sample Thickness: 229 μm
Mass of Coal (dmmf), M_c: 5.80 mg
Treatment Temperature: 150°C

Time (hr)	M_c *(g)*
0.0333	0.0022
0.0667	0.0031
0.1000	0.0044
0.1333	0.0055
0.1667	0.0062
0.2000	0.0073
0.3000	0.0085
0.3333	0 0095
0.5000	0.0113
0.6000	0.0125
0.6667	0.0135
0.8333	0.0149
1.0000	0.0187
1.1667	0.0218
1.3333	0.0255
1.5000	0.0291
2.0000	0.0313
3.0000	0.0345
4.0000	0.0444
5.0000	0.0465
6.0000	0.0473
7.0000	0.0491
8.0000	0.0505

Dynamic Uptake
Coal Type: PSOC 791
Penetrant: Chloroform Vapor
Penetrant Activity = 0.04
Sample Thickness: 229 μm
Mass of Coal (dmmf), M_c: 2.26 mg
Treatment Temperature: 35°C

Time (hr)	M_c *(g)*	*Time (hr)*	M_c *(g)*
0.0333	0.0036	5.0000	0.0884
0.0667	0.0069	6.0000	0.0920
0.1000	0.0102	7.0000	0.0935
0.1333	0.0127	8.0000	0.0978
0.1667	0.0142		
0.2000	0.0164		
0.2333	0.0178		
0.2667	0.0196		
0.3000	0.0218		
0.3667	0.0240		
0.4333	0.0287		
0.5000	0.0335		
0.6000	0.0404		
0.6667	0.0425		
0.7667	0.0449		
0.8333	0.0464		
1.0000	0.0478		
1.1667	0.0498		
1.3333	0.0518		
1.5000	0.0531		
2.0000	0.0560		
3.0000	0.0611		
4.0000	0.0669		

Dynamic Uptake
Coal Type: PSOC 247
Penetrant: Chloroform Vapor
Penetrant Activity = 0.04
Sample Thickness: 229 μm
Mass of Coal (dmmf), M_c: 3.11 mg
Treatment Temperature: 35°C

Time (hr)	M_c *(g)*	*Time (hr)*	M_c *(g)*
0.0333	0.0022	7.0000	0.1271
0.0667	0.0076	8.0000	0.1316
0.1000	0.0091	9.0000	0.1349
0.1333	0.0127	10.000	0.1364
0.1667	0.0149	11.000	0.1375
0.2000	0.0176	12.000	0.1393
0.2333	0.0193		
0.2667	0.0216		
0.3000	0.0236		
0.3333	0.0265		
0.3667	0.0280		
0.4000	0.0298		
0.4667	0.0335		
0.5000	0.0364		
0.6000	0.0400		
0.6667	0.0429		
0.7667	0.0465		
0.8333	0.0504		
0.9333	0.0556		
1.0000	0.0578		
1.1667	0.0624		
1.3333	0.0658		
1.5000	0.0727		
2.0000	0.0815		
3.0000	0.0982		
4.0000	0.1113		
5.0000	0.1185		
6.0000	0.1224		

Dynamic Uptake
Coal Type: PSOC 312
Penetrant: Chloroform Vapor
Penetrant Activity = 0.04
Sample Thickness: 381 μm
Mass of Coal (dmmf), M_c: 4.51 mg
Treatment Temperature: 35°C

Time (hr)	M_c *(g)*
1.0000	0.01020
2.0000	0.01890
3.0000	0.02400
4.0000	0.03310
5.0000	0.04510
6.0000	0.05160
10.000	0.06040
11.000	0.06622
12.000	0.07958
13.000	0.09753
14.000	0.12440
15.000	0.15530

Dynamic Uptake
Coal Type: PSOC 853
Penetrant: Chloroform Vapor
Penetrant Activity = 0.04
Sample Thickness: 229 μm
Mass of Coal (dmmf), M_c: 2.99 mg
Treatment Temperature: 35°C

Time (hr)	M_c *(g)*
0.0333	0.0005
0.1000	0.0011
0.1333	0.0022
0.1667	0.0040
0.2667	0.0065
0.3333	0.0087
0.4333	0.0098
0.5000	0.0105
0.6667	0.0120
0.8333	0.0138
1.0000	0.0152
1.3333	0.0181
1.5000	0.0192
1.6667	0.0214
1.8333	0.0243
2.0000	0.0258
2.5000	0.0276
3.0000	0.0298
3.5000	0.0320
4.0000	0.0345

Dynamic Uptake
Coal Type: PSOC 791
Penetrant: Chloroform Vapor
Penetrant Activity = 0.04
Sample Thickness: 229 μm
Mass of Coal (dmmf), M_c: 1.57 mg
Treatment Temperature: 100°C

Time (hr)	M_c *(g)*	*Time (hr)*	M_c *(g)*
0.0333	0.0033	7.0000	0.0678
0.0667	0.0051		
0.1000	0.0060		
0.1300	0.0069		
0.1667	0.0080		
0.2000	0.0095		
0.2333	0.0116		
0.2667	0.0124		
0.3000	0.0131		
0.3333	0.0145		
0.3667	0.0156		
0.4000	0.0164		
0.5000	0.0185		
0.6000	0.0215		
0.6667	0.0244		
0.8333	0.0284		
1.0000	0.0302		
1.1667	0.0323		
1.5000	0.0356		
1.6667	0.0385		
1.8333	0.0411		
2.0000	0.0444		
2.5000	0.0496		
3.0000	0.0520		
3.5000	0.0571		
4.0000	0.0596		
5.0000	0.0611		
6.0000	0.0654		

Dynamic Uptake
Coal Type: PSOC 247
Penetrant: Chloroform Vapor
Penetrant Activity = 0.04
Sample Thickness: 203 μm
Mass of Coal (dmmf), M_c: 1.77 mg
Treatment Temperature: 100°C

Time (hr)	M_c *(g)*
0.0333	0.0055
0.0667	0.0065
0.1000	0.0084
0.1333	0.0109
0.1667	0.0124
0.2000	0.0142
0.2333	0.0156
0.2667	0.0175
0.3000	0.0185
0.3333	0.0200
0.3667	0.0222
0.4000	0.0229
0.4333	0.0242
0.4667	0.0255
0.5000	0.0267
0.600	0.0284
0.6667	0.0302
0.7667	0.0320
0.8333	0.0338
0.9333	0.0356
1.0000	0.0369
1.1667	0.0396
1.3333	0.0411
1.5000	0.0431
2.0000	0.0473
2.5000	0.0491

Dynamic Uptake
Coal Type: PSOC 312
Penetrant: Chloroform Vapor
Penetrant Activity = 0.04
Sample Thickness: 254 μm
Mass of Coal (dmmf), M_c: 2.88 mg
Treatment Temperature: 100°C

Time (hr)	M_c *(g)*
0.0333	0.0011
0.0667	0.0022
0.1000	0.0033
0.1667	0.0036
0.2667	0.0047
0.3333	0.0058
0.5000	0.0078
0.7000	0.0102
1.0000	0.0113
1.1667	0.0138
1.3333	0.0153
1.5000	0.0180
2.0000	0.0200
3.0000	0.0240

Dynamic Uptake
Coal Type: PSOC 853
Penetrant: Chloroform Vapor
Penetrant Activity = 0.04
Sample Thickness: 203 μm
Mass of Coal (dmmf), M_c: 3.11 mg
Treatment Temperature: 100°C

Time (hr)	M_c *(g)*	*Time (hr)*	M_c *(g)*
0.0333	0.0044	11.000	0.0985
0.0667	0.0065	12.000	0.1018
0.1000	0.0124	13.000	0.1065
0.1333	0.0149	14.000	0.1080
0.1667	0.0167		
0.2000	0.0178		
0.2333	0.0187		
0.2667	0.0211		
0.3000	0.0247		
0.3333	0.0265		
0.3667	0.0280		
0.5000	0.0320		
0.6000	0.0353		
0.6667	0.0375		
0.8333	0.0393		
1.0000	0.0415		
1.1667	0.0433		
1.3333	0.0455		
1.5000	0.0469		
2.0000	0.0556		
2.5000	0.0586		
3.0000	0.0618		
4.0000	0.0705		
5.0000	0.0760		
6.0000	0.0825		
7.0000	0.0873		
8.0000	0.0909		
9.0000	0.0956		

Dynamic Uptake
Coal Type: PSOC 791
Penetrant: Chloroform Vapor
Penetrant Activity = 0.04
Sample Thickness: 356 μm
Mass of Coal (dmmf), M_c: 3.11 mg
Treatment Temperature: 150°C

Time (hr)	M_c *(g)*	*Time (hr)*	M_c *(g)*
0.0333	0.0076	11.000	0.1276
0.0667	0.0113	12.000	0.1298
0.1000	0.0149		
0.1333	0.0185		
0.1667	0.0207		
0.2000	0.0240		
0.2333	0.0280		
0.2667	0.0302		
0.3333	0.0338		
0.4333	0.0385		
0.5000	0.0429		
0.6000	0.0473		
0.6667	0.0502		
0.8333	0.0571		
1.0000	0.0625		
1.1667	0.0676		
1.3333	0.0724		
1.5000	0.0753		
2.0000	0.0847		
2.5000	0.0905		
3.0000	0.0960		
4.0000	0.1030		
5.0000	0.1065		
6.0000	0.1109		
7.0000	0.1145		
8.0000	0.1178		
9.0000	0.1211		
10.000	0.1229		

Dynamic Uptake
Coal Type: PSOC 247
Penetrant: Chloroform Vapor
Penetrant Activity = 0.04
Sample Thickness: 178 μm
Mass of Coal (dmmf), M_c: 1.70 mg
Treatment Temperature: 150°C

Time (hr)	M_c *(g)*	*Time (hr)*	M_c *(g)*
0.0333	0.0015	8.0000	0.0433
0.0667	0.0025	9.0000	0.0451
0.1000	0.0036	10.000	0.0458
0.1333	0.0065	11.000	0.0473
0.1667	0.0091		
0.2000	0.0102		
0.2333	0.0109		
0.2667	0.0116		
0.3000	0.0124		
0.3333	0.0135		
0.3667	0.0142		
0.4000	0.0149		
0.4333	0.0156		
0.4667	0.0167		
0.5000	0.0175		
0.6000	0.0189		
0.6667	0.0204		
0.8333	0.0222		
1.0000	0.0236		
1.1667	0.0255		
1.5000	0.0269		
2.0000	0.0284		
2.5000	0.0302		
3.0000	0.0320		
4.0000	0.0371		
5.0000	0.0389		
6.0000	0.0407		
7.0000	0.0418		

Dynamic Uptake
Coal Type: PSOC 853
Penetrant: Chloroform Vapor
Penetrant Activity = 0.04
Sample Thickness: 203 μm
Mass of Coal (dmmf), M_c: 3.44 mg
Treatment Temperature: 150°C

Time (hr)	M_c *(g)*
0.0333	0.0015
0.0667	0.0022
0.1333	0.0025
0.1667	0.0040
0.2000	0.0051
0.2333	0.0062
0.2667	0.0069
0.3000	0.0080
0.3333	0.0091
0.3667	0.0102
0.4000	0.0113
0.4333	0.0124
0.4667	0.0131
0.6000	0.0149
0.6667	0.0164
0.7667	0.0182
0.8333	0.0196
1.0000	0.0211
1.1667	0.0225
1.3333	0.0255
1.5000	0.0291
2.0000	0.0345
2.5000	0.0389
3.0000	0.0404
4.0000	0.0429
5.0000	0.0436

Microscopy Studies
Coal Type: PSOC 853
Penetrant: DMF liquid
Sample Thickness: 7.6 μm
Temperature: 25°C

Time (min)	*Transition Layer thickness*	*Time (min)*	*Transition Layer thickness*
0.5333	114.7680	12.733	564.5151
0.8500	147.7638	13.216	578.8611
1.1500	183.6288		
1.6166	210.1689		
1.8500	225.9495		
2.1000	243.1647		
2.3000	259.6626		
2.5333	276.8779		
2.8500	287.6375		
3.0666	304.1353		
3.4333	314.1775		
3.8333	345.7385		
4.1166	360.8020		
4.3666	368.6921		
4.7333	380.1689		
5.2833	387.3420		
5.6166	395.9497		
6.0666	400.9707		
6.6166	408.1436		
7.0000	414.5994		
7.4500	422.4897		
7.8166	432.5320		
8.2000	440.4221		
8.7333	449.7471		
9.2000	461.2239		
9.7000	473.4180		
10.100	480.5911		
10.566	494.9370		
11.066	509.2830		
11.500	516.4561		
12.150	537.9751		

Microscopy Studies
Coal Type: PSOC 853
Penetrant: DMF liquid
Sample Thickness: 7.6 μm
Temperature: 25°C

Time (min)	*Distance (μm)*	*Time (min)*	*Distance (μm)*
0.5333	114.7680	10.100	480.5911
0.8500	147.7638	10.566	494.9370
1.1500	183.6288	11.066	509.2830
1.6166	210.1689	11.500	516.4561
1.8500	225.9495	12.150	537.9751
2.1000	243.1647	12.733	564.5151
2.3000	259.6626	13.216	578.8611
2.5333	276.8779	13.550	591.0552
2.8500	287.6375	13.916	599.6628
3.0666	304.1353	14.666	606.8359
3.4333	314.1775	15.333	626.2029
3.8333	345.7385	16.500	632.6587
4.1166	360.8020	17.000	638.3970
4.3666	368.6921	17.533	644.8528
4.7333	380.1689	18.183	652.7429
5.2833	387.3420	19.000	669.9583
5.6166	395.9497	19.666	682.1523
6.0666	400.9707	41.000	985.5703
6.6166	408.1436		
7.0000	414.5994		
7.4500	422.4897		
7.8166	432.5320		
8.2000	440.4221		
8.7333	449.7471		
9.2000	461.2239		
9.7000	473.4180		

Microscopy Studies
Coal Type: PSOC 853
Penetrant: DMF liquid
Sample Thickness: 7.6 μm
Temperature: 40°C

Time (min)	*Distance (μm)*	*Time (min)*	*Distance (μm)*
0.2666	71.73001	23.666	1197.891
0.8333	114.7680	24.483	1212.237
1.7334	143.4600	26.750	1248.102
2.1333	186.4980	27.033	1283.967
2.4666	215.1900	28.000	1298.313
3.1000	286.9199	29.100	1327.005
3.5000	308.4390	30.833	1334.178
4.3333	358.6499		
4.6666	380.1589		
5.1666	401.6880		
5.6666	423.2070		
6.2333	466.2451		
6.8333	494.9370		
7.5000	537.9751		
8.0000	581.0129		
8.4166	616.8779		
8.9500	645.5701		
9.4166	688.6082		
10.416	717.3000		
10.883	738.8191		
11.500	774.6841		
12.133	789.0300		
13.000	824.8950		
13.916	875.1060		
14.416	932.4900		
16.666	975.5281		
18.000	1030.043		
19.983	1063.756		
21.000	1090.296		
21.833	1126.161		
22.500	1176.372		

Microscopy Studies
Coal Type: PSOC 853
Penetrant: DMF liquid
Sample Thickness: 7.6 μm
Temperature: 70°C

Time (min)	*Distance (μm)*
0.2166	356.4980
0.7333	419.6206
0.9666	509.2830
1.5000	606.8359
1.7666	645.5701
2.0500	695.0637
2.3333	773.9668
2.7166	817.7219
3.9333	913.8401
4.3666	977.6799
4.8666	1059.452
5.2333	1113.967
5.6666	1187.849
6.1333	1245.950
7.1666	1345.655
8.0000	1380.085
7.6166	1403.756
9.7000	1425.275
15.933	1453.250

Microscopy Studies
Coal Type: PSOC 853
Penetrant: DMF liquid
Sample Thickness: 7.6 μm
Temperature: 100°C

Time (min)	*Distance (μm)*
0.1500	218.0592
0.3500	351.4771
0.6333	472.7007
0.8666	593.9246
1.1166	619.0300
1.6833	638.3970
2.2166	691.4773
2.6333	770.3801
3.1333	834.9373
3.7000	919.5786
4.3333	1058.735
5.0000	1183.545
5.4500	1291.140
5.7333	1398.735
6.0000	1470.465
7.0666	1578.060
7.4833	1626.836
8.0000	1661.267
9.0000	1699.284
9.7833	1740.887
10.650	1783.925
11.500	1875.740
12.416	1908.018
13.266	1976.879
13.800	2000.549
15.000	2026.373
15.783	2054.346
16.916	2067.258
18.500	2085.191

Microscopy Studies
Coal Type: PSOC 312
Penetrant: DMF liquid
Sample Thickness: 7.6 μm
Temperature: 25°C

Time (min)	*Distance (μm)*	*Time (min)*	*Distance (μm)*
1.0333	206.5824	18.466	1140.507
1.3500	329.2407	19.500	1183.545
1.5833	364.3884	20.149	1240.929
1.9833	424.6416	21.000	1291.140
2.2666	469.8315	22.000	1319.832
2.5500	498.5234	23.433	1341.351
2.9166	534.3884	25.800	1362.870
3.1833	564.5151	26.649	1398.735
3.7500	578.1438	28.133	1434.600
4.1000	615.4434	29.266	1470.465
4.8166	648.4392	31.333	1527.849
5.2333	697.2156	33.850	1578.060
5.5833	711.5615	35.383	1628.271
5.8833	743.1228	38.416	1671.309
6.2666	763.9246	47.000	1793.250
6.7833	773.9668		
7.2000	778.2705		
7.7666	781.1396		
8.3000	791.1819		
8.9333	812.7009		
9.6000	831.3506		
10.283	844.9795		
11.383	893.0386		
11.816	907.3845		
12.266	929.6208		
13.566	964.0513		
14.250	991.3086		
15.016	1037.216		
15.833	1057.300		
16.649	1083.123		
17.417	1111.815		

Microscopy Studies
Coal Type: PSOC 247
Penetrant: DMF liquid
Sample Thickness: 7.6 μm
Temperature: 25°C

Time (min)	*Distance (μm)*
0.6500	256.7935
1.1500	430.3801
1.5333	497.8062
1.8333	506.4138
3.2166	542.9961
3.8833	591.7725
4.7166	619.0300
6.8333	626.9202
7.2833	643.4182
8.9166	652.7429
10.400	670.6755
11.783	681.4351
13.650	685.7388
15.166	685.7388

Microscopy Studies
Coal Type: PSOC 853
Penetrant: Chloroform liquid
Sample Thickness: 7.6 μm
Temperature: 25°C

Time (min)	*Distance (μm)*
0.2666	253.2069
0.4833	296.9622
0.7166	352.9116
0.9166	387.3420
1.8500	405.2744
2.1500	438.9875
3.0666	459.7893
3.3166	495.6543
4.3333	533.6711
5.0166	605.4011
5.6000	648.4392
5.9500	675.6965
6.9500	796.2031
7.3166	831.3506
8.2166	847.1313
8.5000	870.8022
8.8000	895.9077
9.6333	903.0808
10.283	929.6208
11.466	948.9880
12.483	984.1357
14.300	995.6125
17.649	1098.904
18.916	1147.680
19.616	1183.545
20.700	1212.237
22.683	1226.583

Microscopy Studies
Coal Type: PSOC 853
Penetrant: Methylene Chloride liquid
Sample Thickness: 7.6 μm
Temperature: 25°C

Time (min)	*Distance (μm)*
0.1166	182.9115
0.4833	263.2490
0.8500	311.3081
1.2166	350.0425
1.8500	398.1016
2.6000	416.7515

Microscopy Studies
Coal Type: PSOC 853
Penetrant: THF liquid
Sample Thickness: 7.6 μm
Temperature: 25°C

Time (min)	*Distance (μm)*
1.1000	80.33760
1.3166	129.1140
1.5333	156.3714
1.7500	206.5824
2.0000	230.9706
2.1833	265.4011
2.4833	277.5950
2.7500	284.0508
2.9666	294.0930
3.2166	306.2871
3.4500	319.9158
3.7333	330.6753
4.0000	340.0002
4.3500	348.6079
4.5500	358.6499
4.9333	378.7344
5.2333	391.6458
8.8666	413.8821
5.9166	421.0552
6.1666	433.9666
8.2000	469.1143
8.6166	485.6121
8.9500	492.7852
9.5166	503.5447
10.200	520.7598
10.833	527.2156
11.283	534.3884
11.883	537.9751
12.166	540.8442

Microscopy Studies
Coal Type: PSOC 853
Penetrant: Pyridine liquid
Sample Thickness: 7.6 μm
Temperature: 25°C

Time (min)	*Distance (μm)*
0.9166	100.4220
1.1333	141.3081
1.3333	167.1309
1.6666	201.5613
1.8333	222.3630
2.0500	251.7724
2.2500	275.4431
2.5500	297.6794
2.8000	314.1775
2.9666	332.8271
3.5000	347.8906
3.9666	360.0847
4.3166	372.9961
4.9833	380.1689
5.4166	393.7976
5.7333	407.4265
5.9833	423.2070
6.5000	434.6838
6.7833	447.5952
7.0666	451.8989
7.5833	463.3760
8.4000	473.4180
9.0500	489.9160
9.5833	497.0889
10.150	504.2620
10.850	512.8696
11.366	519.3252
12.000	520.7598

END

DATE FILMED

01 / 23 / 91